Enhancement and Redevelopment of the Regional Lake Water Quality Model with Applications

by

Bushra Tasnim

A thesis submitted to the Graduate Faculty of
Auburn University
in partial fulfillment of the
requirements for the Degree of
Master of Science

Auburn, Alabama
August 08, 2020

Keywords: Water Quality, Chlorophyll-a, Phosphorus, Dissolved Oxygen

Approved by

Xing Fang, Chair, Arthur H. Feagin Chair Professor of Civil and Environmental Engineering
Joel S. Hayworth, Associate Professor of Civil and Environmental Engineering Di Tian,
Assistant Professor of Crop, Soil and Environmental Sciences

ABSTRACT

Water quality is a serious issue in most of the world in the 21st century. Many lakes are impaired with Harmful Algal Blooms (HABs). To provide better lake management and restoration, modeling of lakes is of utmost importance. MINLAKE is a very reliable water quality simulation tool that simulates water temperature and DO in all types of lakes. However, this model cannot portray the overall nutrient and phytoplankton scenario of the lake which is important to identify the condition of the lake. To capture these fluctuations, a daily model MINLAKE2020 is developed based on a one-dimensional, deterministic daily-time-step water quality model "MINLAKE2012". MINLAKE2020 simulates chlorophyll-a, phosphorus, biochemical oxygen demand on a daily time step in addition to water temperature and dissolved oxygen simulation. Some of the model parameters were calibrated for six Minnesota lakes which include two shallow lakes, two medium-depth lakes, and two deep lakes. The accuracy of the model was assessed by comparing the chlorophyll-a, phosphorus, and dissolved oxygen with the observed ones at the study lakes. The overall results from the model are satisfactory for all lakes. This model can be successfully used to simulate water quality for all types of lakes. The long-term goal of developing MINLAKE2020 is to include/integrate it with a watershed model, SWAT, a popular watershed water quality simulation model. SWAT simulates reservoirs in a watershed as well-mixed waterbodies, which can be a possible source of error for water quality simulations. MINLAKE2020 simulating nitrogen, inflow, and outflow was developed but should be fully tested before integrating it with the SWAT model.

ACKNOWLEDGEMENT

I would like to wholeheartedly express my warmest gratitude to Dr. Xing Fang, my academic advisor, for providing me the opportunity to pursue my master's degree under his guidance. I appreciate the support, continuous encouragement, patience, and guidance he has shown towards me in accomplishing my goals. He is an excellent professional researcher as well as a very good human being who will always remain as inspiration throughout my life. I am also thankful to my graduate committee members, Dr. Joel S. Hayworth and Dr. Di Tian for their time to review my thesis and provide me with their valuable guidance for further improvements. I would like to present my special gratitude to Dr. Hayworth and Dr. Fang for providing me the chance to pursue my further research and studies.

I would like to thank my parents who worked very hard for my well-being. I would also like to thank my husband for his unconditional support. I am also thankful to Auburn University! War Eagle!

This study is partially supported by funding from Auburn University for the PAIR project "A prototype framework of climate services for decision making." Di Tian is PI, Xing Fang and others are six Co-PIs. This study is also partially supported by funding from the OUC-AU Joint Center for Aquaculture and Environmental Science for the project "*Identifying potential bioaccumulation hotspots of heavy metals in dynamic estuarine systems in Alabama, USA and China."* Matthew N. Waters is PI, Xing Fang and Joel Hayworth are Co-PIs at Auburn University; Jinfen Pan is PI, Min Wang is Co-PI from OUC (Ocean University of China).

Table of Contents

List of Figures

List of Tables

Chapter 1 Introduction

1.1 Background

Water is a necessary element for all living organisms. However, aquatic organisms need water for the respiration process. Water quality is an important research area in this modern era because of the excessive pollution of surface water. Water quality standards vary according to the specific use of water. The water used for industrial production has different guidelines than potable water.

In recent years, surface water bodies around the globe have undergone a lot of challenges. There have been occurrences of non-point source pollution, eroded sediments with heavy metals, fish kill, harmful algal bloom, etc. These blooms of phytoplankton affect public health and ecosystem services globally. Due to freshwater blooms, United States incur economic losses of more than US$4 billion annually, primarily from harm to aquatic food production, recreation and tourism, and drinking water supplies. A recent study used three decades of high-resolution Landsat 5 satellite imagery to investigate the summertime algal bloom trend in 71 lakes in the United States (Ho et al., 2019). However, it was found that 68 percent of the lakes show global exacerbation of bloom intensity since 1980. The reasons for these algal blooms are excessive nutrient availability by runoff, agricultural fertilizer, or some other sources, warm temperature, etc. The problem associated with harmful algal blooms is the pollution of sources of drinking water, impairment of recreational facility, the value of businesses and properties, etc. Lake Erie is the biggest example of the challenges associated with an algal bloom. Forty-five years ago, Lake Erie became so polluted that scientists feared that it would die of suffocation (Geist, 2017). After a massive

cleanup effort by everyone, from local business to state and national policymakers, the lake was back from the brink. In recent years, the lake is suffering from algal bloom again and again. In 2015, an algal bloom of intensity 8 out of 10 occurred at Lake Erie. In July 2019, a severe bloom of blue-green algae (Cyanobacteria) spread over the western half of Lake Erie. By August 13, 2019, the bloom spread over to 620 square miles over the western basin which is almost 7 times the area of Cleveland. Lake Erie's algal bloom is a threat to the health and drinking water of 11 million people. In February 2020, the state of Ohio committed to spending $172 million to clean up Lake Erie.

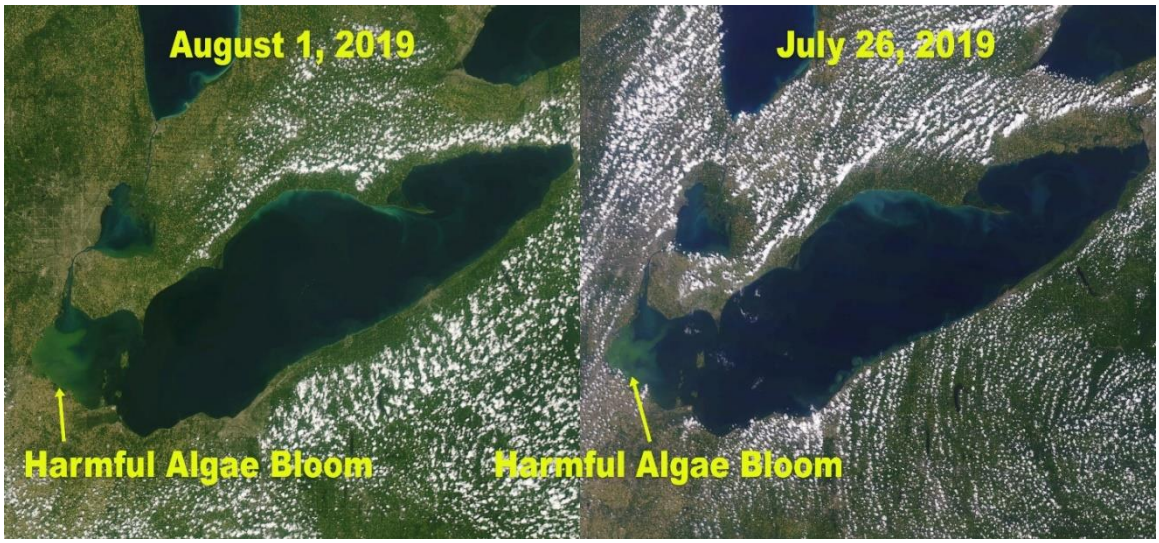

Figure 1.1 Satellite imagery of Lake Erie from July 26, 2019, to August 1, 2019

The main reason behind this harmful algal bloom is the excess nutrients from upstream sources. The excess nutrients cause an overgrowth of algae in a short period. The algae consume oxygen and block sunlight from underwater plants. As a result, aquatic life cannot survive because of the lack of oxygen. The largest dead zone in the United States (about 6,500 square

miles) is in the Gulf of Mexico and occurs every summer as a result of nutrient pollution from the Mississippi River Basin.

Figure 1.2 One of the adverse effects of algal bloom–fish kill observed on the west coast of Lake Erie (Hayes, 2020)

To alleviate the problem of algal bloom and endangerment of aquatic species, it is important to have a broad idea about the driving factors of algal bloom: water temperature, phosphorus, nitrogen, chlorophyll-a, and dissolved oxygen (DO) concentration of lakes. Mathematical modeling can simplify this work. Schooner said, "Modeling is a little like art in the words of Pablo Picasso. It is never completely realistic; it is never the truth. But it contains enough of the truth, hope, and enough realism to gain understanding about the systems being simulated in the model." Mathematical models have been used since to better understand the physical, chemical processes.

In the second half of the twentieth century, due to the advent of modern computers, several numerical models have been developed to predict water quality parameters in different types of water bodies such as riverine systems, estuaries, lakes, and reservoirs. Based on the necessity, limitations, and the type of water body, the modelers have decided whether to develop one-dimensional, two-dimensional, and three- dimensional models.

1.2 Introduction to Water Quality Models

In the 1960s, eutrophication effects were first observed in lakes, especially in those which were used for drinking water supply (Dillon and Rigler, 1974a; Vollenweider and Kerekes, 1982). Eutrophication has been a threat to water bodies since the beginning of the twentieth century in industrialized countries (Le Moal et al., 2018; Moss, 2012; Takolander et al., 2017; Yao et al., 2018). A large proportion of the anthropogenic increase in nitrogen and phosphorus flux due to industrialization is delivered to ground or surface waters through direct runoff, human and animal wastes, and atmospheric deposition. In the long run, excess nutrients are transported to water bodies (Liu et al., 2008; Turner and Rabalais, 2003).

When a waterbody undergoes any human-influenced ecosystem changes such as nutrient loading, extreme weather events, and invasive organisms; algal species (cyanobacteria) can form dense overgrowths known as algal blooms. Since these blooms can produce toxins that are harmful to people and animals, it is mostly known as harmful algal blooms (HAB). As with HABs, oxygen is consumed by algae and the sunlight is blocked from the underwater plants. Moreover, when the algae die, they also consume oxygen. As a result, the oxygen concentration in the waterbody drops causing in a condition named hypoxia. Hypoxia is defined as a naturally-occurring condition where

the concentration of dissolved oxygen in a water column is too low to support living aquatic organisms, typically below 2–4 mg/L of dissolved oxygen (National Science and Technology Council, 2017). Hypoxia and toxins from HABs have the potential to kill fish. Moreover, HABs can cause sickness in people if a sufficient amount of toxin is ingested through drinking water, contaminated food, or contaminated air (Wood, 2016). They can have serious effects on the social health of a community causing a decrease in activity that is dependent on aquatic or seafood harvests or tourism; disruption of social, and cultural practices.

Since water quality of surface water has become a great concern in the twentieth century, many numerical models have been developed to predict water quality parameters in different types of water bodies such as riverine systems, estuaries, lakes, and reservoirs. There is not a complete agreement among the professionals regarding the best approach for modeling rivers, lakes, estuaries, and coastal waters (Ji 2008). It depends on the necessity, limitations, and the type of water body. For example, in freshwater rivers where the dominant gradient of water quality constituents is along the longitudinal axis in the flow direction, a one-dimensional laterally and vertically averaged model is appropriate for describing the flow of water and the mass transport of constituents. However, a one-dimensional model is not appropriate for simulating water quality of the tidal river characterized by pronounced lateral or vertical gradients of salinity. Water quality gradients in broad, shallow lakes generally arise from winds, inflows of freshwater, and outflows along the lateral and longitudinal direction of the flow. A vertically averaged, two-dimensional model is appropriate for this type of waterbody. In deep lakes and reservoirs, vertical mixing is restricted, and vertical gradients of water quality constituents arise from seasonal stratifications and inflows of cold-water rivers into a warmer-water lake or reservoir. If these water bodies are

narrow and deep, they can be simulated by a two-dimensional, laterally averaged model. For some lakes and reservoirs with large surface areas, if the lateral gradients of water quality constituents are significant, a three-dimensional model is appropriate.

In most of the cases, lakes are simulated using one-dimensional models that assume well mixed or uniform conditions along the lateral direction and only recognize the major variations of water quality along the vertical direction. For one-dimensional models, the main concept is that all inflow quantities and constituents are instantaneously dispersed throughout the horizontal layers (USACE 1995).

For a one-dimensional, horizontally averaged model, the vertical dimension of the lake is divided into many well-mixed horizontal layers (assuming no variation in the same depth). Two approaches have been developed to model a one-dimensional water quality gradient in lake models: turbulent diffusion approach and mixed-layer approach. In a turbulent diffusion approach, heat is supplied to the surface of the lake and then is distributed to the lower layers by diffusion (Chapra 2008). The model development is focused on the appropriate specification of the turbulent diffusion coefficients at different depths.

In the mixed-layer approach, a mechanical energy balance is used to predict the thickness of the upper mixed layer (epilimnion) (Chapra 2008). Mixed layer models are generally used in conjunction with diffusion models. Mixed layer models divide a temperature stratified lake into well-mixed surface layers (epilimnion) and diffusion layers below the epilimnion (hypolimnion). The mixed-layer depth and the mixed-layer temperature is simulated either by balancing wind energy with internal potential energy change or by averaging density instabilities due to surface cooling (natural convection) (Fang and Stefan 1994a). In this approach, the thick well-mixed

surface layer includes several horizontal layers with the same water temperature and the hypolimnion is modeled as a series of layers using the turbulent diffusion approach (Figure 1.3).

Though Chapra (2008) has specifically mentioned these methods for the prediction of water temperature, these approaches have been used successfully to model all other water quality parameters in lakes over the years. Fang (1994) has used the same approach in the regional dissolved oxygen model to predict the dissolved oxygen in different lakes in Minnesota. Though the approach remains the same, the source and sink terms differ based on the water quality parameter.

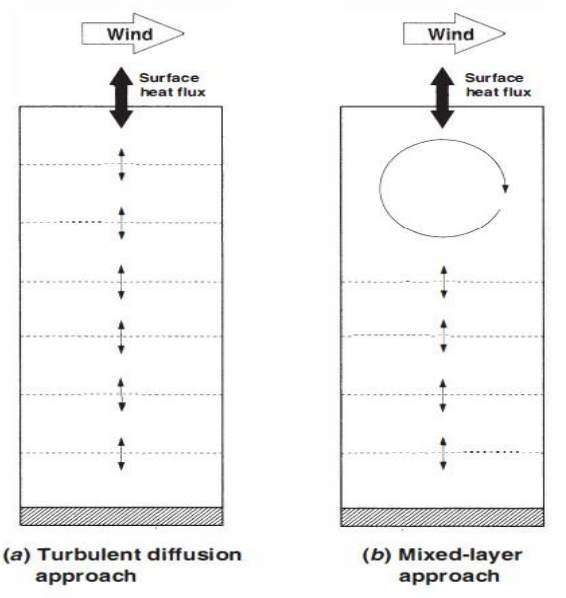

Figure 1.3 Lake water quality modeling approaches in vertical (deep) direction (Chapra 2008)

1.2.1 MINLAKE

The Minnesota Lake Water Quality Management Model (MINLAKE) is a one-dimensional (along depth direction), deterministic water quality model with a time step of one day that was developed in the 1980s (Riley and Stefan, 1988). The model was developed for supporting lake eutrophication studies and modeling lake water quality responding to various control strategies in a

lake (Riley and Stefan 1988). MINLAKE simulates a lake as a series of stacked horizontal layers of varying thickness. Each of the water layers is considered well mixed. Only the surface layer is in contact with the atmosphere during the open water season. These assumptions worked well for temperature and DO simulations over the years. It was observed that the horizontal variations of water temperature and DO in freshwater lakes are relatively small compared to the vertical variations. So, the one-dimensionality of the MINLAKE makes it appropriate for freshwater lakes. The MINLAKE model has been modified several times and has been successfully applied for more than 30 years to simulate the water quality parameters in different types of lakes. MINLAKE can reproduce selected constituent data to relatively high accuracy (Batick 2011).

In MINLAKE88, the description for phytoplankton and nutrient modeling was also provided along with the temperature and dissolved oxygen model. Three different phytoplankton models of different complexity were provided. The first model is a single algal group model with productivity distributed throughout the mixed layer. This model combines all the growth and loss terms into one equation and solves it explicitly. The level-one model equation is subject to two assumptions: the phytoplankton population is assumed to be uniformly distributed throughout the mixed layer and the light intensity at some point in the mixed layer reaches the level for light-saturated photosynthesis to occur (Forsberg and Shapiro, 1980). The model is good for calculating chlorophyll-a concentration quickly but the validity of the assumption has some doubts. The second model is also a single algal group model. The second model represents algal growth by a Michaelis-Menten equation (Monod, 1949) subject to both light and phosphorus limitation and the growth term is unique to each layer. The second model does not incorporate the zooplankton grazing term in phytoplankton simulation. Instead, the grazing is incorporated in simulation by the

use of a high mortality rate if zooplankton is dominant. The third model is considerably more complex than the previous models as three algal classes (diatoms, green algae, and blue-green algae) are simulated instead of one. The algal groups have different rates of growth, respiration, settling, zooplankton grazing, and different nutrient requirements. The nutrient limitation is calculated by the Michaelis-Menten equation and the lowest one among the light and nutrient limitations is chosen for calculation. Among these three models, the third model works the best for simulating phytoplankton.

In 1990, Gu and Stefan (1990) included an ice-cover period simulation in MINALKE88 to make it capable for year-round simulations (for thermal parameters). In 1991, Hondzo and Stefan introduced a more general water temperature simulation model for MINLAKE which can be applied to a wide variety of lakes and regions (Hondzo and Stefan, 1993a).

An important modification of the MINLAKE was accomplished in 1994 when Fang (1994) developed the regional dissolved oxygen model and combined it with MINLAKE to study the impact of global climate warming on lake water quality and fish habitat in Minnesota lakes. Minnesota has 11,842 lakes over 10 acres (4 ha) in surface area. It is impossible to model each lake in Minnesota so that the regional lake model was developed to model different types (categorizing by stratification strength and eutrophication) of the lakes by maximum depths (shallow, medium-depth, and deep), surface area (small, medium area, and large), and trophic status (eutrophic, mesotrophic, and oligotrophic). Therefore, the regional MINLAKE model is comprised of two separate sub-models – a regional water temperature model (Hondzo and Stefan 1993a) and a regional dissolved oxygen model (Fang 1994). The regional DO model is a simplified version of the DO model that did not simulate daily nutrients and Chl*a* concentrations but used the

annual mean Chlorophyll-a concentration with seasonal variation patterns (Fang 1994) for dissolved oxygen simulation. The annual mean Chl*a* concentration could be determined from field measurements in each year (typically based on a few surface Chl*a* data) for individual lake simulations or specified based on lake trophic status for regional lake studies (Fang 1994)

Regional MINLAKE model was first developed to simulate water quality in the open water season (when there is no ice cover over the lake). However, in cold regions such as Minnesota, heat exchange and oxygen transfer processes, which normally occur through the open water surface, are substantially altered by winter ice and snow cover (Fang and Stefan 1994b). Therefore, separate sub-models for winter conditions were developed and integrated with MINLAKE96 to simulate water temperature and dissolved oxygen all year-round (Fang and Stefan 1994b). The horizontal layers include snow, ice, water, and sediment. The year-round water temperature simulation model has been expanded significantly by simulating ice and snow covers above the water, and the heat exchange between each water layer and its adjoining sediment (Fang et al. 2010a). MINLAKE96 model was further modified and refined as it was used in a study in 2010, to simulate water quality conditions in cisco lakes, which are typically deep mesotrophic or oligotrophic lakes (Fang et al. 2010a).

In the MINLAKE96 model, it is assumed that the lake has no inflow or outflow and the lake is horizontally well-mixed. So, it is usually appropriate to use MINLAKE96 for lakes where there are no inflow and/or outflow and where inflows/outflows do not significantly alter water quality conditions in lakes. There are many lakes in Minnesota and over the USA that can be simulated using MINLAKE96. Therefore, Fang et al. (1994) applied MINLAKE96 to project the impact of climate warming on small lakes in the contiguous US. MINLAKE96 predicts the water

temperature and DO in response to daily weather conditions such as air temperature, dew point temperature, solar radiation, sunshine percentage, wind speed, wind direction, and precipitation, and snowfall. The model has been successfully applied to many lakes with satisfactory results for years (Fang 1994; Fang et al. 2010b). MINLAKE was further modified to calculate the hourly water temperature and dissolved oxygen using hourly weather conditions (Jamily 2018).

The MINLAKE96 model was modified by Deborah E. West-Mack and was made capable to simulate phosphorus, nitrogen, and chlorophyll-a simulation in 1998 (West and Stefan, 1998). In MINLAKE98, the third model of phytoplankton simulation used in 1988 is used as it can simulate chlorophyll-a for three algal classes. The mass balance equations for chlorophyll-a, phosphorus, nitrogen, and DO were modified from those of MINLAKE88. The model was tested on two lakes and produced satisfactory results. But due to a lack of observed data and the inability of the model to run for multiple years, the nutrient model was not further developed. The source code of MINLAKE98 was also lost and no longer available for further enhancement and improvement.

MINLAKE models have been applied in various lakes with different maximum depths and surface areas. Stepanenko et al. (2013) applied it to simulate thermal regime in Großer Kossenblatter See, a shallow turbid midlatitude lake in Germany with a mean depth of 2 m and a maximum depth of 5 m and surface area of 168 ha. Typically, MINLAKE is designed for relatively small inland lakes, but Thiery et al. (2014) applied it (with minor modifications on diffusion coefficients) to simulate temperature dynamics in a very large and deep tropical lake, Lake Kivu in Africa (2370 km^2 surface area; 485 m maximum depth; 1463 m a.s.l.).

1.2.2 PCLake

PCLake (1990) is a lake ecosystem model that uses a process-based model to simulate water quality based on ecological interactions in shallow, non-stratifying lakes in the temperate climate zone. The earlier versions of the model describe a completely mixed water body and it includes the water column and the upper sediment layer of the bottom of the lake. It is appropriate for modeling shallow, non-stratified lakes (Wen et al., 2019; Andersen et al., 2020). Mathematically, PCLake employs several coupled differential equations, one for each of the state variables included in the analysis. PCLake simulates the lake as a food web. Other than the food web, PCLake also includes empirical relations between components, such as the effect of fish and macrophytes, described as dry weight (D), nitrogen (N), and phosphorus concentration (P). The uniform time unit for all processes is 1 day. The relevant time scale for the output ranges from 1 week to 1 month. However, the recent version of PCLake, PCLake+ extends the PCLake model to cover a wide range of freshwater lakes that differ in stratification regime and climate-related processes (Janssen et al., 2019). A hypolimnion layer was introduced in PCLake+ that can be configured by different forcing functions or built-in empirical relationships to impose stratification.

1.2.3 LAKE2K

LAKE2K is a one-dimensional lake water quality model that divides the lakes into three vertical layers for simulation. LAKE2K uses a water balance, heat balance, and mass balance related to various physical and biogeochemical constituents to calculate water quality parameters for the epilimnion, metalimnion, and hypolimnion (three layers) of a lake (Chapra and Martin, 2004). However, the water balance is determined by specifying boundaries for the epilimnion,

metalimnion, and hypolimnion. LAKE2K simulates temperature through analyzing the surface heat exchange at the air-water interface of the lake. The model accounts for ice cover conditions. LAKE2K simulates carbon, nitrogen, oxygen, phosphorus, silica concentrations and phytoplankton, and zooplankton biomass. One drawback of Lake2K is that it does not consider heat exchange at the sediment-water interface.

1.2.4 CE-QUAL-W2

CE-QUAL-W2 (USACE-WES) is a two-dimensional hydrodynamic and water quality model which can be used in rivers, lakes, reservoirs, estuaries, and even a combination of rivers segments and multiple reservoirs. This model assumes lateral homogeneity but considers variations in longitudinal (flow direction) and vertical (depth) directions. CE-QUAL-W2 was originally developed by the United States Army Corps of Engineers Waterways Experiment Station (USACE-WES) and continuously enhanced/developed by researchers at the Portland State University in Oregon (http://www.ce.pdx.edu/w2/). This model is suitable for relatively long and narrow water bodies (Cole and Buchak 1995), for example, in Hodges Reservoir (Raymon et al, 2018), the Xiluodu Reservoir (Xie et al., 2017), and Amistad Reservoir (Fang et al., 2007). It can be used to predict water surface elevations, velocities, temperatures, DO, nutrients, phytoplankton, ice cover (onset, growth, and breakthrough), and so on. This model considers inflow and outflow, whereas the regional MINLAKE model did not consider those. One major drawback of CE-QUAL-W2 is the lack of consideration of heat transfer at the sediment-water interface. Though the time step of the model can be user-specified, numerical stability should be given priority while choosing a time step.

1.2.5 EFDC

The environmental fluid dynamic code (EFDC) was initially developed at the Virginia Institute of Marine Science and has been developed extensively over the past two decades. EFDC is a state-of-the-art versatile model used for simulating one-, two- or three-dimensional flow, transport, and biogeochemical process in surface water systems such as rivers, lakes, estuaries, reservoirs, and so on. For example, Chen et al. (2018) applied EFDC in Bankhead river-reservoir system with a thermal power plant (complex thermal discharge, mixing, and recirculation), Devkota, and Fang (2015a, 2015b) simulated temperature and salinity in a tidal river and a shallow estuary using EFDC. It can be used to simulate the process of hydrodynamics, sediment transport, and water quality eutrophication in one, two, and three dimensions. EFDC is a very flexible model that supports different options of creating the mesh such as sigma vertical coordinate, Cartesian or curvilinear, and orthogonal horizontal coordinate. In EFDC, the user can create a mesh of varying cell sizes, which makes the model capable of better representing the physical characteristics of different types of reservoirs. EFDC can use a fixed time step or a dynamic time step depending on the user preference and the safety factor provided by the user. If the safety factor is 0, the model uses a fixed time step (Craig 2012). Though EFDC is very flexible and supports a lot of conditions, it is quite complex and complicated. Therefore, the EFDC model is difficult to apply if there are not enough observed data for comparison.

1.2.6 ELCOM and CAEDYM

ELCOM (Estuary, Lake, and Coastal Ocean Model) is an advanced three-dimensional hydrodynamic model. ELCOM (CWR, University of Western Australia) was designed to

numerically simulate hydrodynamics and thermodynamics for inland and coastal waters in a practical manner. CAEDYM (Computational Aquatic Ecosystem Dynamic Model) is a water quality module that uses ELCOM, if integrated with ELCOM, as a hydrodynamic driver. ELCOM provides a detailed characterization of water movement and mixing in lakes whereas CAEDYM computes interactions between biological organisms and their nutrient cycles. CAEDYM can be integrated with ELCOM after some modifications and together they provide three-dimensional simulation capability for the examination of detailed changes in water quality. ELCOM-CAEDYM can successfully simulate the temporal and spatial variations of several water quality parameters such as temperature, conductivity, Chlorophyll-a, total organic Carbon, Nitrogen, Phosphorus (Hannoun et al., 2006). This model was used to model hypoxia in Lake Erie (Leon et al., 2006). Different agencies also use this model to simulate nutrient and algae for water purification and reservoir management practices (City of San Diego, 2012).

1.3 Considering Watershed Inputs for Lake Modeling

Lake ecosystems are particularly sensitive to nutrient loading from their watershed because of the thermal stratification of the water column during spring and summer periods when the primary production is maximum. However, thermal stratification hardly lasts more than a few hours or days in shallow lakes. The main morphometric (depth, volume) and hydrological (discharge of the tributaries, surface, and land-use in the catchment) characteristics determine the lake vulnerability to eutrophication. To account for eutrophication, it is important to introduce inflow and outflow in the lake water quality model. Also, Lakes and reservoirs are part of the hydrological cycle of their watershed. Lakes play an

essential role in the biogeochemical cycles of continental watersheds. To view the eutrophication scenario in detail, a watershed model coupled with a lake model can be beneficial.

The Soil and Water Assessment Tool (SWAT) is a continuous-time, semi-distributed, process-based river basin model jointly developed by the USDA Agricultural Research Service (USDA-ARS) and Texas A&M AgriLife Research. In 1990, the first version of SWAT was developed to evaluate the effects of alternative management decisions on water resources and nonpoint-source pollution in large river basins. The SWAT model was developed by merging three existing models – CREAMS, EPIC, and GLEAMS (Gassman et al, 2007). The model has been continuously changed and updated over the years.

SWAT is a small watershed to river basin-scale model which is capable of simulating the quality and quantity of surface and groundwater. The impact of land use, land management practices, and climate change on water quality and quantity can be successfully predicted by SWAT. Moreover, SWAT can be used to assess soil erosion prevention and control, non-point source pollution control, and regional management in watersheds. The SWAT model is extensively used in the world for modeling hydrology, water quality, and climatic change (Krysanova and Arnold, 2008, Gassman et al., 2007).

SWAT has several components for simulation such as weather, surface runoff, return flow, percolation, evapotranspiration, transmission losses, pond and reservoir storage, crop growth and irrigation, groundwater flow, reach routing, nutrient and pesticide loading, and water transfer. In SWAT, a watershed is divided into multiple sub-watersheds, which are further subdivided into hydrologic response units (HRUs). HRUs consist of homogeneous land use, management,

topographical, and soil characteristics. As water impacts plant growth and the movement of sediments, nutrients, pesticides, and pathogens, water balance is the driving force behind all the processes simulated in SWAT. Simulation of watershed hydrology is separated into two phases: the land phase and the in-stream or routing phase. The land phase controls the amount of water, sediment, nutrient, and pesticide loadings to the main channel in each subbasin whereas the in-stream phase is the movement of water, sediments, etc., through the channel network of the watershed to the outlet. SWAT is a continuous-time model that operates on a daily time step. SWAT is capable of running simulations for large watersheds without extensive monitoring data and predicting changes in hydrological parameters under different management practices and physical environmental factors (Gassman et al. 2007; Daloglu et al. 2014).

For some watersheds, lakes comprise a major portion. In the SWAT model, lakes are simulated as well-mixed reservoirs which is a potential source of error. In reality, lakes can be stratified or polymictic based on their geometry ratio. Stratification criteria affect the concentration of water quality parameters inside the lake. To correctly simulate watersheds containing lakes, a lake model (which considers stratification criteria) should be incorporated with the SWAT model to correctly simulate lake water quality parameters. This is one option to include watershed inputs for lake modeling. Many applications of current practices are to set and run a watershed model (e.g., SWAT) first, then the outputs of the watershed model were taken as input data for a lake model. This is to develop and operate two separate models.

1.4 Knowledge Gap

- MINLAKE has been used for 33 years by lake modelers to successfully simulate temperature and dissolved Oxygen in lakes. This model applies to all types of lakes: stratified, unstratified, shallow, deep, eutrophic, oligotrophic, etc. The widely used regional DO model of MINLAKE2012 has some limitations. The model can successfully predict dissolved oxygen concentration, but it lacks the ecological aspects of a lake.
- SWAT is a widely used watershed model that has high accuracy in predicting water quality and hydrologic parameters of a watershed. SWAT model can simulate ponds and reservoirs in the watershed. Reservoirs are simulated as in-stream waterbody which has inflow and outflow and ponds are simulated as off-stream waterbody which does not have inflow or outflow. Lakes are simulated as reservoirs and are considered well-mixed in the SWAT model. The hydrologic areas which need modeling attention include complex watersheds, often containing one or more reservoir or ponds. Lakes are stratified where lake depth becomes larger in comparison to its surface area. This assumption of the lake being well-mixed can produce an error in SWAT modeling if the lake is large or has significant inflow or outflow. Hence, the SWAT model should be coupled with a lake model that can successfully simulate water quality parameters for a lake regardless of its stratification status. MINLAKE is the perfect option for this coupling. MINLAKE is a one-dimensional model that is simple and reliable at the same time. Two options can be proposed based on the location of the lake in a watershed: the lake outflow can be used as inflow for SWAT or SWAT outflow can be used as inflow for the lake.

The first step towards this coupling is to upgrade the existing MINLAKE model to include phytoplankton (presented using Chl*a*) and nutrients (phosphorus and/or nitrogen)

simulation. Then, the inflow and outflow should be added to the MINLAKE model to make it capable of coupling with SWAT. The coupled model is supposed to be more accurate as it considers the stratification and detailed ecological process of the lakes. This will be particularly beneficial for large lakes which covers a significant portion of the watershed.

1.5 Scope and Objectives

HABs, hypoxia, fishkill, etc. are results of eutrophication – a process that occurs because of the availability of excessive nutrients and results in increased algae growth. Excess algae as mentioned earlier lead eutrophication and undesirable changes in aquatic resources such as reduced water clarity, hypoxia, harmful algal blooms, fish kills, loss of biodiversity, and increases in nuisance species (Wolfe and Patz, 2002; Townsend et al., 2003). Eutrophication also has a detrimental effect on human health through increased exposure to cyanobacteria toxins (Hudnell, 2010; Hudnell and Dortch, 2008), nitrites, and nitrates (Wolfe and Patz, 2002; Townsend et al., 2003). Furthermore, the economic costs of eutrophication, for restoring the ecosystem services (e.g., housing amenity value, recreation opportunities, freshwater provisioning, and food and fiber production) are high (Moomaw and Birch, 2005; Pretty et al., 2003; Dodds et al., 2009).

The main effects of lake eutrophication are an increase in phytoplankton biomass (dominated by cyanobacteria), a decrease in water transparency, and a clear difference between surface layers and the deoxygenated hypolimnion (Dodds, 2006; Wetzel, 2001). However, the deoxygenated hypolimnion aids the sediment to release an internal phosphorus load, which in turn amplifies the eutrophication of the system (Dodds, 2006). Since most of the cities use surface water as a drinking water source, HABs cause serious problems of off-flavor

odor and taste (sometimes described as earthy or musty). In some cases, the drinking water no longer remains safe to drink and a complete cleanup is needed. For example, the state of Ohio committed to spending $172 million to clean up Lake Erie as HABs were causing severe drinking water problems. During the spring and summer of 2019, some residents of Auburn city reported off-flavor taste and odor in their drinking water. The reason behind this off-flavors was the seasonal algal bloom in Saugahatchee lake which is used as a drinking water source by Opelika Utility.

Though off-flavor producers are attributed to photoautotrophic cyanobacteria and filamentous heterotrophic bacteria, the most frequent source of off-flavor production is now generally attributed to cyanobacterial metabolism and degradation (Tabachek and Yurkowski, 1976; Durrer et al., 1999). Nutrient enrichment, eventually a large population of cyanobacteria in a drinking water supply reservoir causes 2-Methylisoborneol and geosmin production which causes off-flavor taste and smell in drinking water (Olsen et al., 2017). Extensive research has been performed on the occurrence of cyanotoxins but predicting these compounds remains challenging, especially in large, dynamic waterbodies (Watson et al., 2008; Graham et al., 2010).

Despite the number of research works conducted during the last five decades around the globe, eutrophication remains a major concern worldwide (Smith et al., 2006). More than 40% of lakes are eutrophic and affected by algal blooms, which poses a great concern for the nearby community (Bartram et al., 1999). Interactions between nutrients, principally phosphorus which is generally the main cause of lake eutrophication and the ecological functioning, need to be addressed. During the last two decades, new manifestations of eutrophication have emerged (Anderson et al., 2012; Le Moal et al., 2018; Pomati et al., 2017).

The management and restoration solutions to control eutrophication need a detailed overview of the lake's nutrient concentration must be supported by scientific outcomes. Since the 1970s, numerical modeling has been considered to be an effective tool to quantify nutrient concentration (Imboden, 1974; Vollenweider, 1975; Vollenweider and Kerekes, 1982). Many models were developed, to be used for lake management and restoration purposes. The key state variables of those models are those that link primary production to nutrients, principally phosphorus, nitrogen, and sometimes silica (De Senerpont Domis et al., 2014; Reynolds et al., 2001).

Excess nutrients have been reported as the primary cause of lake water quality impairments in the United States Environmental Protection Agency (USEPA) reports to congress for consecutive 8 years (USEPA1994, USEPA 1996, USEPA 1998, USEPA 2000, USEPA 2002). Given the importance of nutrient pollution, the USEPA 1998 requires states to adopt water quality standards with specific numeric nutrient criteria and less than half of the fifty states have complied (USEPA 2009). However, the development of nutrient criteria for lakes requires access to reliable information on nitrogen and phosphorus concentrations at the statewide level (USEPA 1998; Reckhow et al. 2005).

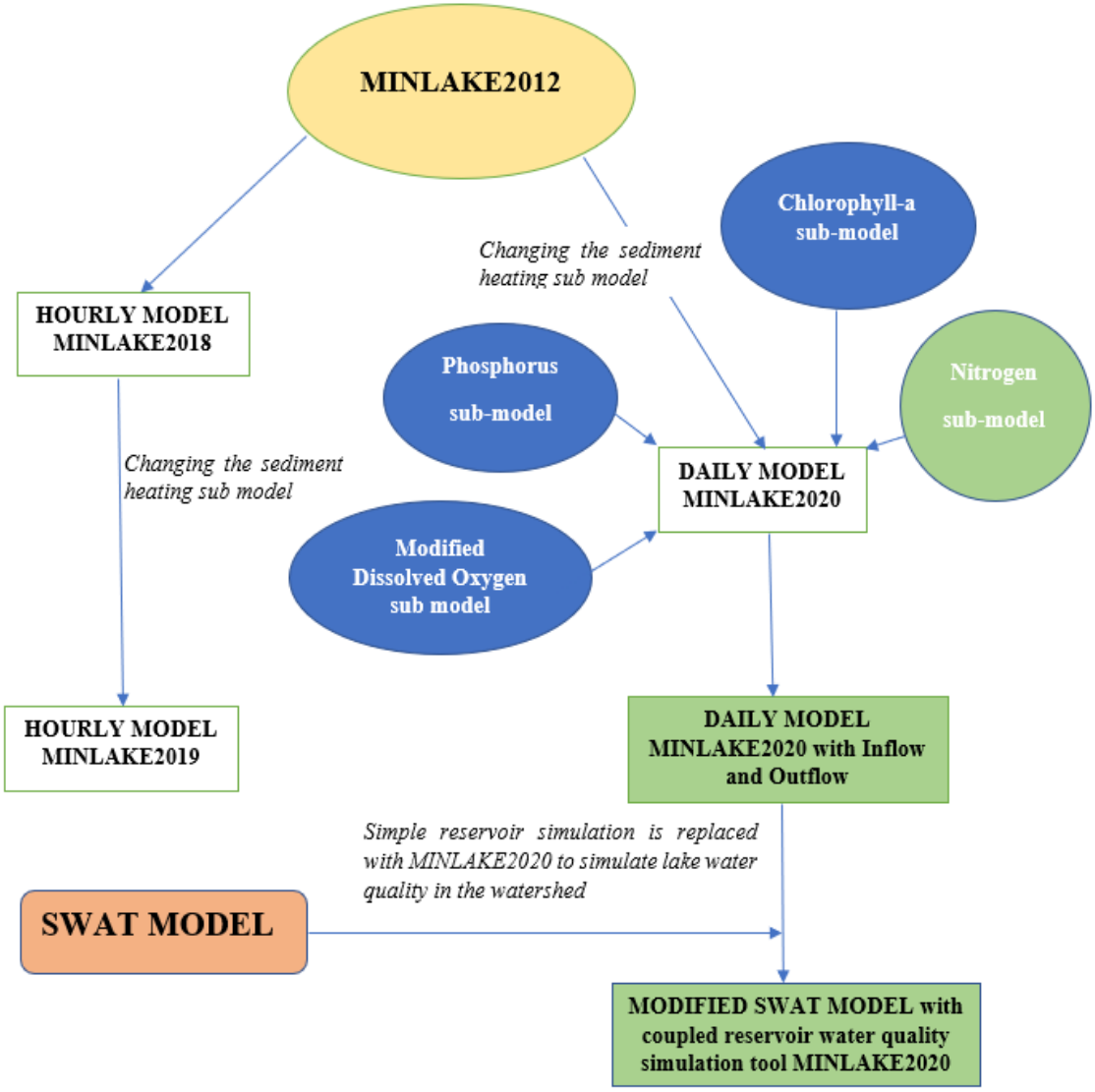

Figure 1.4 Proposed modifications of MINLAKE model

The long-term objective of this study is to merge the SWAT model with MINLAKE model. In this thesis, the development of a lake model with no inflow/outflow, MINLAKE2020 was developed. This model needs further modification to calculate the effect of inflow/outflow. Then this model can be coupled with the SWAT model to simulate for

watersheds. Following is a diagram showing the long-term objective of the MINLAKE2020 model.

Several lake water quality models have been developed over the past two decades, but each model has some limitations such as modeling for a certain type of waterbody or certain nutrients. Here, we have tried to introduce a reliable water quality simulation tool, MINLAKE2020, based on the lake water quality model MINLAKE2012. The model is capable of simulating the temperature, Chlorophyll a (Chl*a*), Phosphorus, Biochemical Oxygen Demand (BOD), DO for all types of lakes accurately. In this study, only Phosphorus is considered (among the nutrients), as it is known to be the primary nutrient controlling the trophic state of lakes in the Upper Midwest and Canada (Dillon and Rigler 1974; Vollenweider 1968). The nitrogen nutrient model was developed and coded in MINLAKE2020 but has not been tested against field data.

The objectives of this study are set as:

1. Change the MINLAKE2012 model to include subroutines for Chl*a*, Phosphorus, Nitrogen, and BOD simulation
2. To include a different subroutine for DO simulation which will take into account the Chl*a* and nutrient concentration
3. To include the direct solar heating concept of sediment in the model, changing the sediment subroutine
4. To calibrate the model MINLAKE2020 using observed data of the study lake
5. To apply the model to different lakes of varying depths to validate its suitability

It is worth mentioning that this study is based on the previous studies and efforts made to simulate water quality parameters in lakes. The base for this study is the MINLAKE2012, a one-dimensional deterministic year-round lake water quality model for small lakes (< 10 km^2) in the USA. The main concept and calibration parameters for Lake Elmo and Lake Riley were taken from an older version of MINLAKE, MINLAKE98 (West and Stefan, 1998).

1.6 Thesis Organization

This thesis includes five chapters. Chapter 1 includes background, the introduction of water quality models, and the objectives of this study. Chapter 2 includes the model description and model operating process. Chapter 3 includes a description of model calibration and a description of the study lakes. In Chapter 4, the simulation results for the study lakes are presented. Chapter 5 includes the summary and future scope of this work.

Chapter 2 MODEL DEVELOPMENT

2.1 Comprehensive Review of MINLAKE 2012

MINLAKE2012 model is comprised of two separate mathematical models for daily water quality simulation: a water temperature model and a DO model. In this model, the water temperature model is solved first, since most of the water quality parameters are temperature dependent. The DO model uses the simulated water temperature for calculating saturated DO and other temperature correction terms.

2.1.1 Water Temperature Model

Water temperature simulation is the basis of all other water quality parameters. The temperature of a waterbody is affected by the ambient weather conditions and the temperature of inflow. In in-land lakes that do not receive a significant inflow, weather conditions like solar radiation, sky condition, wind speed, wind directions, air temperature, and precipitation affect the change in water temperature. However, in cold regions such as Minnesota, the thickness of the ice layer and the snow depth impact solar radiation penetration into the lake water during the winter. As a result, the thermal condition of the lake water during the winter in cold regions is affected by the ice layer and snow layer on the surface of the lake. The lake is divided into horizontal layers of varying thickness, and one-dimensional, unsteady heat transfer equation (2.1) is solved for each layer to simulate the vertical water temperature profiles along with the depth in lakes.

$$\frac{\partial T_w}{\partial t} = \frac{1}{A}\frac{\partial}{\partial z}\left(K_z A \frac{\partial T_w}{\partial z}\right) + \frac{H_w}{\rho C_p} \tag{2.1}$$

Here, water temperature (oC) is expressed as $T_w(z, t)$, which is a function of depth (z) and time (t). A(z) (m^2) is the horizontal area of each water layer that is a function of the depth (based on lake bathymetry). H_w (J/m^3-day) is the total amount of heat absorbed by source and sink terms per unit volume of water. K_z (m^2/day) is the vertical turbulent heat diffusion coefficient, and ρC_p (J/m^3 - ^oC) represents the heat capacity of water per unit volume.

Equation 2.1 was solved numerically using an implicit finite difference scheme and a Gaussian elimination method with time steps of one day. MINLAKE2012 model represents the lake and its environment in the open-water and winter ice-covered seasons. Furthermore, the effects of heat transfer through lake sediment, the ice cover, and the snow cover are also included in the model by separate sub-models. MINLAKE's water temperature and lake environment during the open-water season and ice cover period is shown in the schematic diagram (Figure 2.1).

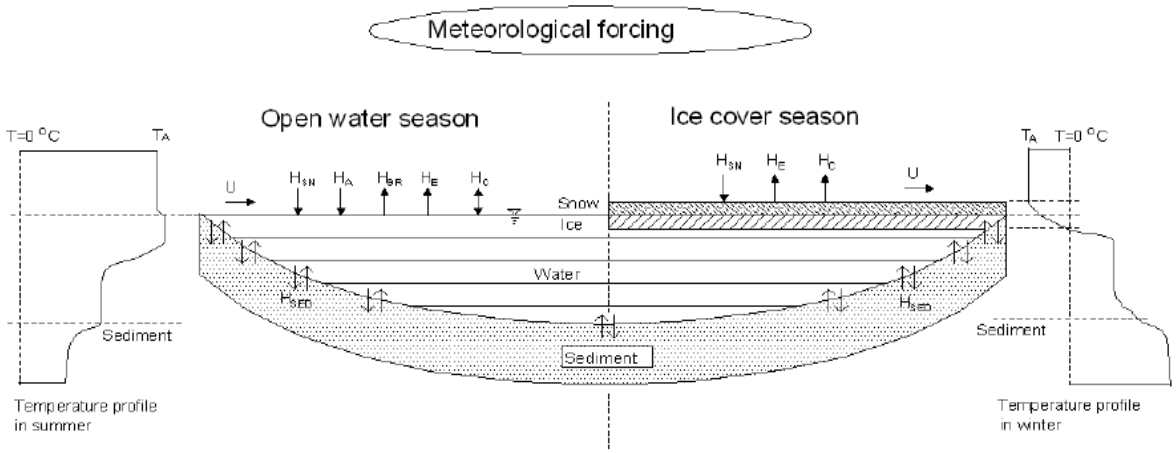

Figure 2.1 Schematic of a stratified lake showing water temperature profiles in the open water season and ice-cover period. It also shows the sediment layers below the lake including heat transfer components and sediment temperature profiles (Fang and Stefan 1998).

A heat balance equation was developed for modeling the heat budget at the water surface (Chapra 2008). The source terms for water temperature simulation are shortwave solar radiation (H_{SN}) and atmospheric longwave radiation (H_A) whereas the sink terms are water longwave radiation (H_{BR}), conduction (H_C), and evaporation (H_E). The surface heat exchange through the water surface during the open water season is given by the following equation:

$$\Delta H = H_{SN} + H_A - (H_{BR} + H_C + H_E) \quad (2.2)$$

Evaporation can be positive (condensation) or negative. The heat flux entering the water body and leaving the water body is constantly changing due to the changing characteristics of the various climate variables.

The snow and ice thickness sub-models originally developed by Gu and Stefan (1990) were modified by Fang and Stefan (1996) and integrated with the MINLAKE model to account for snow and ice thickness. In many lake water temperature models, modelers have ignored the heat flux transfer between the lake water and sediment. Fang and Stefan (1996) found that the heat fluxes between lake water and sediment can be substantial for lake water temperature simulations. From field measurements and MINLAKE model results, it was found that shallow lakes can become 1–2^{o}C warmer under a thick winter ice/snow cover without significant radiation penetration through the winter covered surface or significant flow into and out of a lake (Fang and Stefan 1996a). In such cases, the source of this heat is the underlying sediment. Similarly, heat transfer between water and sediment in the littoral region of a lake also causes dampening of the temperature fluctuations during the open water season (Fang and Stefan 1996a). To account for the water-sediment heat exchange, a separate sub-model was developed which calculates the temperature profiles in the sediment below the water-sediment interface (Fang and Stefan 1996a). The sediment

subroutine can calculate heat transfer by lake sediment during both the open water season and the ice-covered period. However, sediment heat fluxes play an important role in shallow lakes, especially during the ice-cover period.

In shallow lakes and littoral zones of deeper lakes, the solar radiation can penetrate all water layers and directly heat the sediment. This direct warming of lake sediment due to solar radiation has not been considered in MINLAKE2012. In MINLAKE2020, the sediment subroutine was modified to successfully represent the direct heating of lake sediment (explained later in section 2.3).

During the winter ice-cover period, the model simulates ice and snow thickness, and sediment temperature profiles first. Then the model determines the heat source/sink terms and solves the heat transfer equation in Equation (2.1). At the air-snow interface or air-ice interface, when snow is absent, the net heat flux from the atmosphere into or out of the snow/ice cover is calculated (Fang et al. 2010a). Contributions of heat flux are made by solar radiation (H_{SN}), evaporation (H_E), and convection (H_C) during the winter as shown in Figure 2.1. In MINLAKE2012, snow thickness is calculated from snow accumulation (precipitation), followed by compaction and snow melting. This model simulates the melting of snow by surface heat input (convection, rainfall, and solar radiation), melting within the snow layer due to internal absorption of shortwave solar radiation, and the transformation of wetted snow to ice (Fang et al. 2010a).

2.1.2 Dissolved Oxygen Model

The regional dissolved oxygen (DO) model (Fang 1994) was first integrated with the year-round water temperature model in MINLAKE96. Later on, the model was modified, and the final

version is integrated with MINLAKE2012. The model solves the vertical unsteady mass transport equation (2.3) to estimate the vertical profiles of DO in a lake daily over many years. MINLAKE2012 solves the one-dimensional mass transfer equation (2.3) to simulate the DO profiles in lakes

$$\frac{\partial C}{\partial t} = \frac{1}{A}\frac{\partial}{\partial z}\left(K_z A \frac{\partial C}{\partial z}\right) + S \tag{2.3}$$

Here, C(z, t) is the DO concentration (mg/L) which is a function of depth (z) and time (t), K_z (m^2/day) is the vertical turbulent mass diffusion coefficient, which is similar to the one used for temperature calculation, And S(z, t) represents the total of all the source and sink terms of DO (mg/L-day).

The main sources of dissolved oxygen in a lake with no considerable inflow and outflow (considered in MINLAKE2012) are the surface reaeration and the oxygen production due to photosynthesis while the main sinks of the DO are respiration process in the water body, sediment oxygen demand, biochemical oxygen demand, and plant respiration processes. Therefore, the source and sink terms are described in detail.

$$S = P - R - S_{SOD} - S_{BOD} + F_s \tag{2.4}$$

Here P(z, t) represents the amount of oxygen produced through photosynthesis every day, F_s is surface reaeration, R(z, t) is the amount of oxygen used by the plants and aquatic animals due to respiration, S_{BOD}(z, t) is the biochemical oxygen demand (BOD), which includes Carbonaceous and Nitrogenous oxygen demand and other oxidation processes; and S_{SOD}(z, t) is the sediment oxygen demand through chemical and/or biological reactions. A schematic diagram of DO source and sink terms in three representing layers is shown in Figure 2.2.

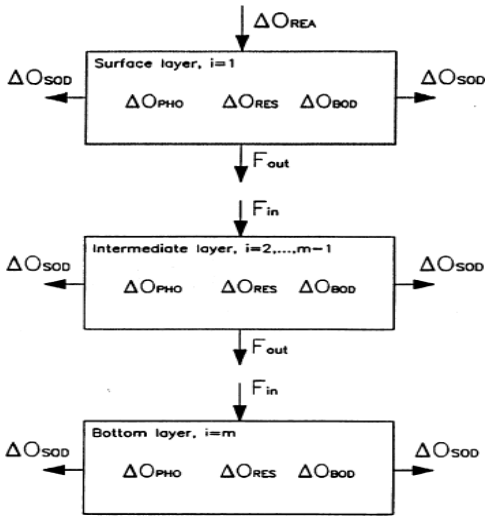

Figure 2.2 Source and sink terms of DO in a lake (Fang, 1994)

Several modifications were applied to the regional DO model to account for the presence of ice and snow cover in simulating the DO in a lake over the winter season. These modifications include: (a) surface oxygen transfer reaeration is set to zero, (b) respiration rate coefficient is set to zero, (c) water column oxygen demand, by detrital and other organic matter, is set constant (0.01 g O_2 m^{-3} day^{-1}) (d) sedimentary oxygen demand (S_b) is made dependent on trophic state and is set equal to 0.226, 0.152, and 0.075 (g O_2 m^{-2} day^{-1}) for eutrophic, mesotrophic, and oligotrophic lakes, respectively (Fang and Stefan 1994)

2.1.3 Diffusion Coefficient

The determination of the turbulent diffusion coefficient has been discussed by Fang (1994). In MINLAKE, the mixed depth is calculated in a separate subroutine after which the stratification starts. In the mixed layer, the water temperature gradient is usually zero or near zero. In the

regional daily water temperature MINLAKE model, the vertical heat diffusion coefficient K_z for epilimnion and hypolimnion is calculated using the following formula:

$$K_z = 8.17 \times 10^{-4} \times \frac{As^{0.56}}{(N^2)^{0.43}} \quad (2.5)$$

Here, K_z is the vertical diffusion coefficient in cm^2/sec (1 cm^2/sec = 8.64 m^2/day = 0.36 m^2/hr), A_s is the surface area of the lake (km^2), N^2 is the Brunt-Vaisala stability frequency of the stratification (sec^{-2}). The value of N^2 is a small constant value (N^2 = 0.000075) that leads to the largest diffusion coefficient in epilimnion whereas the value of Brunt Vaisala stability frequency is related to the water density in each layer in layers below the mixed layer. The equation for calculating Brunt Vaisala frequency is given below:

$$N^2 = -\frac{g\, d\rho}{\rho\, dz} \quad (2.6)$$

Here, ρ(z, t) is the density of water as a function of water temperature which varies with depth and time (day), g is the acceleration of gravity, and dρ/dz is the density gradient between water layers. In MINLAKE2012, N^2 is determined by using the already known water temperature profile calculated in the previous time step (Fang and Stefan 1994b).

2.2 Development of MINLAKE2020

MINLAKE2020 model was developed using MINLAKE2012 as a model base. MINLAKE2012 has a water temperature model and regional DO model. The temperature model was not modified except for small modifications in the sediment temperature model. Regional DO model was developed based on two assumptions:

- The Chlorophyll-a concentration varies in a seasonal pattern, i.e., variations from annual mean Chl*a* concentration, which can be estimated from observed data

- The BOD concentration is constant with time and throughout all depths (BOD is not functional when DO becomes zero)

Though the model was used successfully to predict DO concentration in past and future climate scenarios, the model could not provide useful details on some water quality parameters. Moreover, the generalized assumption based on inadequate field data could be a possible source of error. Nutrients (Phosphorus, Nitrogen, Silica) affect the Chlorophyll-a concentration in a lake and so, the nutrient simulation is very important for predicting lake water quality. The Fortran code of MINLAKE2012 was modified to include subroutines for Chl*a* representing phytoplankton, P, N, and BOD simulation. In MINLAKE2020, water temperature is simulated first, then Chl*a*, P, N, and BOD are simulated in chronological order daily. After that, DO is simulated since it depends on the aforementioned parameters. The modifications applied to the MINLAKE2012 is presented in this section. A diagram of the processes affecting lake water quality is present in Figure 2.3. A detailed description of modifications applied to the MINLAKE model is given below.

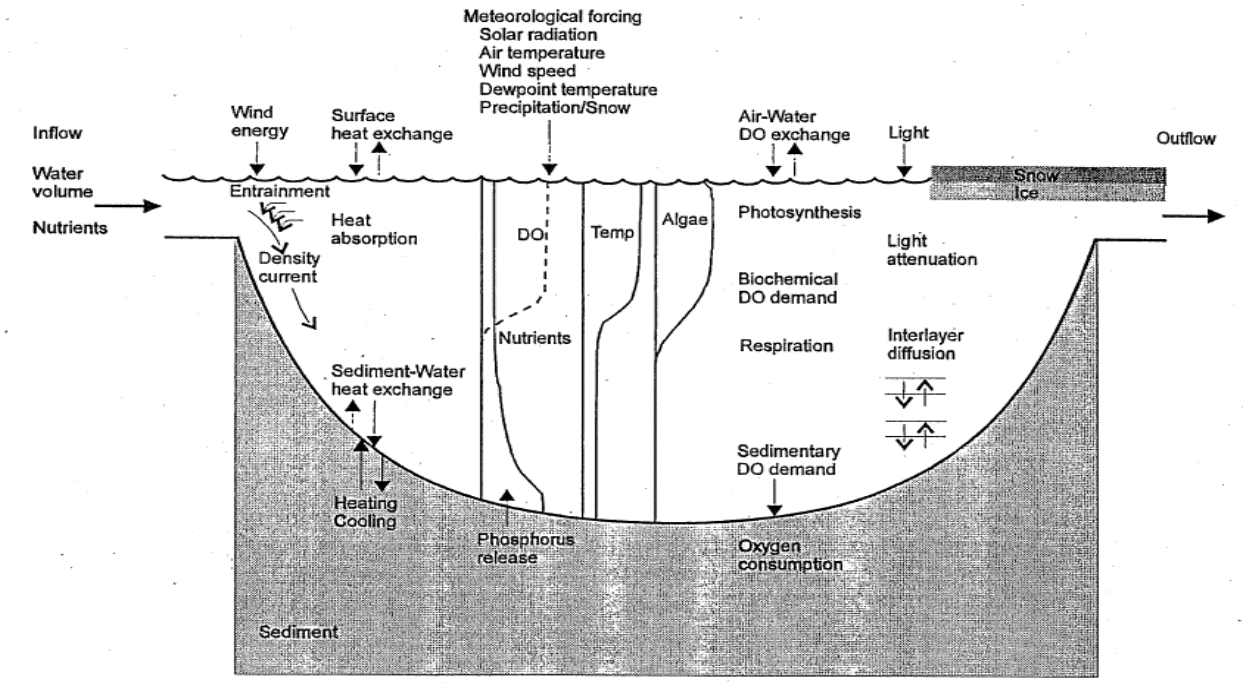

Figure 2.3 Schematic representation of processes in MINLAKE2020 (adopted from West and Stefan, 1998)

2.2.1 Chlorophyll-a Simulation

In MINLAKE2012, a seasonal pattern was used to predict daily chlorophyll-a concentration from the observed data. In MINLAKE2020, a separate subroutine was developed and added to simulate daily Chlorophyll-a for each water layer. Chlorophyll-a is considered as an indicator of primary productivity in MINLAKE2020. The model can simulate up to three algal groups (diatoms, green algae, and blue-green algae). Different coefficients and rates are used to represent a specific group. Some algal groups have a specific affinity towards some nutrients. Minlake2020 took into account the nature of the algal group and simulated accordingly.

A schematic diagram of the phytoplankton cycle applicable to all algal groups is presented in Figure 2.4. Phytoplankton growth is simulated by external nutrient limitation using a Michaelis

Menten growth function. Light and phosphorus limitations are simulated and tested in six lakes in this study. Nitrogen limitation for green algae as well as silica limitation for diatoms was implemented in MINLAKE2020 but not tested for this study. Phytoplankton respiration and mortality have different parameters and rates in MINLAKE2020. However, respiration removes chlorophyll-a and releases a proportional amount of nutrients directly to the water column. Mortality contributes to the detrital mass (BOD) but does not release nutrients to the water. The diffusion rate is calculated while simulating temperature and the same rate is used for Chlorophyll-a. Zooplankton grazing is an important sink term as it is the result of the mobility of zooplankton. Another sink term, settling removes chlorophyll from a layer and adds to the next layer or the sediment.

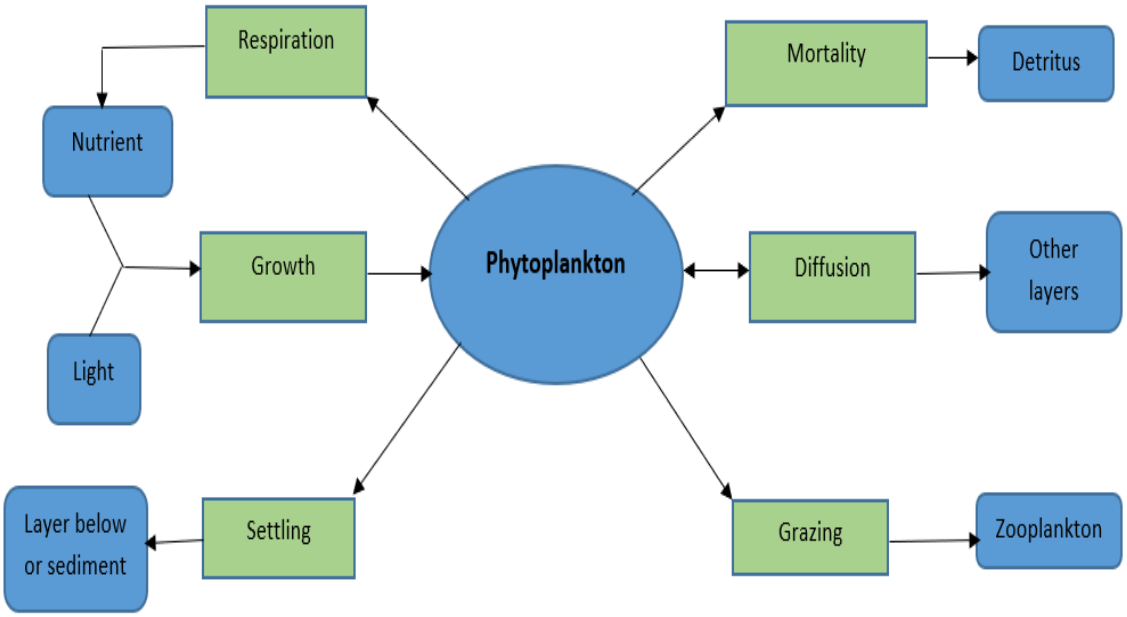

Figure 2.4 Schematic diagram of chlorophyll-a cycle

The differential equation representing Chlorophyll-a in the one-dimensional model is given as Equation 2.7. Chlorophyll-a is lost by nonpredatory mortality, zooplankton grazing, and

respiration. These parameters are introduced as first-order sink terms in the equation whereas phytoplankton growth is calculated as a zero-order source term.

$$\frac{\partial \mathrm{Chla}}{\partial t} - \frac{1}{A}\frac{\partial}{\partial z}\left(AK_z \frac{\partial \mathrm{Chla}}{\partial z}\right) + \frac{V}{A}\frac{\partial(A\mathrm{Chla})}{\partial z} + K_m \theta_m^{T-20}\mathrm{Chla} + K_r \theta_r^{T-20}\mathrm{Chla}$$

$$+ Gr_{max}\frac{\mathrm{Chla} - \mathrm{Chla}_{min}}{\mathrm{Chla} - \mathrm{Chla}_{min} + HSC}\theta_z^{T-20} ZP\ \Delta t\ V_r\ CF$$

$$- G_{max}\, f(T)\left[\frac{I(1+2\sqrt{\frac{K_1}{K_2}})}{I+K_1+\frac{I^2}{K_2}} : \frac{P}{K_P+P} : \frac{N}{K_N+N} : \frac{Si}{K_{Si}+Si}\right]_{min} \mathrm{Chla} = 0 \qquad (2.7)$$

where

Chl*a* = chlorophyll-a concentration (mg/L)

A = Area (m^2)

K_z = eddy diffusivity (m^2/day)

V = settling velocity (m/day)

K_m, K_r = mortality and respiration rate (/day)

Θ = temperature adjustment coefficient

T = temperature (^oC)

G_{max} = maximum growth rate (/day)

f(T) = temperature function for growth

Gr_{max} = maximum grazing rate (mg Chl*a* per individual zooplankton per day)

Chla_{min} = minimum chlorophyll concentration for grazing to occur (mg/L)

HSC = half-saturation constant for grazing (mg/L)

I = intensity of photosynthetically active radiation ($\mu E.m^{-2}hr^{-1}$)

K_1, K_2=light limitation and inhibition coefficients, respectively($\mu E.m^{-2}hr^{-1}$)

K_P, K_N, K_{Si} = half saturation constant for phosphorus, nitrogen, and silica, respectively (mg/L)

P, N, Si = available concentration of phosphorus, nitrogen, and silica, respectively (mg/L)

ZP = zooplankton concentration or density, i.e., number of zooplankton per volume ($\#/m^3$)

Δt = time zooplankton spent in layer i to graze (day).

V_r = volume day depth/layer ratio

CF = unit conversion from L to m^3 (0.001).

2.2.1.1 Phytoplankton Growth

Phytoplankton growth depends on six factors: (1) the maximum growth rate of the algae, (2) the nutrient half-saturation coefficient, (3) the water temperature, (4) the solar irradiance, (5) the external nutrient concentration, and (6) the current chlorophyll concentration.

The maximum growth rate of algae varies for different classes of algae. Maximum growth rates vary upon a wide range, minimum being 0.2/day, and maximum being 11/day (EPA, 1985). In MINLAKE2020, the broad classification of algae (green algae, blue-green algae) is used. The maximum growth rate is a calibration parameter. For each class of algae, the growth rate should be in the range suggested by Table 2.3. Within this range, different values are calibrated so that the simulated results are matched reasonably well with the chlorophyll-a field data.

Another important parameter that affects the growth of phytoplankton is water temperature. MINLAKE2020 uses a function provided by Lehman(1975) where the maximum yield occurs at an optimal temperature, $T_{opt;}$ the growth rate coefficient decreases both above and below this temperature. The minimum temperature (T_{min}) is the low temperature at which phytoplankton growth is reduced by 90 percent. T_{min} can be any number. For some species, the minimum temperature is greater than zero. Also, at the maximum temperature (T_{max}), the growth is reduced by 90 percent. T_{min}, T_{opt}, T_{max} are input parameters that give flexibility in simulating temperature limitation for Chlorophyll-a growth. The equations used to simulate the temperature correction on Chlorophyll-a growth is given below:

$$f(T) = \exp\left(-2.3\left(\frac{T-T_{opt}}{T_{opt}-T_{min}}\right)^2\right) \qquad \text{for } T < T_{opt} \tag{2.8a}$$

$$f(T) = \exp\left(-2.3\left(\frac{T-T_{opt}}{T_{max}-T_{opt}}\right)^2\right) \qquad \text{for } T > T_{opt} \tag{2.8b}$$

Table 2.1 summarizes a suitable range of optimum, maximum, and minimum temperatures for algae growth of three phytoplankton groups.

Table 2.1 Optimum, minimum, and maximum temperature values for phytoplankton. (U.S. Army Corps of Engineers, 1982)

Algal Type	Optimum Temperature (^oC)	Maximum Temperature (^oC)	Minimum Temperature (^oC)
Total Phytoplankton	10–40	15–42	0–18
Green	20–40	40–42	0–7
Blue-green	20–29	-	4
Diatoms	20–33	30–36	0–12

Phytoplankton growth is usually limited by either light or phosphorus (which has the lowest limitation factor). When nitrogen and silica are also modeled the lowest growth-limiting factor of light, phosphorus, nitrogen, and silica (diatoms only) is used to calculate the phytoplankton growth. Since Carbon is considered to be in excess, the limitation for carbon is not calculated.

The light limitation is very important for algal growth simulation. Sometimes in eutrophic lakes, the light becomes the limiting constituent as the algae beneath the surface layer do not get enough sunlight for photosynthesis. A Haldane equation (Megard et al., 1984) is used in MINLAKE2020 to calculate the light limitation for algal growth, which was used in the regional DO model also.

$$f(I) = \frac{I(1+2\sqrt{\frac{K_1}{K_2}})}{I+K_1+\frac{I^2}{K_2}} \quad (2.9a)$$

$$I = \frac{27.25}{TD} * RAD \quad (2.9b)$$

Here, f(I) is the light limitation coefficient (dimensionless), I is the photosynthetically active radiation (PAR), TD is photoperiod (hr), RAD is solar radiation, K_1 and K_2 are the light limitation and inhibition coefficients, respectively. All the units for input variables are in μEinstein/m^2/sec. In MINLAKE88 and MINLAKE98, light limitation and inhibition coefficients were specified by the user. Fang used temperature-dependent empirical equations to calculate light limitation and inhibition coefficients in the regional DO model (Fang et al., 1996). These equations worked well in all the upgraded versions of MINLAKE96 (including MINLAKE 2012). In MINLAKE2020, light limitation and inhibition coefficients are calculated using the same equations as in MINLAKE2012. The light limitation coefficient is specified as a temperature-dependent relationship fitted to experimental data (Megard et al., 1984).

$$K_1 = \frac{0.687}{0.0036} * 1.086^{T-20} \quad (2.10)$$

$$K_2 = \frac{10}{0.0036}$$

Here, K_1 and K_2 have units of μEinstein/m^2/sec (0.0036 is a unit conversion from Einstein/m^2/hr). In MINLAKE2020, it is assumed that the nutrient composition of the algal cells is constant. Moreover, the growth of the algae is assumed to be a function of the external nutrient concentration using a Michaelis-Menten relationship. The growth-limiting factor for Phosphorus, Nitrogen, and Silica is calculated using Equation 2.11.

$$f(S) = \frac{S}{K_S+S} \quad (2.11)$$

Here, f(S) is the Michaelis-Menten growth-limiting factor (dimensionless), S is the concentration of the nutrient (P, N, or Si) in water (mg/L) and K_S is the half-saturation constant for the nutrient (mg/L).

Both the concentration of the nutrient and the half-saturation constant for each nutrient are very important in calculating the limiting factor. Each species of phytoplankton has a different half-saturation constant for a given nutrient. Most of the half-saturation values for phosphorus are between 0.001 mg/L and 0.02 mg/L (EPA,1985). Most of the half-saturation values for nitrogen are between 0.03 mg/L and 0.1 mg/L (EPA,1985). The half-saturation values for silica are between 0.03 mg/Land 0.1 mg/L (EPA,1985). However, silica limitation is calculated for diatoms only.

In all lake simulations, the maximum growth rate, nutrient half-saturation constants are calibration parameters. It is important to note that the parameter values should stay in the range listed in Table 2.2.

Table 2.2 Phytoplankton maximum growth rates and Half-Saturation constants for phosphorus, nitrogen, and silica. (EPA, 1985)

Algal Type	Maximum Growth Rate (1/d)	Half Saturation Constant for P (mg/L)	Half Saturation Constant for N (mg/L)	Half Saturation Constant for Si (mg/L)
Total Phytoplankton	0.2–8.0	0.0005–0.08	0.0014–0.4	-
Green	0.7–9.2	0.002–0.475	0.001–1.236	-
Blue-green	0.2–11.0	0.0025–0.06	0.0–4.34	-
Diatoms	0.55–5.0 ·	0.001–0.163	0.003–0.923	0.03–0.1

Values are from experimental measurements reported in the literature and from documented models.

2.2.1.2 Mortality

The mortality of Phytoplankton is simulated as a temperature-dependent phenomenon. In MINLAKE1988, the mortality of phytoplankton was integrated with the respiration rate. It was later identified that mortality and respiration affect the model in a similar way but in different time frames. Respiration affects the available phosphorus and dissolved oxygen immediately whereas mortality contributes with a time lag through detrital decay. There was not enough data on the mortality rates.

2.2.1.3 Respiration

Respiration rate does not vary as greatly as settling rates. Most respiration rates are between 0.02/d and 0.05/d. Table 2.3 summarizes the suggested range of settling velocity, respiration rate, mortality rate, and zooplankton grazing rate for three algal groups.

Table 2.3 Phytoplankton settling velocities, respiration rates, non-predatory mortality rates, and zooplankton grazing rates. (EPA, 1985)

Algal Type	Settling Velocity (1/d)	Respiration Rate (1/d)	Non-Predatory Mortality Rate (1/d)	Zooplankton Grazing Rate (mg Chl*a*/day)
Total Phytoplankton	0.0–30.0	0.005–0.8	0.003–0.17	
Green	0.02–0.89	0.01–0.46	-	0.0015
Blue-green	0.0–0.2	0.03–0.92	-	0
Diatoms	0.02–17.1	0.03–0.59	0.03	

Values are from experimental measurements reported in the literature and from the documented model.

2.2.1.4 Zooplankton Grazing

Zooplankton grazing is simulated only to represent the dynamics of algae. Zooplankton grazing rate varies with different classes of algae. For example, zooplankton is more likely to feed on green algae than blue-green algae. In MINLAKE2020, a single class of zooplankton is simulated. To simulate the chlorophyll-a lost by grazing of zooplankton, the zooplankton population (ZP(t), #/m^3) should be simulated in each day. In MINLAKE2020, a separate subroutine is included for zooplankton simulation. Grazing by zooplankton is assumed to take place in the evening when zooplankton rises to the upper layers. Grazing within a layer depends on the temperature and Chlorophyll-a concentration. A Michaelis-Menten ratio is used to express the effect of Chlorophyll-a concentration on grazing. It is assumed that no grazing occurs below a threshold Chlorophyll-a concentration (Chl$a_{\min}$ in Equation 2.7). Grazing in a layer $\mathrm{GRAZE(k, I)}$ is proportional to the Chlorophyll-a concentration in the layer compared to the total Chlorophyll-a concentration from the day depth to the surface.

$$\mathrm{GRAZE(k, I)} \propto \Delta t(I) = (1 - \frac{TD}{24})(\frac{\sum_{k=1}^{3} \mathrm{Chla(k,I)}}{\sum_{I=1}^{IZ}\sum_{k=1}^{3} \mathrm{Chla(k,I)}}) \quad (2.12)$$

Here, Δt(I) is the time increment for layer I (day), TD is the photoperiod (hr) from sunrise to sunset, Chl*a*(k, I) is the Chlorophyll-a concentration of phytoplankton group k in layer I, and IZ is the day-depth layer, where DO ≥ 0.5 mg/L.

Zooplankton grazing of phytoplankton (Chl*a*) occurs during the nocturnal migration at the day depth. The nocturnal grazing rate is calculated for each layer (I = 1, IZ) between the day depth and the surface using the volume day depth/layer ratio Vr = V(IZ)/V(I).

2.2.1.5 Advection

Settling velocity of algae is a very important and sensitive parameter of MINLAKE2020 model. The settling velocity of each algal class is set and calibrated by the user. There is a wide range of values for each of the algae classes. In general, the blue-green algae are lighter and exhibit the lowest rates and the diatoms are heavier and have the highest rates. MINLAKE2020 does not simulate the ability of some phytoplankton to float due to buoyancy but this can be accounted for by adjusting the settling rate. The model could predict very large or unreasonable Chlorophyll-a concentrations if the settling velocity is set to be too small.

2.2.2 Zooplankton Simulation

MINLAKE2020 includes a zooplankton model to be able to correctly simulate (1) Chl*a* lost by zooplankton grazing and (2) DO consumed by zooplankton respiration. A single class of zooplankton is simulated in the lake environment. To simulate the chlorophyll-a lost by grazing of zooplankton, the zooplankton population should be simulated in each day. Zooplankton simulation is different than that of other parameters because of the complex nature of the zooplankton movement. During the day, zooplankton retreats to deeper water seeking refuge from visual predators. They begin to rise to the surface at dusk while grazing and return to deeper layers at dawn. Zooplankton activity of these two periods is treated separately in the model.

The zooplankton is assumed to have a constant reproduction rate and time-varying predation rate for determining the zooplankton population ZP(t). The reproduction rate is constant as the Chlorophyll-a concentration cannot significantly affect the reproduction rate. The day depth, light level at the day depth, and predation on zooplankton are calculated as the first step in zooplankton simulation. The day depth of zooplankton is identified as the deepest layer in which

dissolved oxygen concentration is greater than 0.5 mg/L and therefore changes with time depending on DO vertical distribution along with the depth. Predation on zooplankton is assumed to be a function of light availability at the day depth (Wright et al., 1980). In MINLAKE2020, dual effects of seasonal predation and light limitation are included to simulate biomanipulation techniques related to methods of increasing the zooplankton population (Shapiro et al., 1982). The dominant zooplankton predators are assumed to visual predators and the zooplankton predation only occurs in the daytime. The light limitation assumes a linear variation of predation between two light levels (Wright et al., 1980).

$$P_d' = P_d \frac{XI - XI_{min}}{XI_{max} - XI_{min}} \tag{2.13}$$

$$0 \leq \frac{XI - XI_{min}}{XI_{max} - XI_{min}} \leq 1$$

Here, P_d' is the predation rate (day^{-1}), P_d is the daily predation rate (day^{-1}) calculated in Equation 2.14. XI is the light intensity at the day depth ($\mu E/m^2/s$), XI_{min} is the light intensity at which no predation occurs ($\mu E/m^2/s$) and XI_{max} is light intensity above which predation is not light inhibited ($\mu E/m^2/s$).

Both daytime and nocturnal predation are calculated in MINLAKE2020. The daytime predation combines light limitation on with a time-varying maximum predation rate. A linear function is used to calculate the time-varying predation rate given in the equation.

$$P_d = P_{min} + (P_{max} - P_{min})\left(\frac{DY - D_{min}}{D_{max} - D_{min}}\right) \tag{2.14}$$

$$0 < \frac{DY - D_{min}}{D_{max} - D_{min}} < 1$$

Here, P_d is the daytime predation rate (day^{-1}). P_{min} and P_{max} are minimum and maximum predation rates (day^{-1}), respectively. DY is Julian day, D_{min} is Julian day of last day of minimum predation

rate and D_{max} is Julian day of the beginning of maximum predation rate. For example, for Elmo Lake, West and Stefan (1998) set P_{min}, P_{max}, D_{min}, as D_{max} as 0.05 day^{-1}, 0.7 day^{-1}, 140, and 180; it means P_{min} occur on May 19th and P_{max} occur on June 28th.

Zooplankton density in the daytime is determined using Equation (2.15) including reproduction and daytime predation.

$$ZP(t) = ZP(t-1) - P'_d(ZP - ZP_{min})\frac{TD}{24} + ZP(t-1) * Repro \quad (2.15)$$

Here, Repro is the reproduction rate (day^{-1} population in the day depth layer in the previous day) and ZP(t-1) is the zooplankton density in the previous day.

Nocturnal predation occurs during the nocturnal migration at the day depth. The nocturnal predation rate is calculated for each layer between the day depth and the surface.

$$P(I) = P_n\left(ZP\frac{V(IZ)}{V(I)} - ZP_{min}\right)\Delta t(I) \quad (2.16)$$

Here, P(I) is the nocturnal predation rate in layer I during migration (#/m^3) and P_n is the nocturnal predation rate (/day). ZP is the zooplankton population in the day depth layer calculated using Equation (2.15) and ZP_{min} is the minimum concentration of zooplankton for predation to occur (#/m^3). V(IZ) and V(I) are the volumes of the day depth layer and layer I (m^3), respectively. $\Delta t(I)$ is the time that zooplankton spent in layer I during the night (day). ZP(t) minus P(I) will finally give the zooplankton population for the next day.

The second part of zooplankton simulation is the simulation of grazing by zooplankton which begins with a vertical rise in the evening. Temperature and Chlorophyll-a concentration affects grazing in the water layer. A Michaelis-Menten ratio is used to express the effect of Chlorophyll-a concentration on grazing with a refugium effect for no grazing below a threshold

Chlorophyll-a concentration. Grazing by zooplankton is described in detail in section 2.2.1.4 using Equations (2.7) and (2.12).

2.2.3 Phosphorus Simulation

Figure 2.5 gives a schematic diagram of the mas balance (source and sink terms) for phosphorus simulation simulated in MINLAKE2020. In most of the cases, phosphorus is known to be the primary nutrient controlling the trophic state of lakes in the Upper Midwest USA and Canada (Dillon and Rigler 1974; Vollenweider 1968). The model simulates only the readily accessible phosphate composed of orthophosphate and polyphosphate ions referred to as soluble reactive phosphorus (SRP). Therefore, the model does not consider/simulate the settling for SRP even normally phosphorus could attach with sediment and settle downward. Phytoplankton growth removes SRP from the water. Respiration releases phosphorus into the water column. Mortality does not directly release phosphorus to the water column but contributes to the detrital mass (BOD); the phosphorus is released from the detrital mass through decay. Though diffusion of phosphorus occurs between layers, phosphorus is also transported indirectly between layers by phytoplankton and detritus settling.

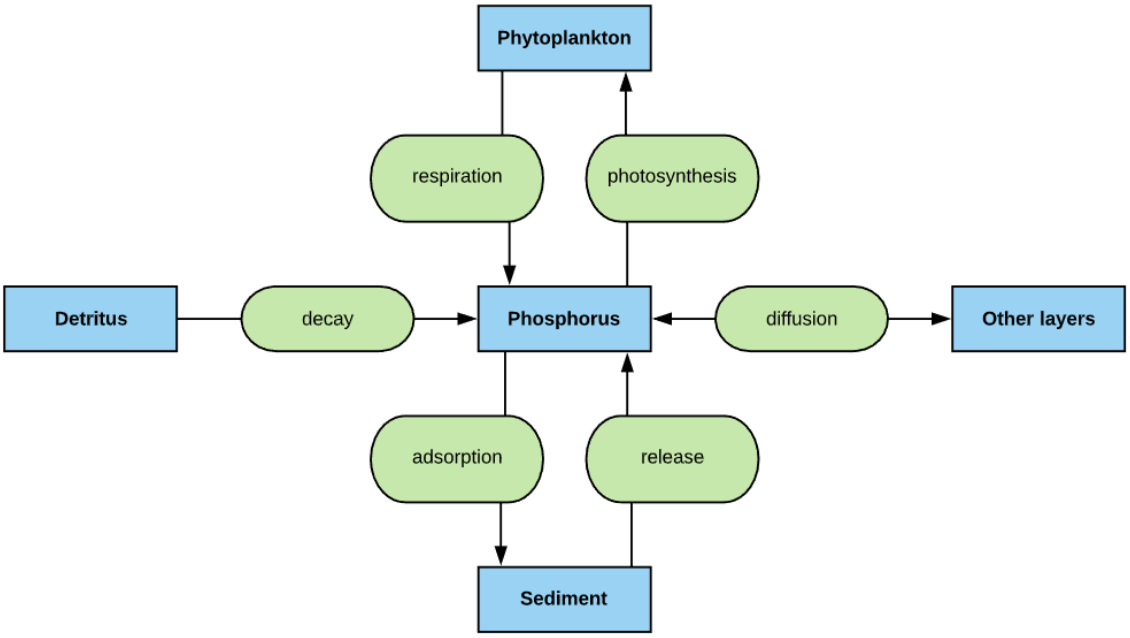

Figure 2.5 Schematic diagram of phosphorus source and sink terms

The differential equation representing phosphorus transport is presented as Equation 2.15. The uptake of SRP due to phytoplankton (Chlorophyll -a) growth is calculated as a zero-order sink term using the mass yield ratio of phosphorus to chlorophyll (Y_{PChla}). Phosphorus concentration at the previous time step (day) was used for the Michaelis-Menten relationship. Phosphorus releases due to detrital decay and respiration (for each algal group) are also considered to be zero-order source terms. The release of phosphorus from the lake sediment is calculated as a zero-order source/sink term depending on the dissolved oxygen concentration in the overlying water.

$$\frac{\partial P}{\partial t} - \frac{1}{A}\frac{\partial}{\partial z}\left(AK_z\frac{\partial P}{\partial z}\right) + Y_{PChla}\sum_{n=1}^{3} G_{max} f(T)\left[\frac{I(1+2\sqrt{\frac{K_1}{K_2}})}{I + K_1 + \frac{I^2}{K_2}} : \frac{P}{K_P + P} : \frac{N}{K_N + N} : \frac{Si}{K_{Si} + Si}\right]_{min} Chla$$

$$-Y_{PBOD}K_{BOD}\theta_{BOD}^{T-20}BOD \pm \frac{S_P}{A}\frac{\partial A}{\partial z} - Y_{PChla}\sum_{n=1}^{3} K_{rn}\theta_{rn}^{T-20}Chla = 0 \qquad (2.15)$$

P = available phosphorus concentration (mg/l)

A = Area (m^2)

K_z = eddy diffusivity (m/day)

KBOD, K_{rn} = decay and respiration rate (/day)

θ=temperature adjustment coefficient

T = temperature (oC)

G_{max} = maximum growth rate (/day)

f(T) = temperature function for growth

S_P = rate of phosphorus released at the water-sediment interface ($g/m^2/d$)

Chl*a* = chlorophyll-a concentration (mg/l)

Y_{PChla} = mass yield ratio of phosphorus to chlorophyll

I = intensity of photosynthetically active radiation ($\mu E.m^{-2}hr^{-1}$)

K_1, K_2=light limitation and inhibition coefficients respectively($\mu E.m^{-2}hr^{-1}$)

K_P, K_N, K_{Si} = half saturation constant for phosphorus, nitrogen and silica, respectively (mg/L)

P, N, Si = available concentration of phosphorus, nitrogen and silica, respectively (mg/L)

Y_{PBOD} = mass yield ratio of phosphorus to BOD

2.2.3.1 Phytoplankton Growth to Remove Phosphorus

The phosphorus, accumulated from the inflow, detrital biomass, sediment release, and respiration, is used by the phytoplankton, in the presence of sunlight, for growth. Algae need both nitrogen and phosphorus for growth. However, phosphorus is particularly important for algal growth as it is usually in short supply compared to other nutrients. If it is assumed that nitrogen is in abundant supply, phosphorus becomes the only limiting nutrient for algal growth (green and blue-green alga), which is being modeled in the application of MINLAKE2020 in

this study. The only sink term in phosphorus simulation shown in Equation 2.15 is the uptake by algae. This uptake depends on the maximum growth rate, light limitation, nutrient limitation, chlorophyll-a concentration at that time, and the yield ratio of P to Chl*a*.

A phosphorus/chlorophyll a yield coefficient (Y_{PChla}) is used to determine the amount of phosphorus consumed during photosynthesis as well as the amount of phosphorus released during algal respiration. In MINLAKE98, the value of Y_{PChla} was derived from the mass yield coefficient of phosphorus to BOD divided by the mass yield coefficient of chlorophyll to BOD. This value is 1.1 mg P/mg Chl*a* for Y_{PChla}, which was assumed to be constant in MINLAKE1998, which is close to that presented by Thomann and Mueller (1987) of 1.0 µg P/µg Chl*a*. However, the phytoplankton biomass does not depend on phosphorus solely, it also depends on the nitrogen concentration. Hessen et al. (2006) did a study of 400, mostly oligotrophic, lakes to assess the yield ratio of phosphorus to Chlorophyll-a and the yield ratio of zooplankton to phytoplankton. It was found that higher phytoplankton yield per unit total P should be expected in lowland lakes which are rich in Calcium and Nitrogen. So, using a fixed value for Y_{PChla} (which is derived from a mathematical equation) might cause unsatisfactory results. In MINLAKE2020, Y_{PChla} is used as a calibration parameter, since the yield coefficient of P to Chl*a* can change according to a lot of factors.

There are three source terms for Phosphorus: detrital decay (death of phytoplankton), sediment release, and phytoplankton respiration. Here, a constant phosphorus release rate is used for phosphorus simulation. Two alternatives were tied depending on the dissolved oxygen concentration. This phosphate flux rate must be calibrated to the hypolimnetic phosphorus profile under anoxic conditions.

2.2.3.2 Detrital decay

Phosphorus is released into the water through detrital decay. This term is related to biochemical oxygen demand (BOD). The equation for the detrital decay is given below:

$$\text{P from decayed biomass} = Y_{PBOD} K_{BOD} \theta_{BOD}^{T-20} BOD \quad (2.16)$$

The mass yield ratio of Phosphorus to BOD is used to convert the BOD concentration to released P concentration. Since detrital decay is dependent on the temperature, a temperature correction term is also introduced. In MINLAKE2020, a separate subroutine is introduced for BOD calculation.

2.2.3.3 Respiration

Respiration is a very important biological process in the lake ecosystem. Respiration rate depends on the algal class. The class-dependent respiration rates are given in Table 2.3. The aquatic plants use oxygen and release carbon dioxide and energy. This energy is quantified by the algal biomass, Chl*a*; the phosphorus is returned to the water as a ratio of Y_{PChla}. The equation used for respiration is given below.

$$\text{P from Respiration} = Y_{PChla} \sum_{n=1}^{3} K_{rn} \theta_{rn}^{T-20} Chla \quad (2.17)$$

2.2.3.4 Sediment Release

An important source of phosphorus is the release from sediment. For many lakes which have a history of progressive eutrophication, the lake sediments have now become the primary source of phosphorus to the water. If the sediment-water interface is anoxic, phosphate ions

go to the water at an increased rate, dependent upon the concentration difference between porewaters and the overlying water (Home and Goldman, 1994). In MINLAKE2020, the soluble reactive phosphorus SRP was released back to water when the dissolved oxygen becomes zero.

However, the sediment release rate, the mass yield ratio of phosphorus to Chl*a*, and the maximum growth rate are sensitive input parameters. In MINLAKE2020, these are used as calibration parameters. If any of the parameter values is too high, the simulation will result in excessive chlorophyll-a, which will cause the simulation to break.

2.2.4 BOD Simulation

The biochemical oxygen demand (BOD) is an important parameter in dissolved oxygen, phosphorus, and nitrogen cycles. The microbial decay or decomposition of organic matter consumes oxygen so that the amount of organic matter is represented as BOD, an oxygen equivalent. However, dissolved oxygen directly affects biological decay processes and phosphorus release under anoxic conditions. In the regional DO model (Fang 1994), a constant rate for BOD was used for each simulation lake but varies with lake trophic state. But BOD is an important parameter for nutrient cycles and DO cycle and is affected by mortality, organic decay, diffusion, and advection. A schematic diagram is presented below to better understand the BOD cycle.

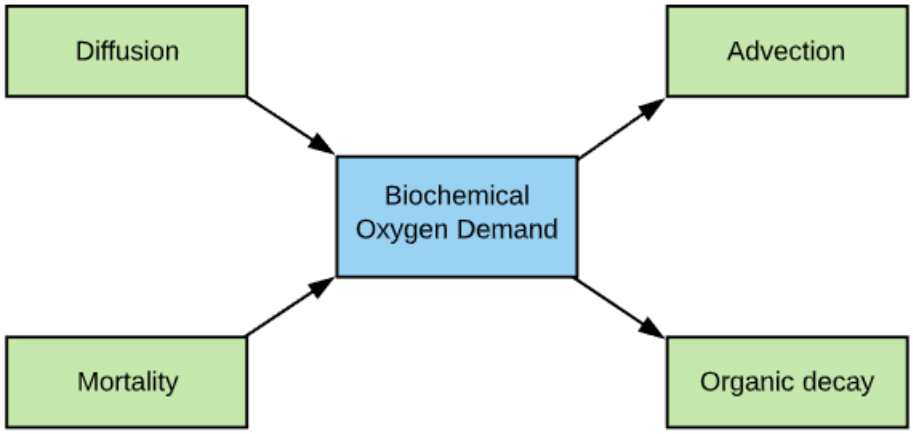

Figure 2.6 Schematic diagram of BOD source and sink terms

In the model, BOD is increased from two sources. First, detritus travels to adjacent layers via diffusion. Secondly, the mortality of the phytoplankton adds to the detritus concentration. BOD has two sink terms: advection (in the vertical direction) and organic decay. Detritus has a fall velocity. Detritus falls from the concerning layers and goes to another layer or the sediment. Organic decay is a natural biochemical process. The microorganisms cause the decay of the organic matter and add up to the nutrients. This cycle is very important for nutrient calculation as it directly adds to the nutrient through detrital decay.

The microbial decay of organic matter follows the same pattern as nitrification. It is a function of the detrital mass expressed in oxygen equivalents. The mortality of cells and a fraction of the grazed phytoplankton are converted from chlorophyll-a concentrations to oxygen equivalents using the constant carbon/chlorophyll-a ratio and stoichiometric relationships. The result is a one-to-one correspondence between detrital decay and the utilization of oxygen. The following equation represents the mechanism behind BOD calculation in MINLAKE2020.

$$\frac{\partial BOD}{\partial t} - \frac{1}{A}\frac{\partial}{\partial z}\left(AK_z\frac{BOD}{z}\right) + \frac{V}{A}\frac{\partial A\, BOD}{\partial z} - \frac{1}{Y_{CHBOD}}\sum_{n=1}^{3} K_m\theta_m^{T-20}Chla + K_{BOD}\theta_{BOD}^{T-20}BOD = 0 \quad (2.18)$$

BOD = available biochemical oxygen demand (mg/l)

A = Area (m^2)

K_z = eddy diffusivity (m/day)

K_m = mortality rate coefficient (/day)

K_{BOD} = organic decomposition rate (/day)

θ = temperature adjustment coefficient

T = temperature (^oC)

V= Fall velocity of detritus (m/day)

Y_{CHBOD} = mass yield ratio of chlorophyll-a to BOD

Chl*a* = available chlorophyll-a concentration (mg/L)

2.2.5 DO Simulation

Dissolved oxygen or DO is one of the vital parameters of lake water quality simulation. Aquatic organisms and fish depend on the availability of DO in the waterbody (ref.). A schematic diagram of the processes contributing to the dissolved oxygen concentration is given in Figure 2.7. Phytoplankton (Chlorophyll-a) can add dissolved oxygen to the water layer through photosynthesis to the point where water is supersaturated with DO. These dynamic processes can happen in time scales of less than one day (the timestep of the simulation). Therefore, the simulated DO profiles are an average over the day. Dissolved oxygen removal from the water layer through respiration is simulated to occur at a constant rate throughout the day while photosynthesis occurs only during the hours with solar radiation. The sediment oxygen demand is proportional to the sediment surface area in contact with the water layer (applicable to all layers). Calibration of the sediment oxygen demand is very important for simulating DO in the hypolimnion. The diffusion of dissolved oxygen occurs between the water layers in the hypolimnion. Even though the zooplankton migrates during the simulated day to graze on phytoplankton, zooplankton respiration is simulated at the day depth only. The zooplankton usually spends the largest amount of their time in the day depth

layer. Biochemical oxygen demand (BOD) removes oxygen from the water layer through the decay of detritus. Nitrification removes oxygen from the water layer through the conversion of organic nitrogen to inorganic nitrogen. Nitrification is applied to the DO model only if nitrogen is simulated.

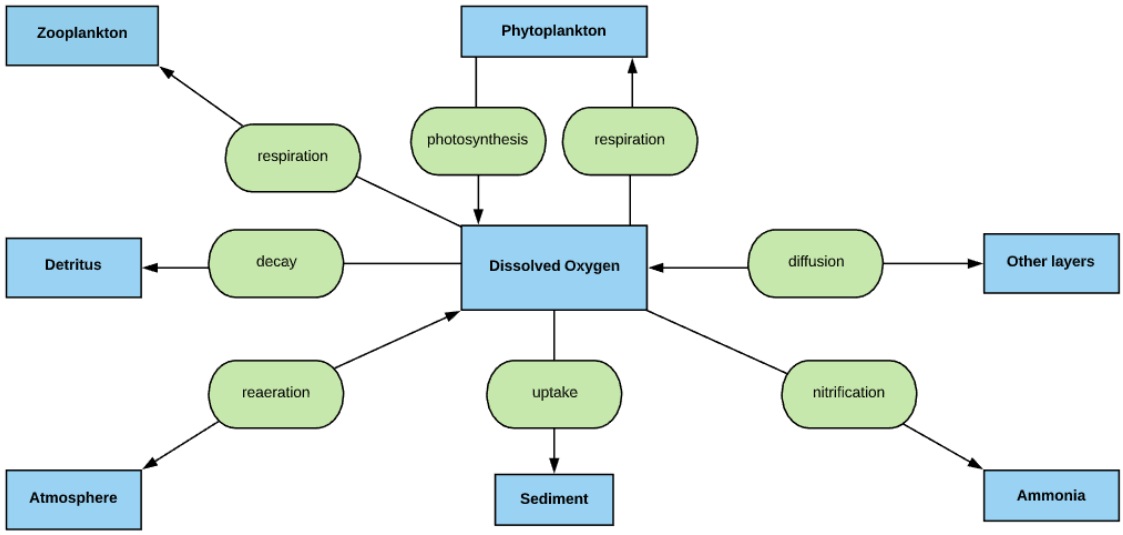

Figure 2.7 Schematic diagram of DO source and sink terms

A differential equation (2.19) is used to simulate DO concentration layer by layer. The equation incorporates all the source and sink terms.

$$\frac{\partial DO}{\partial t} - \frac{1}{A}\frac{\partial}{\partial z}\left(AK_z\frac{\partial DO}{\partial z}\right) + \frac{1}{Y_{CHO_2}}\sum_{n=1}^{3}\{K_{rn}\theta_{rn}^{T-20} -$$

$$G_{max}f(T)\left[\frac{I(1+2\sqrt{\frac{K_1}{K_2}})}{I+K_1+\frac{I^2}{K_2}} : \frac{P}{K_P+P} : \frac{N}{K_N+N} : \frac{Si}{K_{Si}+Si}\right]_{min}\}Chla + K_{BOD}\theta_{BOD}^{T-20}BOD + \frac{S_b}{A}\frac{\partial A}{\partial z}\theta_{SOD}^{T-20} +$$

$$\frac{1}{Y_{NHO2}}K_{NH}\theta_{NH}^{T-20}NH - k(DO_{sat} - DO)_{surface} + \frac{TD}{24}K_{zr}\theta_{zr}^{T-20}ZP\frac{0.001}{V_{iz}} = 0 \qquad (2.19)$$

where

DO = available dissolved oxygen concentration (mg/l)	I = intensity of photosynthetically active radiation ($\mu E.m^{-2}hr^{-1}$)
A = Area (m^2)	K_1, K_2=light limitation and inhibition coefficients respectively($\mu E.m^{-2}hr^{-1}$)
K_z = eddy diffusivity (m/day)	K_P, K_N, K_{Si} = half saturation constant for phosphorus, nitrogen and silica, respectively (mg/L)
K_{BOD}, K_{rn} = decay and respiration rate (/day)	P, N, Si = available concentration of phosphorus, nitrogen, and silica, respectively (mg/L)
Kzr = Zooplankton respiration rate	DO_{sat} = Saturated DO concentration (mg/L)
θ=temperature adjustment coefficient	YCHO2= Mass ratio of Chlorophyll-a to Oxygen
T = temperature (^oC)	YNHO2= Mass ratio of Ammonium to Oxygen
G_{max} = maximum growth rate (/day)	K_{NH}= Nitrification rate (/day)
f(T) = temperature function for growth	
Chla = chlorophyll-a concentration (mg/l)	
S_b = Sedimentary Oxygen Demand coefficient at 20^oC (/day)	
TD = Photoperiod (hr)	

Reaeration at the surface layer is calculated as a first-order source/sink term. Respiration, photosynthesis, zooplankton respiration, sediment oxygen demand (SOD), BOD, and nitrification are calculated as zero-order (with regard to oxygen) source/sink terms. The diffusion of dissolved oxygen between layers is calculated in a process similar to heat. However, the maximum epilimnetic diffusion coefficient used for mass diffusion is different from that used for heat diffusion and is a function of the wind speed (Walters, 1978). The hypolimnetic diffusion coefficient is calculated as a function of the density and the surface area of the lake.

2.2.5.1 Oxygen Production by Photosynthesis

MINLAKE2020 simulates both chlorophyll-a and nutrients. The light intensity is used to calculate the light limitation component of the photosynthetic growth of phytoplankton. DO production in the photosynthesis is calculated from the biomass (Chlorophyll-a) production using a ratio of mg chlorophyll/mg oxygen (Y_{CHO2}) released. The calculation of light limitation and nutrient limitation is described in detail in section 2.2.1.

2.2.5.2 Oxygen Consumption by Respiration

Respiration rates K_{rn} depend on the algal classes and are simulated separately for each of them. Respiration used for DO includes a ratio of mg Chlorophyll-a/mg oxygen (Y_{CHO2}). The respiration rates are dependent upon temperature. Respiration rates are presented in Section 2.2.1 and temperature adjustment coefficients are presented in Table 2.4.

Table 2. 4 Temperature adjustment coefficients for dissolved oxygen sources and sinks

Source or Sink	**Range**	**MINLAKE2020**
Phytoplankton respiration	1.08	1.08
BOD	1.02–1.15	1.047
SOD	1.02–1.13	1.065
Nitrification	1.0548–1.0997	1.08
Zooplankton respiration	-	1.06

Values are from experimental measurements (Thomann and Mueller, 1987 and EPA1985).

MINLAKE2020 following MINLAKE98 uses a stepwise function to reduce the respiration rate (K_{rn}) with decreasing DO concentration. The user-defined rate is reduced to half of its value when DO concentrations fall below 1.0 mg/L and set to zero for DO concentrations less than 0.2 mg/L. In MINLAKE2020, the adjustments for the low DO levels follow Edwards and Owens's (1965) formula. When DO falls below 1 mg/L, the following equation is used for coefficient adjustment for the respiration rate to have a smooth decrease with DO.

$$\text{Adjusted rate} = K_{rn} * DO^{0.45} \quad (2.20)$$

2.2.5.3 Oxygen Consumption by BOD

Biochemical oxygen demand calculates the oxygen consumed by the detrital biomass. This is particularly important in winter when the respiration is considerably low. The BOD decay rate, K_{BOD}, depends on temperature. A range of values is presented in Table 2.5 (EPA. 1985). In MINLAKE2020, BOD decay rate is used as a calibration parameter. In most of the lakes, a rate of 0.05/ day was used. However, the user-defined rate is modified according to Edwards and Owens (1965) formula, the same way presented in Equation (2.20).

Table 2.5 Rate coefficients for DO sources and sinks (EPA,1985)

Source or Sink	Range	MINLAKE2020
BOD	0.02–3.4 /day	0.05 /day
SOD	1.04–1.13 g/m^2/day	0.5–2.0 g/m^2/day
Nitrification	0.10–9.0 /day	0.25 /day
Zooplankton respiration	0.001–0.772 /day	0.002 /day

The widely used temperature adjustment coefficient value of l.047 is used for BOD in MINLAKE 2020. Some researchers have found that this value is valid only when the temperature ranges between 20°C and 30°C and suggest higher values for lower temperatures (Fair et al., 1968). As the BOD concentration in a lake is not measured frequently and simulation can only be grossly calibrated, the temperature adjustment coefficient will be held constant. Moreover, this constant has produced desirable results for many lakes (Fang 1994).

2.2.5.4 Sediment Oxygen Demand

Sedimentary oxygen demand SOD is treated as a sink term for all layers as each layer is in contact with sediments. SOD depends upon temperature. A temperature correction coefficient of 1.065 is used. MINLAKE2020 uses equation (2.20) to adjust the sediment oxygen demand coefficient when DO falls below 1 mg/L. SOD occurs for each layer and it is treated as a sink term in the one-dimensional (vertical) transport equation (Thomann and Mueller 1987; Fang 1994). Oxygen uptake of the sediment depends on the area and composition of bottom materials in contact with the water (Henderson-Sellers 1984; Fang 1994).

Several factors are commonly considered influential for SOD variation in a water body. The most important of them are temperature near the sediment-water interface (Utley et al. 2008), the velocity of the water overlying the sediment (Truax et al. 1995), the organic content of the sediment and the oxygen concentration of the overlying water (Chapra 2008). The sedimentary oxygen demand coefficient S_b is related to the lake maximum depth (Hutchinson 1957) as reported by Fang (1994). In the regional DO model MINLAKE1994, a coefficient EMCOE (2) has been introduced to manipulate the SOD coefficient below the euphotic zone.

2.2.5.5 Nitrification

The consumption of oxygen through nitrification is simulated when nitrogen concentrations are modeled. Nitrification removes oxygen from the water layer through the conversion of organic nitrogen to inorganic nitrogen. A range of values for the nitrification rate, determined by several researchers is presented in Table 2.5 (EPA, 1985). The nitrification rate depends on the DO concentration. In the applications of MINLAKE2020, nitrogen was not simulated and then the nitrification was zero in the DO simulation.

2.2.5.6 Surface Reaeration

Oxygen transfer through the water-atmosphere interface is a major factor in modeling DO. The oxygen mass flux across the air-water interface is assumed to be proportional to the DO deficit in the water body (Rubin 2001).

In the regional DO model, surface oxygen flux at the air-water interface is not treated as a boundary condition but treated as a source term in the surface layer in the DO transport equation (Fang 1994). Reaeration is calculated based on the theory presented by Holley (1977).

$$F_s = K_e(C_s - C_1)A_s \tag{2.21}$$

Here k_e is the bulk surface oxygen transfer velocity (m/day), A_s is the lake surface area (m^2), C_1 (mg/L) is the actual oxygen concentration in the surface layer, C_s is the DO saturation concentration (mg/L) at surface temperature. C_s for freshwater is dependent on temperature and lake elevation and is calculated according to work by the American Public Health Association (Fang 1994).

$$\ln(C_{so}) = -139.34411 + \frac{1.575701*10^5}{T} - \frac{6.642308*10^7}{T^2} + \frac{1.2438*10^{10}}{T^3} - \frac{8.621949*10^{11}}{T^4} \quad (2.22)$$

$$C_s = C_{so} * (1 - 0.000035 * \Delta H) \quad (2.23)$$

Here, T is water temperature and ΔH is the elevation of the lake above sea level (m). The oxygen exchange coefficient can be written as presented below (Fang and Stefan, 1994b).

$$k_e = 0.108 U_{10}^{1.64} \left(\frac{600}{S_{ct}}\right)^{0.5} \quad (2.24)$$

Here U_{10} is the wind speed (m/s) at 10 m above the lake surface, and S_{ct} is the Schmidt number of oxygen at the surface water temperature. The available wind speed used as input in the model is usually measured in weather stations.

The oxygen gas transfer coefficient is affected by surface water temperature and wind speed. To simulate DO in a lake during the winter ice cover period, the modifications were made to account for the presence of ice cover and low temperature (Fang 1994). In that condition, reaeration is set to zero because the lake ice cover prevents any significant gas exchange between the atmosphere and the water body.

2.2.5.7 Zooplankton Respiration

Zooplankton respiration is simulated for the number of hours of daylight at the day depth only in MINLAKE2020. The day depth identifies the layer in which the zooplankton are seeking refuge during the day as they are hiding from the predators. It is assumed that the zooplankton tends to remain in the lowest layer of a lake where there is at least 0.5 mg/L of dissolved oxygen. No zooplankton respiration is simulated during non-daylight hours. It is assumed that while migrating the zooplankton do not remain in one layer for enough time to significantly impact

the dissolved oxygen concentration in the other layer. Zooplankton population in each day is simulated in a separate subroutine (section 2.2.2).

2.3 Sediment Temperature

One of the most important issues in water temperature modeling is sediment heat transfer between water and sediment. Many lake models have ignored the effect of sediment heat transfer while simulating water temperature. However, in mixed shallow lakes, the direction of the heat flux reverses frequently on daily or hourly timescales. Therefore, the sediment heat exchange has been included in the year-round daily water temperature model by Fang and Stefan (1996a) for all layers, from the water surface to the lake bottom. The sediment temperature model simulates the sediment temperature up to 10 m below the sediment/water interface (divided into 10 layers).

$$\frac{\partial T_s}{\partial t} = K_s\left(\frac{\partial^2 T_s}{\partial z^2}\right) \tag{2.25}$$

Where $T_s(z)$ (^oC) is the sediment temperature at depth z in the sediment and K_s (m^2/day) is the sediment thermal diffusivity. The boundary conditions for sediment temperature model is given by the following equations

$$T_s = T_{w(i)} \quad \text{at water-sediment interface} \tag{2.26}$$

$$\frac{\partial T_s}{\partial z} = 0 \quad \text{at 10m below the lake bottom}$$

$T_{w(i)}$ is the simulated water temperature in each water layer (i) at the previous time step. The first boundary condition assures the continuity of temperature at the water-sediment interface. The second boundary condition implies an adiabatic boundary (there is no heat transfer) at 10 m below the sediment surface. Seasonal temperature fluctuations are damped out at this boundary. The initial sediment temperature at the sediment-water interface is set equal to the initial water

temperature at the sediment surface. It, then, increases exponentially with the sediment depth until it reaches nearly a constant value at 10 m below the sediment/water interface. The sediment temperature at 10 m below the sediment-water interface (T_{S10}) is a very important point on this profile (Fang and Stefan 1998).

In shallow lakes, solar radiation is likely to penetrate the whole water depth and directly heat the bottom sediment below the water. In MINLAKE2012 model, the heat absorbed by any water layer was quantified as a subtraction of the heat reached the bottom and top surfaces of the layer as shown in Equation (2.27), and the direct solar heating to sediment was ignored.

To account for the direct solar radiation heating up the sediment in all water layers, the equation to quantify the heat absorbed by a layer of water was modified as

$$HQ(i) = H_{sn(i)}A_{(i+1)}[1 - \exp(-k\Delta z_i)] + \int_0^{A_{(i)}-A_{(i+1)}} H_{sn(i)}[1 - \exp(-kdz)]dA \qquad (2.27)$$

The second part of equation (2.28) more accurately accounts for the absorbed solar radiation by the water in the area of A(i) – A(i+1) since some of the solar radiation heats the bottom sediment, not the water. The lake horizontal area A(i) is not uniform across all water depths due to the slope gradient of the lake bottom, small area dA, and depth dz was introduced for the integration. Equation (2.28) was integrated and further simplified into equation (2.29) by assuming each horizontal area is circular.

$$HQ(i) = H_{sn(i)}A_{(i+1)}[1 - \exp(-k\Delta z_i)] + H_{sn(i)}\left(A_{(i)} - A_{(i+1)}\right) - \frac{2\pi H_{sn(i)}}{k\tan\alpha}\left[\left(r_{(i)} - \frac{1}{k\tan\alpha}\right) - \left(r_{(i+1)} - \frac{1}{k\tan\alpha}\right)\exp(-k\Delta z_i)\right] \qquad (2.28)$$

where $r_{(i)}$ and $r_{(i+1)}$ are radius of the top and bottom surface areas of the water layer i, respectively; and tanα is equal to $[r_{(i)} - r_{(i+1)}]/ \Delta z_i$ and approximates the slope of the lake bottom for the layer i

with respect to the vertical line. The heat reached to the lake sediment can then be calculated using equation (2.29)

$$\mathrm{HQsed(i)} = \frac{2\pi H_{sn(i)}}{k\tan\alpha}\left[\left(r_{(i)} - \frac{1}{k\tan\alpha}\right) - \left(r_{(i+1)} - \frac{1}{k\tan\alpha}\right)\exp(-k\Delta z_i)\right] \quad (2.29)$$

where $\mathrm{HQsed(i)}$ became a heat source term for the first sediment layer to more accurately simulate the sediment temperature profile. These changes subsequently changed the sediment temperature and sediment heat flux of the lake.

2.4 Model Operating Process

MINLAKE is a lake modeling program written in Fortran Language. It is compiled using Visual Studio 2010. After compilation, an executable file is generated. The required files to run the program should be collected in a folder. The name of the folders and files should not contain space. Space in the file or folder name will give an error in the Fortran program. There should be two sub-folders in the common folder - #COMMON and another folder for each specific lake. Inside the #COMMON folder, all the important common files are placed which do not change for each specific lake. The executable file for the MINLAKE model should be placed inside the #COMMON folder. There are two sub-folders – FIXED_INPUT and Weather. MINLAKE2020 model is designed in such a way that the user can choose to run the regional DO (RegDO) model (MINLAKE2012) or the nutrient-Chl*a*-DO (NCDO) model (added in MINLAKE2020) using the same spreadsheet.

The weather folder contains all the weather data for the years that you need to simulate the water temperature and DO. For the weather station closest to the lake, each year a separate file needs to be created. In the FIXED_INPUT folder, several important files do not change for any

specific lake. **Chl_a.dat** is the file that contains the simplified general pattern of chlorophyll-a concentration for the RegDO model, which was developed by Marshall and Peters (1989) and simplified by (Fang 1994). This file is not required to run the NCDO model but is kept in the Fixed Input folder to give users the flexibility to run the RegDO model. **Station.dat file** lists all the weather stations that have been used in the previous studies for model lakes in the USA using MINLAKE and a few lakes in other parts of the world. In this file, the location of the stations (latitude, longitude, and the State in which the station is located) is specified. A numerical ID is assigned for each State in the USA and a specific name is assigned to the weather data files that are gathered from each of these stations. The filename has six letters and two digits. The first two letters refer to the State in which the station is located, the next four letters refer to the name of the station, and the last two digits refer to the year for which the weather data is collected, e.g., MNDULU87.dat has the 1987 daily weather data in Duluth, MN. **Temp_Gwater.dat** contains the annual mean air temperatures and the average air temperatures in January of 1961–1979 for over 209 weather stations in the United States. These are used to calculate the groundwater temperature and the initial sediment temperature at the bottom of the sediment layers in the sediment temperature sub-model. The elevations of weather stations are also added to this file. The information in this file is linked with the weather station through the numerical ID that is assigned for each station. Ts10_profile.dat contains information for setting the initial sediment temperature profiles.

In the folder for each specific lake, four necessary files need to be added to run the model. **Minlake2020_Carrie.xlsm** is an excel file used as a graphical user interface (GUI) for the Fortran code. It is very tedious, tiring, and time-consuming to change a large number of parameters in the main program. Therefore, this GUI helps to input the lake specific parameter data to the model,

including the observed water temperature and DO profiles for model calibration, chlorophyll-a concentrations at each specific time. This Excel file contains several worksheets. The MINLAKE worksheet is the main worksheet of the MINLAKE GUI in which the specific information for each lake and each simulation can be entered. Since lake water quality parameters change significantly during the summer, the typical start date of simulation can be set as April 16th for Minnesota lakes.

The **"Initial Conditions"** worksheet lets the user divide the depth of the lake into many horizontal layers of different depths. The first three layers (< 0.1 m) need to be very thin to simulate the ice formation in winter accurately. The first ten layers are within 1.0 m from the surface water. MINLAKE considers that a lake has a perfect flatwater surface (no waves). The maximum numbers of layers cannot exceed 80 layers in current MINLAKE model. Moreover, the initial values of water temperature, DO, BOD, Chlorophyll-a concentration, and some other parameters are entered in this worksheet. However, the user has the choice to set a uniform profile of these parameters by entering only one value and choosing the uniform profile option when the lake is completely mixed initially. Otherwise, the initial parameter values can be entered for each water depth.

In the "DO Parameters" worksheet, the parameters that are necessary for simulating the DO concentration such as BOD, S_{b20}, respiration rate, maximum oxygen production rate by photosynthesis, etc. can be entered. The user can select in how many depths and at what depths the time series of water temperature and DO to be outputted.

Two new worksheets, 'Fixed Input' and 'WQ Parameter' are added to the MINLAKE excel file for the NCDO model simulation. The parameters in the Fixed Input worksheet were previously written in the Fixed_input.dat file and saved in the 'Fixed_Input' folder for

MINLAKE2012 model. For nutrient simulations, some of the parameters in fixed input could be changed for better model results such as benthic Phosphorus release rate. In the 'WQ Parameters' worksheet, input parameters related to zooplankton, phosphorus, nitrogen, and chlorophyll-a are provided such as the respiration rate, maximum growth rate, mortality lake (for phytoplankton), etc.

In the "Field Data" worksheet, the number of days and years with available observed data are entered. The month and the date on which the field data is available should be entered as a combined number (month×100+date, 807 for August 7). Separate chlorophyll-a concentration for the specified dates can be entered for epilimnion and hypolimnion layers. The observed water temperature and DO profiles should be entered for the specified days for each depth. However, a separate excel file (with Visual Basic for Applications or VBA code) is used to organize the field data in the required format. After organizing, the data can be copied to the 'Field Data' spreadsheet.

In the "Bathymetry" worksheet, the program calculates the cumulative volume, depth increment, and volume increment provided that the depths and the corresponding horizontal areas are entered in the worksheet. The program can generate depth-area and depth-volume graph of the bathymetry.

After organizing and entering the input parameters in the spreadsheets, the model can be run by clicking the "Run Minlake2020" on the 'MINLAKE' spreadsheet. The program reads all the data from the GUI and writes them in two separate files (Lake_Area.sdf and Lake_Input.ini) in the folder specified for the lake. Lake_Area.sdf contains the bathymetry data of the lake and Lake_Input.ini contains all the other information from the excel file that is specific to each lake.

RunMinlake.Bat is a text file that contains information on the desired version of MINLAKE to execute and this file is called by GUI to force the executable file "MINLAKE_.exe" available in the #COMMON folder to run. During the calculation, the name of the lake and the years of simulation are shown on the computer screen.

After running the model, two sub-folders (#ANALYSIS and #OUTPUT) are added to the main folder by the program when the lake is run the first time. The outputted information is stored in separate folders inside the #OUTPUT subfolder. One folder contains all the simulated time series of water temperature and DO year by year while the other contains the water temperature and DO profiles and times series for plots on the GUI. These data can be evaluated visually by loading them on the GUI. After the program stops calculation, the user can click the "Load Output Files" button to load the outputted information into the GUI to visually evaluate the results. The user can assess the statistical error parameters calculated by comparing the simulated data and observed data in the "Sens_Error" worksheet. The "Lake_Error" worksheet shows the maximum and minimum errors for each day that has measured profiles. The worksheets "Tem_Sim_FD and DO_Sim_FD" compare simulated water temperature and DO with the measured water temperature and DO, respectively, as shown in Figure 2.8. The "Tem_Sim_Series", "DO_Sim_Series", "Chl*a*_Sim_Series", "P_Sim_Series", "BOD_Sim_Series" worksheets show the time series of simulated water temperature, DO, Chl*a*, P and BOD compared with the field data at specified depths as shown in Figure 2.9. In MINLAKE2012, only "Tem_Sim_Series and "DO_Sim_Series" worksheets are generated. The measured data are organized and added in the "Mea_Tsrs" worksheet. The winter ice layer thickness, snow depth, and snowfall are represented in the "SnowIce_Sim" worksheet.

In MINLAKE2012, a separate spreadsheet was used to plot the water temperature and DO profiles on the days that have observed data. In addition to that, MINLAKE2020 uses another spreadsheet to plot the profiles of Chlorophyll-a, P, and BOD on the days that have observed data for these parameters.

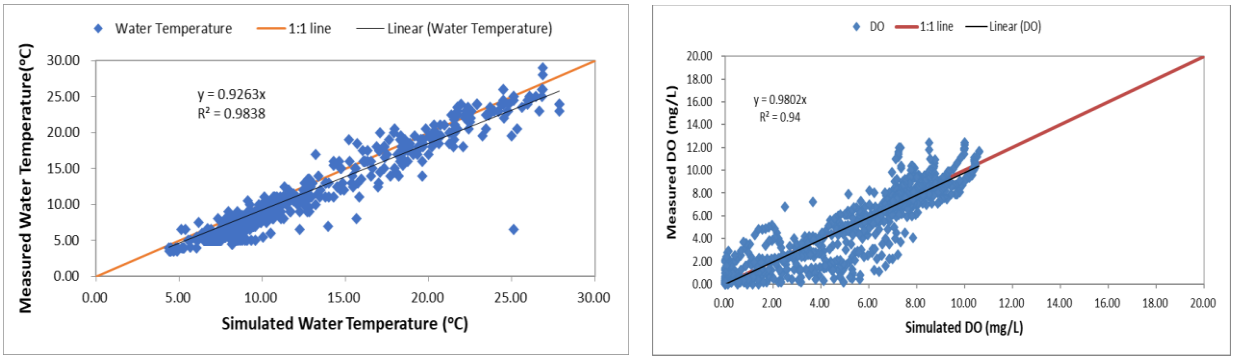

Figure 2.8 Statistical comparison of simulated and observed parameters

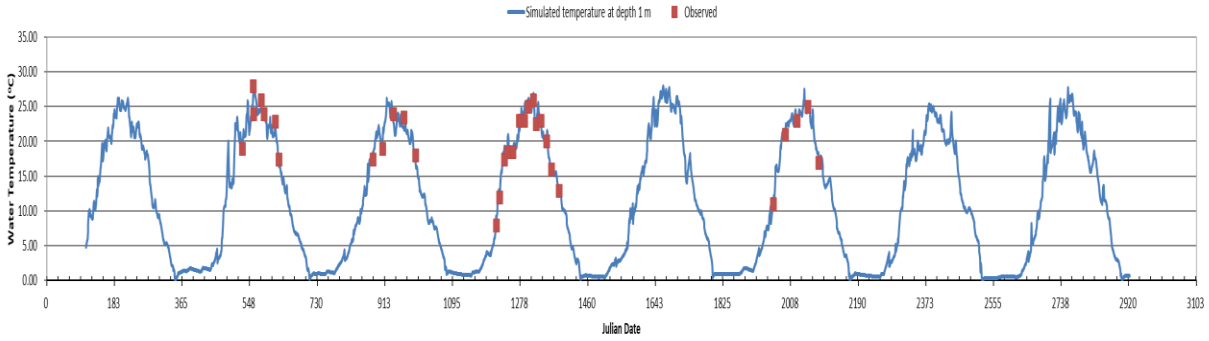

Figure 2.9 Simulated water temperature time series compared with the field data for five years

2.5 Model Input Parameters

Each lake has different characteristics. The variation in lake characteristics is reflected in the model input parameters. Using the user-specified model input parameters, MINLAKE2020 simulates lakes in a daily time step. The lake bathymetry is input data that needs to be supplied to the model. The depth-area curve can be developed from the lake's depth

contour lines by using GIS. The depth contour lines for all lakes in Minnesota were downloaded from the Minnesota Department of Natural Resource (DNR) website.

Weather data file is an important input for the MINLAKE model. MINLAKE calculates water temperature, nutrients, phytoplankton, and DO dynamics in response to the change of weather data. The meteorological data input is organized as daily weather data files, for each station and each year. The weather data include daily air temperature (^{o}F), dew point temperature (^{o}F), wind speed (mph), solar radiation (Langley), sunshine percentage, and precipitation including rainfall (cm) and snowfall (mm).

In MINLAKE2020, the user can choose the model to be run for DO simulation (RegDO or NCDO model). The number of algal classes and light attenuation coefficient are important input parameters for the simulation. Moreover, the snow and ice model require different coefficients as input parameters. Required model input coefficients used in the water temperature model is used in Table 2.6. The inclusion of phytoplankton and zooplankton simulation in MINLAKE calls for many additional input parameters or model coefficients. The maximum growth, respiration rate, mortality rate, benthic phosphorus release rate, etc. are input parameters that can be changed for each lake. These calibration parameters are discussed and tabulated in Section 3.1. The constant input parameters for Phytoplankton, P and DO simulation are given in Table 2.6 and Table 2.7.

Table 2.6 Parameters and coefficient values used in the hydrothermal model (from Stefan et al. 1994).

Coefficients and symbols		**Units**	**Range and references**	**Selected value**
Open water season				
Radiation absorption for water	β_w	-	0.4[a]	0.4
Sediment specific heat	cpsed	kcal kg^{-1} $^oC^{-1}$	0.2 - 0.3[b]	0.28
Sediment thermal conductivity	ksed	kcal day^{-1} $^oC^{-1}$ m^{-1}	8.64 - 51.8[b]	19.25
Radiation attenuation by Chl*a*	μchh	m^2 g^{-1} Chl*a*	0.2 - 31.5[c]	20.0
Radiation attenuation by water	μ_w	m^{-1}	0.33 - 1.03[d]	0.51
Sediment density	ρsed	kg m^{-3}	1650 - 2300[b]	1970
Wind sheltering	W_{str}	-	0.01 - 1.0[e]	varies
Winter ice cover				
Surface reflectivity for ice	α_i	-	0.55[h]	0.55
Surface reflectivity for snow	α_{sw}	-	0.4 - 0.95[l]	0.80
Radiation absorption for ice	β_i	-	0.17 - 0.32[f]	0.17
Radiation absorption for snow	β_{sw}	-	0.17 - 0.34[g]	0.34
Snow compaction	c_{sw}	-	0.125 - 0.5[l]	0.4
Ice thermal conductivity	k_i	kcal day^{-1} $^oC^{-1}$ m^{-1}	45.8[b]	53.6
Snow thermal conductivity	k_{sw}	kcal day^{-1} $^oC^{-1}$ m^{-1}	2.16[b]	5.57
Ice density	ρ_i	kg m^{-3}	920[b]	920.0
Snow density	ρ_{sw}	kg m^{-3}	100 - 400[l]	300.0
Radiation attenuation by ice	μ_i	m^{-1}	1.6 - 7.0[j]	1.6
Radiation attenuation by snow	μ_{sw}	m^{-1}	20 - 40[i]	40.0
Ice latent heat of fusion	λ_i	kcal kg^{-1}	80[k]	80.0
Snow latent heat of fusion	λ_{sw}	kcal kg^{-1}	80[k]	80.0

[a] Dake and Harleman (1969)
[b] Carslaw and Jaeger (1959)
[c] Bannister (1974)
[d] Megard et al. (1979)
[e] Riley and Stefan (1988)
[f] Wake and Rumer (1979)
[g] Scott (1964)
[h] Bolsenga (1977)
[I] Greene (1981)
[j] Pivovarov (1972)
[k] Ashton (1986)
[l] Lock (1990)

Table 2.7 Parameters and coefficient values in the Nutrient model

Coefficients and Symbols		Units	Range and references	Selected value
Respiration rate coefficient	k_r	day^{-1}	0.05-0.5[a]	0.1
BOD temperature adjustment	θ_b	-	1.047[a]	1.047
Photosynthesis temperature adjustment	θ_p	-	1.066[e]	1.036
Respiration temperature adjustment	θ_r	-	1.045[c], 1.047[b]	1.047
Sediment temperature adjustment	θ_s	-	1.034-1.13[f]	1.065
Mass ratio of chlorophyll-a to oxygen	Y_{CHO2}	-	0.0083[d]	0.0083
Mass ratio of phosphorus to oxygen in detritus	Y_{PBOD}		.0091[g]	.0091
Zooplankton respiration rate	XKRZP	day^{-1}	.002[g]	.002
Zooplankton reproduction rate	REPRO	day^{-1}	.02[g]	.02
Minimum light intensity for zooplankton predation	XIMIN	$\mu E(m^2s)^{-1}$	0[g]	0
Light intensity for maximum zooplankton predation	XIMAX	$\mu E(m^2s)^{-1}$	0.1[g]	0.1
Julian day for the end of low predation period	MINDAY		110[g]	110
Julian day for the beginning of maximum predation period	MAXDAY		140[g]	140
Minimum seasonal day time predation rate	PRMIN	day^{-1}	0.05[g]	0.05
Maximum seasonal day time predation rate	PRMAX	day^{-1}	0.7[g]	0.7
Overnight predation rate	PREDMIN	day^{-1}	0.03[g]	0.03

[a] QUAL2E (Brown and Barnwell 1987);
[b] MINLAKE (Riley and Stefan 1988)
[c] EUTR04 (Ambrose et al. 1988)
[d] (Stumm and Morgan. 1981)
[e] (Thomann and Mueller 1987)
[f] (Zison et al. 1978)
[g] (West and Stefan 1998)

Chapter 3 Model Calibration and Description of Study Lakes

3.1 Model Calibration

After developing the NCDO simulation model–MINLAKE2020, the model was tested and used to simulate water quality in six lakes in Minnesota. To get the desired results from the model, the model needs to be calibrated specifically for the selected lake. Six lakes – Carrie Lake, Pearl Lake, Thrush Lake, Riley Lake, Lake Elmo, and Lake Carlos (very deep) were selected for this study. The calibration was performed for water temperature simulation and later for nutrient, Chl*a*, and DO simulations. For classic modeling study, the model is calibrated first using a part of observed data and then the model is validated against the remaining part of observed data for the calibrated parameters. This is a common practice for many hydrologic modeling when long-term time series of streamflow data are available. For these six study lakes, most of the lakes had few days of observed water quality data in a simulation year with a maximum of 100 days of data for Carlos lakes. Traditionally lake modeling studies having a relatively small amount of observed data using all observed for model calibration without validation (Stefan et al. 1993). Therefore, no validation study was performed after calibrating the parameters for a lake.

These lakes have different characteristics as described in Section 3.2. Minnesota Department of Natural Resources has recorded water quality data for all the study lakes except for Thrush lake. The data for Thrush lake were collected from a previous study (Fang et al., 1995). These six study lakes include two deep lakes (Lake Carlos and Lake Elmo), two medium-depth lakes (Thrush and Riley lake), and two shallow lakes (Pearl and Carrie lake).

3.1.1 Calibration Parameters for MINLAKE2012

The daily MINLAKE2020 model is calibrated using the observed data in six study lakes. First, the water temperature model was calibrated, and then the nutrient and dissolved oxygen (DO) model was calibrated. The model was calibrated against the following parameters (Table 3.1).

Table 3.1 Calibration parameters MINLAKE2012 model (Fang et al. 2010)

Calibration parameter	Unit	Effect on model results	Description of the parameter
Wstr		Temperature and DO profiles	Wind sheltering coefficient
K_{BOD}	1/day	DO Profiles	Biochemical oxygen demand rate depending on lake trophic status
Sb20	$g/m^2/day$	DO Profiles	Sediment oxygen demand rate, lake tropic dependent
EMCOE(1)		Temperature and DO Profiles	Multiplier for diffusion coefficient in the metalimnion
EMCOE(2)		DO Profiles	Multiplier for SOD below the mixed layer
EMCOE(4)		Temperature and DO Profiles	Multiplier for diffusion coefficient in hypolimnion
EMCOE(5)		DO Profiles	Multiplier for chlorophyll–a below the mixed layer

Note: EMCOE stands for Empirical Coefficient. EMCOE is an array in the MINLAKE program. EMCOE(3) was used in the program for another purpose.

The wind sheltering coefficient (W_{str}) is very important model calibration parameter for lakes and represents the fraction of wind energy available for lake mixing (Riley and Stefan 1988). The wind sheltering coefficient for the model input file was first calculated using Equation 4.1 as a function of lake surface area, which was developed by Hondzo and Stefan (1993a) for the regional lake study of Minnesota lakes subjected to the past and future climate scenarios.

$$W_{str} = 1.0 - \exp(-0.3 \times A_s) \quad (3.1)$$

Here, A_s is the lake surface area in km^2. The theoretical maximum value for the wind sheltering coefficient is 1.0, and the minimum is 0. Equation 3.1 indicates that for lakes with large surface area W_{str} is larger than the ones for lakes with the smaller surface area. A value of 1.0 indicates no wind sheltering, i.e., 100% wind energy calculated by MINLAKE model was used to mix lake water; and a value of 0 has complete wind sheltering (no wind effects).

Even though wind sheltering coefficient is calculated for each lake using Equation (3.1), in real lakes with the same surface area can have different W_{str} values because the surroundings of a lake, in terms of tree canopies, buildings, etc. can have a significant effect on wind sheltering, especially for small lakes (Markfort et al. 2010). If a small lake is surrounded by tall and dense vegetation (forest) or buildings (residential area) wind sheltering for that lake is stronger than that of a lake with wide-open space around its periphery. Even single rows of trees or buildings along the shoreline of a lake can shelter a larger portion of a small lake; hence W_{str} needs to be calibrated for individual lakes to simulate the wind mixing properly. Areal images by using GIS can help in determining the values of W_{str}.

Biochemical oxygen demand (K_{BOD}) is defined for each lake based on trophic status. The values of K_{BOD} is calibrated for each lake. For MINLAKE2020, K_{BOD} affects phosphorus and DO concentration. The calibrated value ranges between 0.05–0.1 /day.

Sediment oxygen demand coefficient (S_{b20}) is directly related to lake trophic status. It is estimated based on suggested values from previous studies and then calibrated for each lake separately.

EMCOE(2) is a multiplier of sediment oxygen demand (SOD) below the mixed layer. This coefficient was added to the model in a study of cisco lakes (Fang et al. 2010b). It was calibrated for deep stratified lakes in the previous study. In this study, the value of EMCOE(2) was calibrated for shallow lakes also. EMCOE(2) = 1.0 means that the rate of sedimentary oxygen demand in the epilimnion (the mixed layer) and below the mixed layer is the same. Since shallow lakes are usually mixed, it is expected that the impact of EMCOE(2) is very insignificant for shallow mixed lakes.

EMCOE(5) is a multiplier of chlorophyll-a concentration below the mixed layer. For the RegDO model, the same values (time series) of chlorophyll-a concentrations in the epilimnion and the hypolimnion were used in earlier studies for model simulations. The multiplier, EMCOE(5), was therefore introduced to increase chlorophyll-a concentration below the epilimnion for oligotrophic lakes (Stefan et al. 1995a). The multiplier EMCOE(5) as a calibration parameter is easy to implement in the program and more user-friendly than changing values of the chlorophyll-a concentration time series below the epilimnion. EMCOE(5) was only used for Thrush Lake in this study. The same value of chlorophyll-a is used for epilimnion and hypolimnion, i.e., EMCOE(5)=1 for the other five lakes. This parameter is also not used for the NCDO model since the chlorophyll-a vertical profile is simulated by the model day by day.

EMCOE(1) and EMCOE(4) are multipliers for metalimnetic and hypolimnetic diffusion coefficients, respectively. These coefficients were added to the model in the cisco lakes study (Fang et al. 2010b) when it was found that in some cases metalimnetic and hypolimnetic diffusion rates determined from the model formula were higher or lower than indicated by the field temperature and DO profiles.

Overall, the water temperature model of MINLAKE2012 and MINLAKE2020 should be calibrated first by adjusting W_{str}, EMCOE(1), and EMCOE(4) to determine how heat and then mass diffuses in a lake. The calibration results can be evaluated using (1) statistical error parameters (e.g., the root mean squared error RMSE, Nash–Sutcliffe model efficiency coefficient) computed between simulated and measured values, (2) checking the plot of measured versus simulated water temperatures, (3) checking time series plots of water temperatures at five depths to see whether temperatures at certain were under- or over-predicted, and (4) checking profile plots at all dates with field data to see whether the mixed layer depths are under- or over-predicted and other model issues. In addition to the above three parameters, light attenuation coefficient and wind coefficient for convective heat loss can be also used for temperature model calibration.

3.1.2 Additional Calibration Parameters for MINLAKE2020

In addition to the calibration parameters mentioned in 3.1.1, MINLAKE2020 has introduced some calibration parameters for Chl*a* and P simulation.

Maximum Growth Rate of algae $G_{max}(K)$ is the maximum growth rate of algae. It depends on the class of algae and should be in the range mentioned in Table 2.2. Maximum growth rate is a calibration parameter since it depends on a lot of other factors. Moreover, the growth rate of a particular class of algae in a particular lake environment cannot be measured or predicted. Though the growth rate affects Chl*a*, P and DO, matching the simulation results with Chlorophyll-a data should be given priority. Other parameters depend on Chl*a*.

Table 3.2 Additional calibration parameters for MINLAKE2020

Calibration Parameter	Unit	Effect on model results	Description of the parameter
$G_{max}(K)$	day^{-1}	Chl*a*, P, DO Profiles	Maximum growth rate of algae
$K_r(K)$	day^{-1}	Chl*a*, P, BOD, and DO Profiles	Respiration rate of algae
$K_m(K)$	day^{-1}	Chl*a* and BOD Profiles	Non-predatory mortality rate of algae
$K_P(K)$	m/day	Chl*a*, P and DO Profiles	Half saturation coefficient for Phosphorus
S_P	g/m^2-day	P and DO Profiles	Sediment Phosphorus release rate
V(K)	m/day	Chl*a* and DO Profiles	Settling velocity of algae
V(BOD)	m/day	Chl*a* and DO Profiles	Settling velocity of detritus
T_{opt}	^oC	Chl*a*, P and DO Profiles	Optimum temperature for growth of algae
T_{max}	^oC	Chl*a*, P and DO Profiles	Maximum temperature for growth of algae
T_{min}	^oC	Chl*a*, P and DO Profiles	Minimum temperature for growth of algae
ZP	$/m^3$	Chl*a* and DO Profiles	Zooplankton population
ZPMIN	$/m^3$	Chl*a* and DO Profiles	Minimum zooplankton population for predation
YPChl*a*	mg P/mg Chl*a*	P Profiles	Mass yield of Phosphorus to Chlorophyll-*a*

Note: K is the number of total algal classes

Respiration Rate of Algae $K_r(K)$ is the respiration rate of algae. In MINLAKE2012, $K_r(1)$ is considered as a constant having a value of 0.1/day as only one algal class is simulated. Moreover, it was considered as a constant having a value of 0.1/day. But, in MINLAKE2020, a maximum of three algal classes can be simulated. So, different respiration rates are assigned for different classes of algae-based on the range given in Table 2.3.

Mortality Rate of Algae ($K_m(K)$) is the mortality rate of algae. The mortality of algae is calculated for Chlorophyll-a and BOD calculation. In MINLAKE2012, $K_m(K)$ was not used as

Chl*a*, and BOD was not simulated for the RegDO model. Different mortality rates are assigned to different algae classes. The calibrated value for each algal class should fall in the range of the mortality rates given in Table 2.3. The documented rates are from experimental measurements and are recorded by EPA (1985).

Half Saturation Coefficient of Phosphorus K_P(K) is the half-saturation coefficient of phosphorus. It is used in the Michaelis-Menten equation to determine phosphorus limitation. Phytoplankton growth is dependent on light and nutrient limitation. In most cases, Phosphorus is the limiting nutrient for algal growth and so, the half-saturation coefficient depends on the algae class.

Sediment release Rate of Phosphorus S_P(K) is the sediment release rate of phosphorus. This is a very sensitive parameter for chlorophyll-a calculation though it is not directly used in chlorophyll-a simulation. However, when the sediment release of phosphorus is set too high, the simulated chlorophyll-a concentration becomes too high. The model stops at that point. The increase in phosphorus concentration during summer months is directly related to the sediment release of phosphorus.

Settling Velocity of Algae and Detritus is important for chlorophyll-a and DO simulation. This is known as the advection velocity as well. Settling removes phytoplankton and detritus from one layer and adds it to the underlying layer. The calibrated settling velocity should fall in the suggested range mentioned in Table 2.3. In general, the blue-green algae exhibits the lowest settling rate among all the algal classes.

Optimum Temperature for Algal Growth (T_{opt}) is the optimum temperature for algae growth which depends on the algal class. Temperature plays an important role in the growth of

algae. The model is set up in a way to incorporate the highest production at the optimum temperature, declining production at both increasing and decreasing temperatures.

Maximum Temperature for Algal Growth (T_{max}) is the maximum temperature at which the algal growth can still occur. There is much smaller algal growth if the temperature is greater than T_{max}. At T_{max}, the growth rate is reduced to 90 percent of the maximum growth rate.

Minimum Temperature for Algal Growth (T_{min}) is the minimum temperature at which algal growth can occur. At T_{min}, the growth rate is reduced to 90 percent of the maximum growth rate. Riley assumed the minimum temperature to be 0 ^{o}C (Riley and Stefan, 1998). Though this is a good approximation, some phytoplankton species might have the different minimum temperatures for growth. In MINLAKE98, T_{min} was first introduced and the temperature correction equation (Equation 2.8) was modified (West and Stefan, 1998).

Initial Zooplankton Population (ZP): MINLAKE2020 simulates the zooplankton population over the simulation period. The initial zooplankton population per unit volume (#/m^3) is difficult to measure and considered as a calibration parameter to be set by the user. Zooplankton population is important as it reduces the chlorophyll-a concentration through grazing and consumes DO through respiration.

The minimum Zooplankton Population for Predation (ZPMIN) affects the zooplankton simulation. It defines the minimum zooplankton population per unit volume (#/m^3) for predation to occur. ZPMIN is used to simulate nocturnal predation.

The mass Yield ratio of Phosphorus to Chlorophyll-a (Y_{PChla}) is important for simulating phosphorus concentration. The phytoplankton mass for photosynthesis and respiration is converted to phosphorus concentration multiplying by Y_{PChla}. In MINLAKE1998, Y_{PChla} was used as a

constant, 1.1 mg P/mg Chl*a*. No specific guideline was found regarding the suitable value for Y_{PChla} except for some observation present in the literature (Thomann and Mueller, 1987). Y_{PChla} depends on a lot of factors and should not be used as constant. Therefore, in MINLAKE2020, Y_{PChla} is presented as a calibration parameter with a maximum value of 1.1 mg P/mg Chl*a*.

3.2 Characteristics of Study Lake

The daily MINLAKE2020 model was applied to six lakes (Table 3.3) with different characteristics. Two lakes (Pearl and Carrie) are relatively shallow, two lakes are of medium depth (Riley and Thrush) while lake Carlos and Elmo are very deep. All of the lakes are located in Minnesota. Three of the study lakes (Pearl, Carrie, and Carlos) are a part of sentinel lakes that are monitored in 2008–2012 and studied extensively by the Minnesota Department of Natural Resources (MNDNR). Lake Elmo and Riley were extensively monitored in the late 80s and 90s by the Metropolitan Council (Osgod,1983). MINLAKE98 was applied to these two lakes and so, these lakes were used for MINLAKE2020 simulation to compare results. Inflow data was also observed for Lake Riley in 1982 which will be beneficial for future studies. Thrush Lake has observed data for 1985–1987. One advantage of Thrush Lake is the availability of the chlorophyll-a data at the bottom of the lake as well as the surface.

The weather data used as input for simulating lake water quality parameters are not available on the lake. Therefore, the data are collected from the closest weather stations. The closest weather station to Carrie Lake, Pearl Lake, and Carlos Lake is Saint Cloud Regional Airport, and the closest weather station to Thrush Lake and Riley Lake is Duluth International Airport. The closest weather station to Lake Elmo is Minneapolis/St. Paul International Airport.

Table 3.3 Geographic location of six study lakes in Minnesota

Lake Name	**Lake DNR ID**	**County in Minnesota**	**Nearest Town**	**Latitude (^{0})**	**Longitude (^{0})**
Pearl Lake	37003700	Stearns	Cold Spring	45.39949	-94.306674
Carrie Lake	34003200	Kandiyohi	Atwater	45.08210	-94.786700
Riley	47004901	Carver	Chanhassen	44.8361	-93.5231
Thrush	29025000	Cook	Grand Marais	47.8966	-90.5002
Riley	18038600	Crow Wing	Brainerd	44.9958	-92.8794
Lake Carlos	21005700	Washington	Lake Riley	45.94930	-95.361900

The trophic status of lakes, in this study, was assessed by Secchi depth and chlorophyll-a concentration. Secchi depths of 1.2, 2.5, and 4.5 m were used to determine whether the lake is eutrophic, mesotrophic, or oligotrophic (Fang 1994). Besides, yearly and long-term averaged chlorophyll-a concentrations in each lake were assessed. Mean chlorophyll-a concentrations of 15, 6, and 2 (µg/L) were used for eutrophic, mesotrophic, oligotrophic lakes, respectively.

The Geometry Ratio ($GR = As^{0.25}/H_{max}$) was used to determine the lake stratification characteristics (Figure 4.4). According to Gorham and Boyce (1989), the value of geometry ratio is higher in polymictic lakes ($GR > 5$), while strongly stratified dimictic lakes have lower numbers of GR. The transition occurs between 3 and 5 (Fang et al. 2010a). On the x-axis of Figure 4.4, the Secchi depths are shown that indicate the clarity of the lake. It is also an indicator of the trophic status of the lake. The observed data (water temperature, DO, Chl*a*, and phosphorus profiles) at these lakes (except Thrush Lake) were downloaded from the DNR website (LakeFinder, https://www.dnr.state.mn.us/lakefind/index.html). Besides, The DNR website provides us with some of the model input data such as Secchi depth.

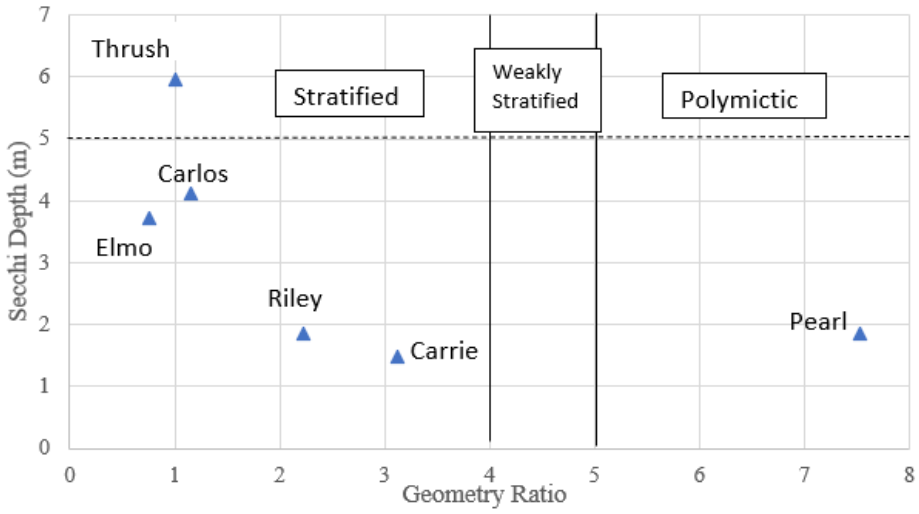

Figure 3.1 Lake stratification classification of six Minnesota lakes

Table 3.4 summarizes the morphometric characteristics, wind sheltering coefficient, and trophic status of six study lakes. Detailed descriptions of the study lakes are given below.

Table 3.4 Characteristics of six study lakes

Lake Name	**Surface area (km^2)**	**Max depth (m)**	**Geometry Ratio ($m^{0.5}$)**	**Mean Secchi Depth (m)**	**Mean Chl*a* (mg/L)**	**Trophic Status**
Pearl	3.05	5.55	7.53	1.85	16.91	Eutrophic
Carrie	0.37	7.90	3.12	1.48	6.71	Eutrophic
Riley	1.19	14.9	2.22	1.85	24.00	Eutrophic
Thrush	0.048	14.63	1.014	5.97	1.71	Oligotrophic
Riley	1.039	42.63	0.75	3.72	4.45	Mesotrophic
Carlos	10.54	50.00	1.15	4.11	3.84	Mesotrophic

3.2.1 Carrie Lake

Carrie Lake (DNR ID: 34003200; Latitude 45º04’55” N, Longitude 94º47’12” W) is a shallow lake located in Kandiyohi County of Minnesota. Carrie Lake has a maximum

depth of 7.9 m and a surface area of 0.37 km^2. Since the geometry ratio ($As^{0.25}/H_{max}$) of Carrie lake is 3.12, the lake is considered to be stratified. Lakes having a geometry ratio of less than 4 is considered to be stratified in this study. Since its geometry ratio (3.12) is close to 4, its stratification strength is close to weak. From the field data, the long-term average Secchi depth at Carrie Lake is found to be 1.48 m, and long-term average chlorophyll-a concentration is 6.7 µg/L. Carrie lake is classified as eutrophic lake based on the mean Secchi depth (SD = 1.48 m <1.8 m, Stefan et al., 1993). But based on the mean chlorophyll-a concentration (Chl*a* = 6.7 µg/L< 15 µg/L) it is classified as a mesotrophic lake. Since the Secchi depth of Carrie lake is very close to the eutrophication limit (1.2 m), Carrie lake is considered mesotrophic considering all aspects. The bathymetry data of Carrie Lake was extracted from the data downloaded from the DNR website (Figure 3.2).

Figure 3.2 Carrie Lake bathymetry contour lines (5 ft increment)

The depth, area, cumulative volume from the lake bottom (deepest point), depth increment, and volume increment of Carrie Lake are presented in Table 3.5. Figure 3.3 illustrates the Carrie Lake bathymetry (area-depth and volume-depth) graph plotted from Table 3.5.

Table 3.5 Carrie Lake bathymetry data

Depth (m)	**Area (m^2)**	**Volume (m^3)**	**Depth increment (m)**	**Volume increment (m^3)**
0.00	0.00	0	0	0
0.28	1930.81	270.3139	0.28	270.3139
1.80	36549.16	29515.1	1.52	29244.78
3.33	81480.33	119807.7	1.53	90292.56
4.85	110124.51	265427.3	1.52	145619.7
6.38	143243.64	459254	1.53	193826.6
7.90	369275.65	848768.6	1.52	389514.7

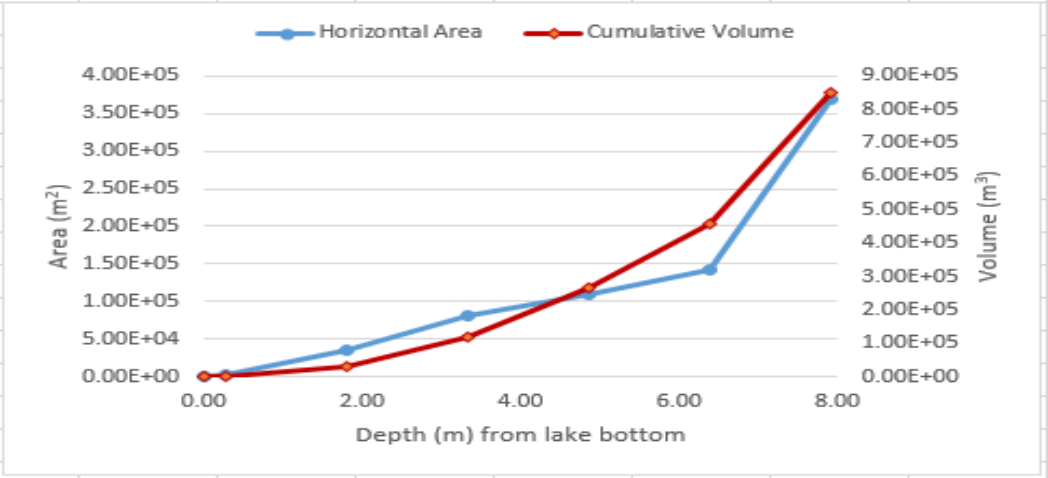

Figure 3.3 Bathymetry curve of Carrie Lake

Observed water temperature, DO concentration data at different depths of Carrie Lake were collected from the DNR website. The Secchi depth data was also collected for

multiple years. However, for Carrie lake, the chlorophyll-a data were available at the surface layer only. Figure 4.7 shows the annual mean, maximum, minimum; and the long-term average of observed Secchi depths at Carrie Lake. Measured Secchi depths were available in each year from 2004 to 2014, and the annual mean of observed Secchi depth is presented in Figure 3.4 from 2008–2012. In the model, the long term average of Secchi depth is used for extinction coefficient calculation. Similar information for chlorophyll-a data from 2008–2012 is given in Figure 3.5.

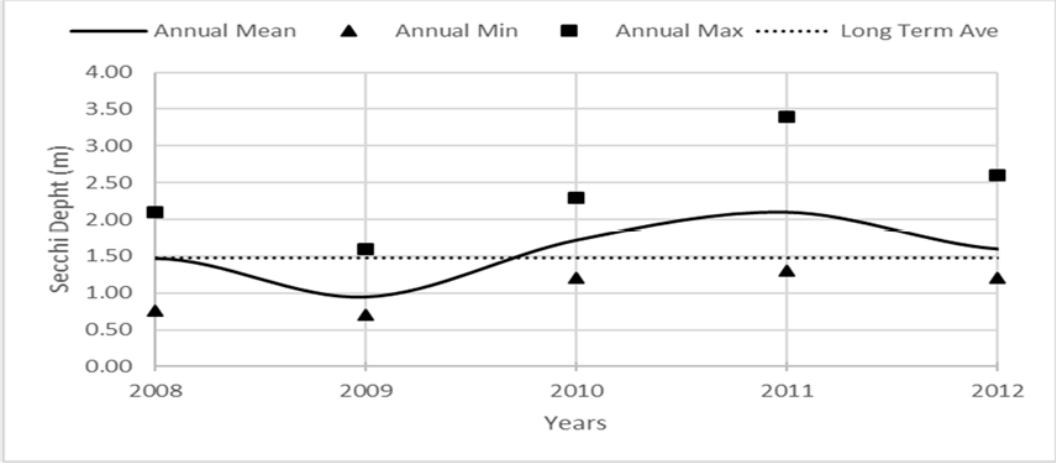

Figure 3.4 Long-term Secchi depth trend at Carrie Lake based on limited observed data

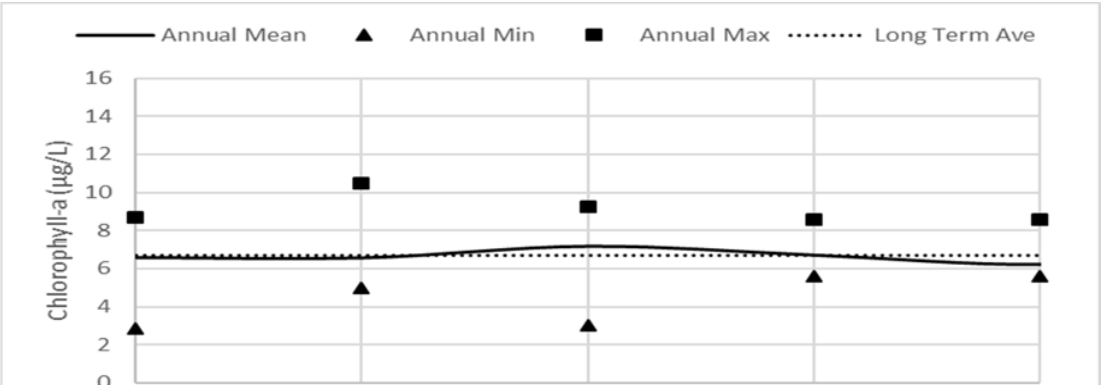

Figure 3.5 Long-term Chlorophyll-*a* trend at Carrie Lake based on limited observed data

In MINLAKE2012, the daily chlorophyll-a concentrations used in DO simulations are generated from the yearly average of observed chlorophyll-a concentrations following the general trend for Chl*a* of the lake. As the model use the same trend for different years, daily chlorophyll-a concentrations used in 2008–2012 are similar.

3.2.2 Pearl Lake

Pearl Lake (DNR ID: 73003700; Latitude: 45º25'58" N; Longitude: 94º18'24" W) is a very shallow lake located in Stearns County. Pearl Lake has a maximum depth of 5.55 m and a surface area of 3.05 km^2. Since the geometry ratio ($As^{0.25}/H_{max}$) of Pearl Lake is 7.53, it is considered as a polymictic lake (mix many times in a year). Among the six study lakes, five of them are stratified lakes whereas Pearl is a polymictic lake. From the field data of several years, the long-term average Secchi depth at Pearl Lake is found to be 1.85 m whereas the long-term average chlorophyll-a concentration is found as 16.91 µg/L. Based on the mean Secchi depth (SD = 1.85m >1.80 m), Pearl Lake can be classified as a mesotrophic lake. On the contrary, Pearl lake can be classified as a eutrophic lake based on the Chlorophyll-a concentration. Since the Secchi depth was very close to the eutrophication criteria, the lake can be considered as eutrophic. The bathymetry data of Pearl Lake were collected from the DNR website. Figure 3.6 shows the depth contour lines of rounded Pearl Lake and Figure 3.7 shows the depth-area and depth-volume graph.

Figure 3.6 Pearl Lake depth contour lines (5 ft increment)

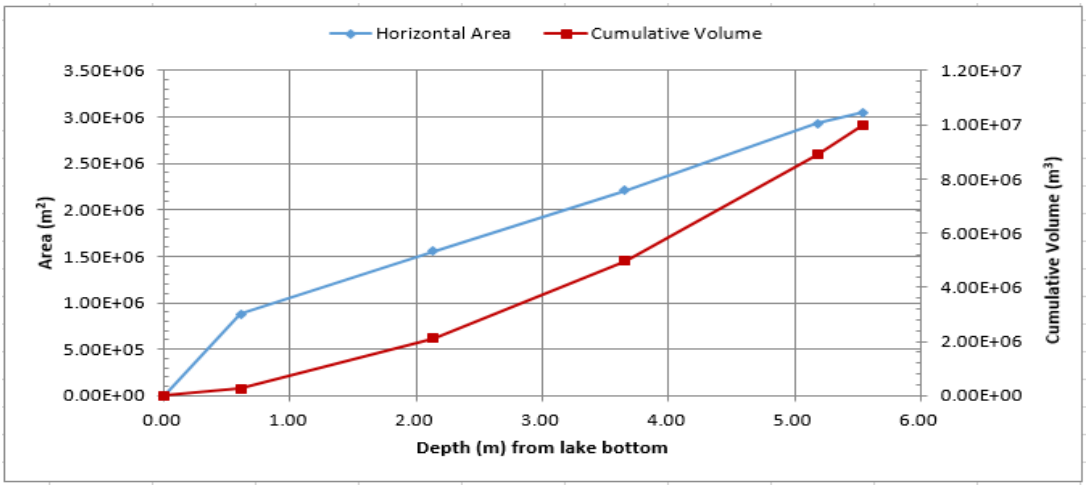

Figure 3.7 Bathymetry curve of Pearl Lake

Observed water temperature, DO concentration, Chl*a*, and phosphorus concentration data at different depths of Pearl Lake were collected from the DNR website. The Secchi depth data were also collected for multiple years. However, for Pearl Lake, the chlorophyll-a data were available at the surface layer only. Figure 3.8 shows the annual mean, maximum, minimum; and the long-term average of observed Secchi depths at Pearl Lake. As can be

seen from Figure 3.9, in 2010 and 2011, the annual mean is higher than that of other years. Since the chlorophyll-a concentration varies from year to year, annual mean Secchi depth is also different for each year as shown in Figure 3.8.

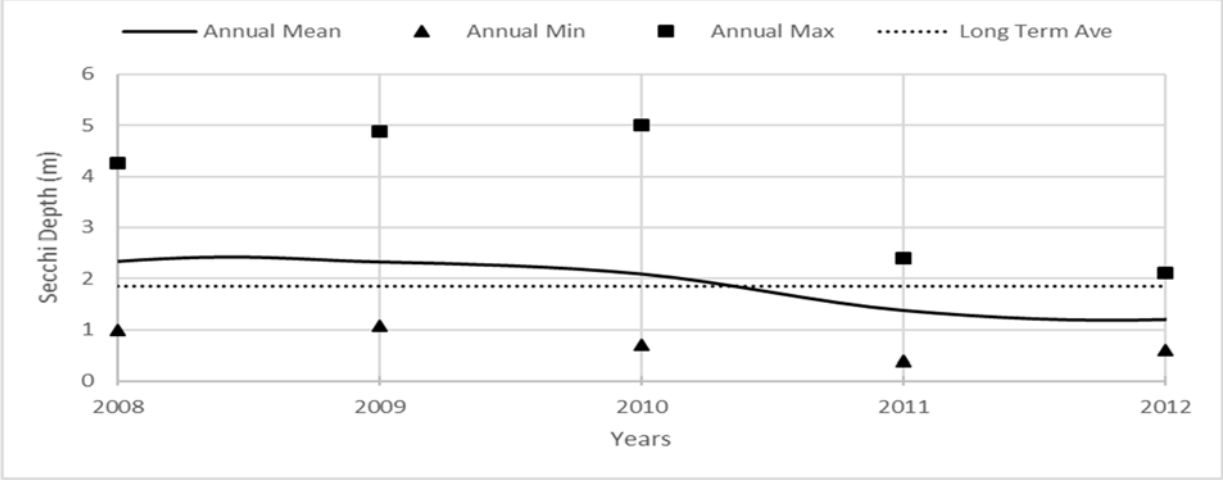

Figure 3.8 Secchi depth trend at Pearl Lake 2008–2012

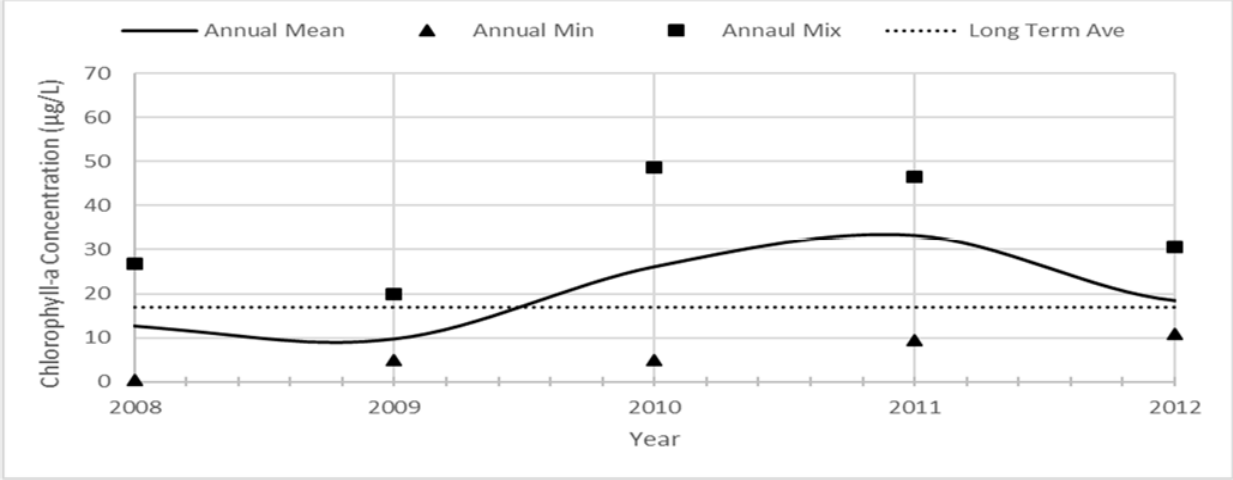

Figure 3.9 Chlorophyll-a concentration at Pearl Lake 2008–2012

3.2.3 Lake Carlos

Lake Carlos (DNR ID 21005700, latitude 45°56’57” N, and longitude 95°21’43” W) is a dimictic lake located in Douglas County, near the Carlos Town. It has a surface area of 10.20 km^2 and a maximum depth of 50 m. It has a geometry ratio ($As^{0.25}/H_{max}$) of 1.13 and is classified as a stratified deep lake. It has a mean Secchi depth of 4.11 m and is classified as a mesotrophic lake. Long-term average chlorophyll-a concentration at Lake Carlos is 3.84 µg/L.

Figure 3.10 Lake Carlos bathymetry contour lines

The bathymetry of Carlos Lake (elongated) was extracted from the lake depth contour lines downloaded from the DNR website using GIS. Figure 3.10 shows the lake bathymetry contour lines and the depth-area and depth-volume curves.

Secchi depth, chlorophyll-a concentration, phosphorus concentration, and water temperature and DO profiles for Lake Carlos were collected from the DNR website. Figure 3.11 shows the annual average (a smooth line connecting annual observed mean Secchi depths), maximum, minimum, and long-term average Secchi depth observed at Carlos from 2008–2012. The long-term average of Secchi depth is used to compute the attenuation coefficient. Figure 3.12 shows the observed chlorophyll-a concentration at Lake Carlos, annual mean, maximum, minimum, and long-term average. As can be seen from Figure 3.12, the annual mean of chlorophyll-a concentration is not much different from year to year.

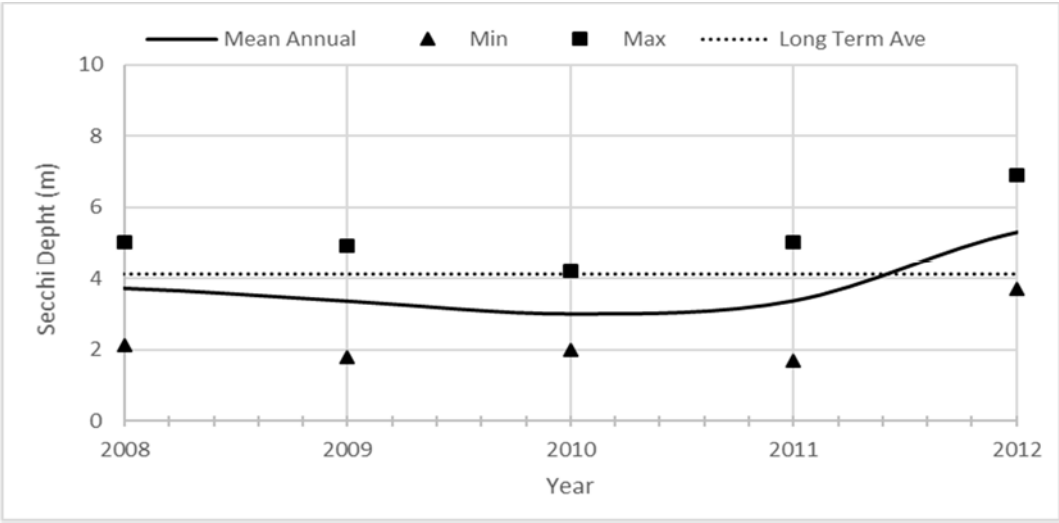

Figure 3.11 Chlorophyll-a concentration at Lake Carlos in 2008-2012

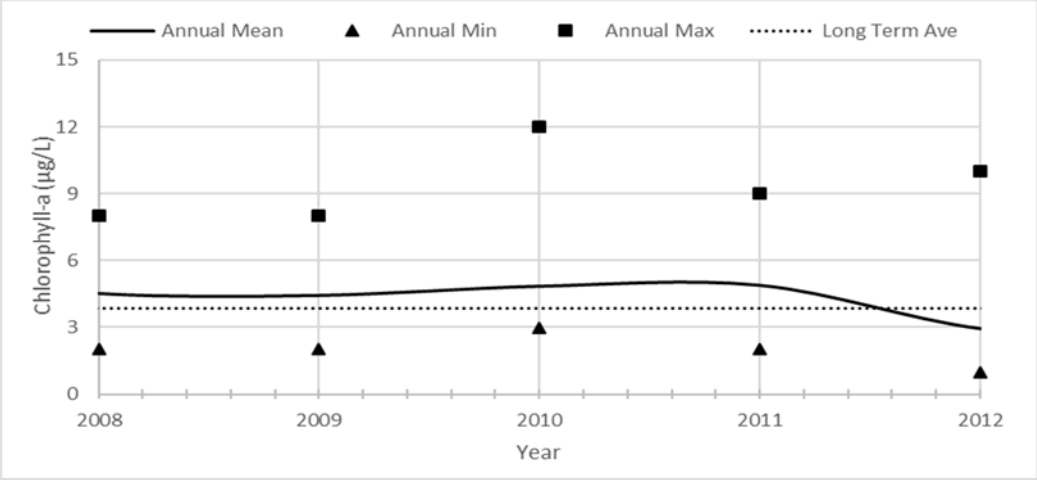

Figure 3.12 Chlorophyll-a average for 2008-2012 for Lake Carlos

3.2.4 Lake Elmo

Elmo Lake (DNR ID: 82010600; Latitude 44°59'44.88" N, Longitude 92°52'45.84" W) is located approximately 10 miles east of St. Paul in Washington County of Minnesota. Elmo Lake has a surface area of 0.37 km^2 and a maximum depth of 48 m. The geometry ration ($As^{0.25}/H_{max}$) of Elmo Lake is 0.75 $m^{-0.5}$. Therefore, it has been considered a strongly stratified lake. Since its geometry ratio (0.75) is much less than 3, its stratification strength is strong. The lake is oriented away from the prevailing wind direction which, along with its depth, allows for stable seasonal stratification. The long-term average Secchi depth at Lake Elmo is 3.72 m, and long-term average chlorophyll-a concentration is 4.45 µg/L. Based on the mean Secchi depth (SD = 3.72 m >1.8 m, Stefan et al., 1993) and mean chlorophyll-a concentration (Chl*a* = 4.45 µg/L< 15 µg/L), Elmo Lake is classified as mesotrophic lake. Its bathymetry data were extracted from the data downloaded from the topozone website (Figure 3.13).

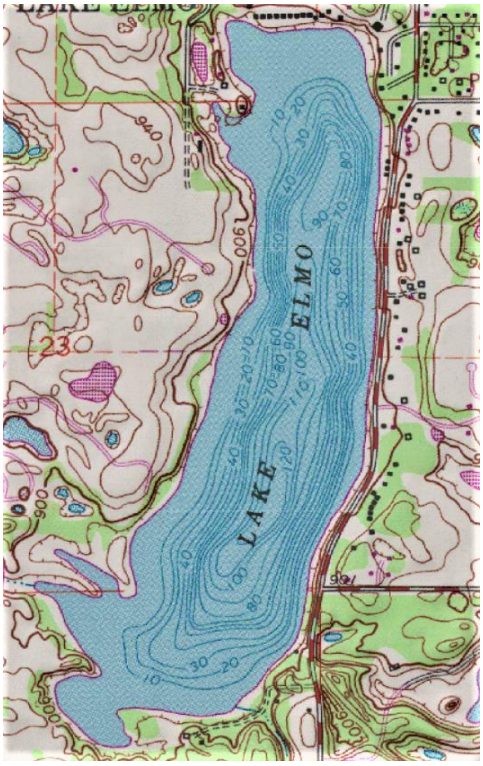

Figure 3.13 Bathymetry of Lake Elmo

Observed or measured Secchi depths, chlorophyll-a concentrations, phosphorus, water temperature and DO profiles for Elmo lake were collected from the DNR website. One main reason for simulation Elmo lake first is the availability of observed data from 1988 to 2018. The lake has observed data of 74 days on a span of 10 years. The chlorophyll-a was measured at the surface, but the phosphorus was observed at different depths, which is important for the validation of the multi-layer model in our study.

Figure 3.14 shows the maximum, minimum, and mean Secchi depth for a time-period of 1980–2018 for Lake Elmo. In recent years, the lake Secchi depth seems to be lower than that in the 1980s. This corresponds to a decrease in Chlorophyll-a concentration in recent years as can be seen from Figure 3.15

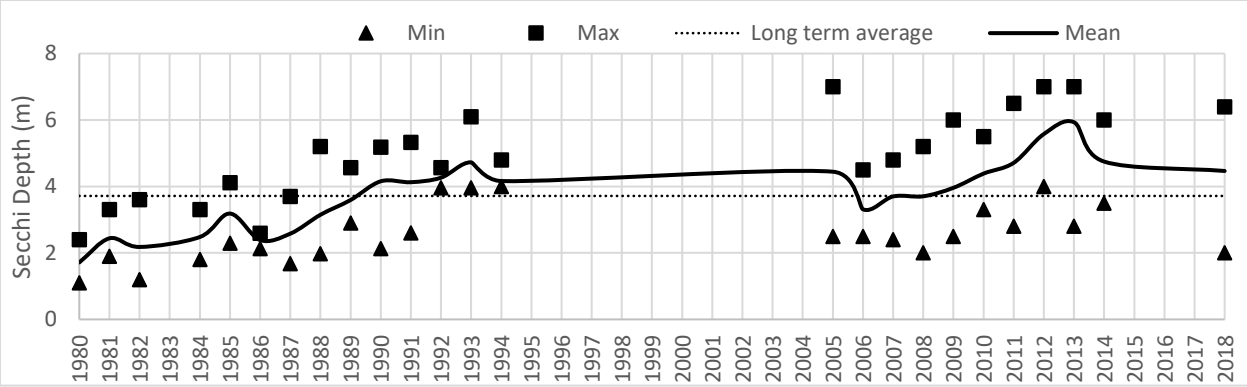

Figure 3.14 Secchi depth average in 1980 – 2018 for Lake Elmo

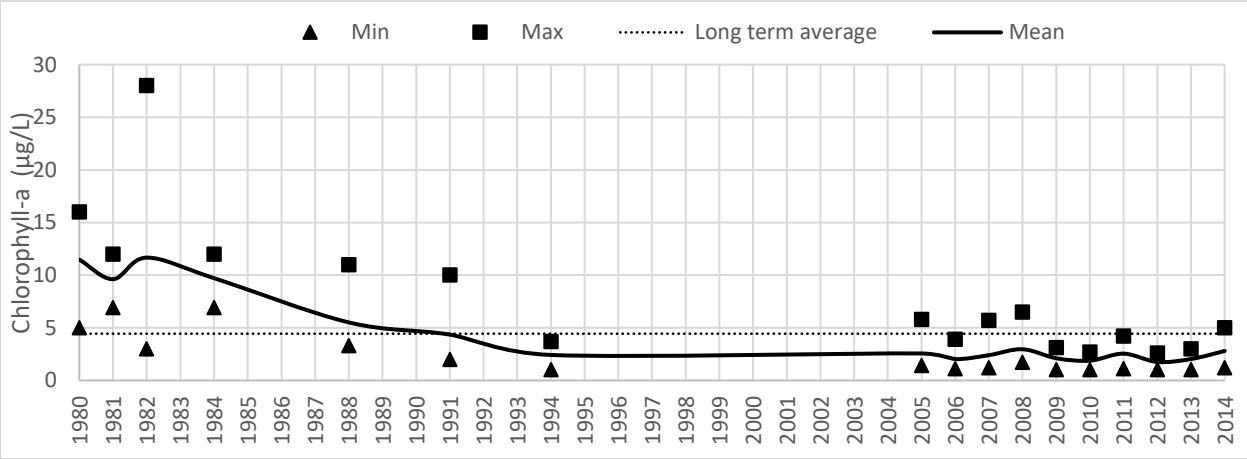

Figure 3.15 Chlorophyll-a concentration trend in 1980 – 2018 for Lake Elmo

3.2.5 Lake Riley

Riley Lake (DNR ID: 47004901; Latitude 44º50'9.96" N, Longitude 93º31'23.16" W) is located in the Carver County of Minnesota. Riley Lake has a surface area of 0.06 km^2 and a maximum depth of 14.63 m. The geometry ratio ($As^{0.25}/H_{max}$) of Riley Lake is 2.22 $m^{-0.5}$. Therefore, it has been considered a stratified lake since its geometry ratio (2.22) is less than 3. The

long-term average Secchi depth at Riley Lake is 1.85 m, and long-term average chlorophyll-a concentration is 24 µg/L. Based on the mean Secchi depth (SD = 1.85 m >1.8 m, Stefan et al. 1993) and mean chlorophyll-a concentration (Chl*a* = 24 µg/L > 15 µg/L), Riley Lake is classified as a eutrophic lake. From the observed Chlorophyll-a data, the lake can be identified as a highly productive lake. Its bathymetry data were extracted from the data downloaded from the topozone website (Figure 3.16).

Figure 3.16 Bathymetry of Lake Riley

Observed water temperature, chlorophyll-a concentration, phosphorus concentration and DO concentration data at different depths of Riley Lake were collected from the DNR website. For Riley lake, only two years (1982 and 1986) of field data were available. The average Secchi depth in 1982 and 1986 is 1.9 m and 1.6 m, respectively. The average Chlorophyll-a in 1982 and 1986 are 22.58 µg/L and 42.6 µg/L, respectively.

3.2.6 Thrush Lake

Thrush Lake (DNR ID: 16019100; Latitude 44º50'9.96" N, Longitude 93º31'23.16" W) is located in the Cook County of Minnesota. Thrush Lake has a surface area of 0.06 km^2 and a maximum depth of 14.63 m. The geometry ration ($As^{0.25}/H_{max}$) of Thrush Lake is 1.014 $m^{-0.5}$. Therefore, it has been considered a stratified lake. Since its geometry ratio (1.014) is much less than 3, its stratification strength is strong. The long-term average Secchi depth at Thrush Lake is 5.97 m, and long-term average chlorophyll-a concentration is 1.71 µg/L. Based on the mean Secchi depth and mean chlorophyll-a concentration, Thrush Lake is classified as an oligotrophic lake.

Observed water temperature, chlorophyll-a concentration and DO concentration data at different depths of Thrush Lake were not available on the DNR website. Fang simulated Thrush Lake for a previous study in 1996 and the data were collected from him. All other lakes in the study have chlorophyll-a data at the surface only. Thrush Lake was included in the study as it has chlorophyll-a concentration data in both epilimnion and hypolimnion. The figure shows the annual maximum and minimum chlorophyll-a concentration at the surface and bottom of Thrush lake in 1985–1991.

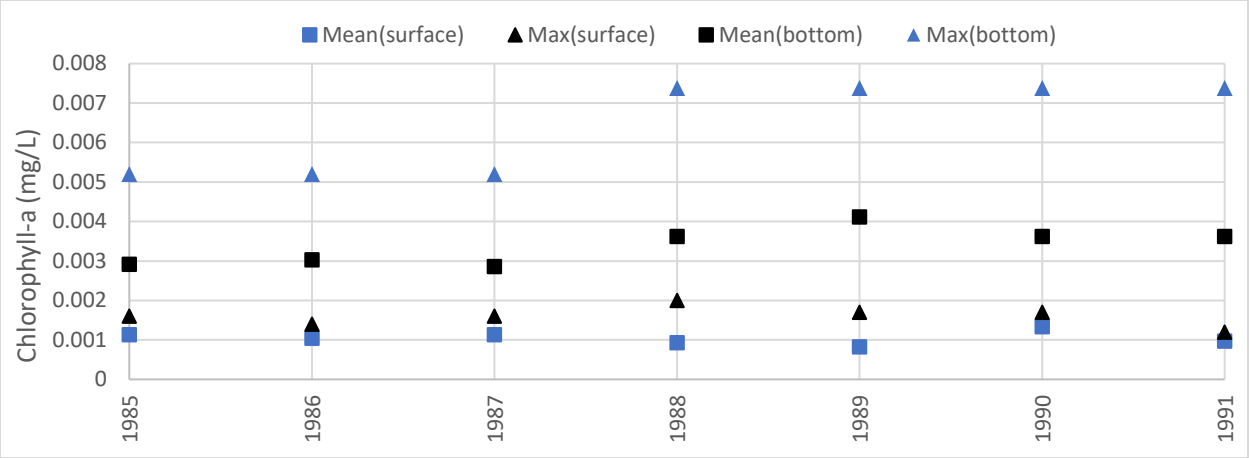

Figure 3.17 Maximum and minimum Chl*a* concentration at the surface and bottom of Thrush lake (1985–1991)

Chapter 4 Simulation Results and Discussion

In Chapter 2 and Chapter 3, the model description and calibration were discussed. In this chapter, the results of lake water quality simulation using the NCDO model MINLAKE2020 will be presented. A total of six lakes with varying depths and trophic status were simulated using MINLAKE2020. The results of DO were compared with that of the RegDO model of MINLAKE2012.

4.1 Lake Elmo Simulations

Lake Elmo was simulated using the NCDO model and the RegDO model. Since there was a large amount of field data for lake Elmo, three different simulation runs were performed to better understand the results. The first run is from 1987–1988, the second run is for 2007–2009 and the third one is a multiple-year study (1979–2009). With contrary to the RegDO model, the chlorophyll-a concentration was simulated day by day using the code. Two algae classes (green algae and blue-green algae) were simulated. Many model parameters and coefficients were introduced to simulate for the NCDO model, and most of them were taken from the previous study of Elmo Lake (West and Stefan, 1998). Some of the parameters were further calibrated to get the best results as we were not using the same program as the previous study.

4.1.1 Lake Elmo Simulation for 2007–2009

Elmo Lake was simulated for 1979–1988 in previous literature and this study for model validation. After that, it was simulated for the 2007–2009 time period that has adequate observed data for comparison.

The statistical results show that temperature is simulated with a slope of 1.022 and a regression coefficient of 0.99. A comparison of the observed and simulated values is presented in Figure 4.1. Field data are available for the open water season. The plotted points are very close to the 1:1 line indicating a good match between simulated water temperature and the observed data.

Dissolved oxygen is also simulated well with a slope of 0.97 and a regression coefficient of 0.92. Despite some difficulties in simulating the complex DO profiles the standard error is low, 1.42 mg/L DO considering DO data of all depths (deeper layer has a higher standard error). Phosphorus is simulated with a slope of 1.037 and a regression coefficient of 0.61. Simulated chlorophyll-a values have the lowest statistical correlation with field observations. Chlorophyll-a is simulated with a slope of 2.6 and a regression coefficient of 0.35. The model, in general, overpredicted the chlorophyll-a concentration (Figure 4.1 b). Lake Elmo has limited observed data for chlorophyll-a and phosphorus.

Ice thickness on Lake Elmo from 2007 to 2009 is presented in Figure 4.2. Lake Elmo has ice cover from December to Mid-April every year. During this time, the lake surface temperature is very close to zero whereas the deeper layers are warmer as shown in Figure 4.3. Figure 4.3 represents the simulated and observed water temperature at 1 m, 6 m, 12 m, 20 m, and 30 m below the surface. The water temperature starts increasing in Mid-April and decreases from August to November. From December to March, the water temperature remains stable because of ice cover.

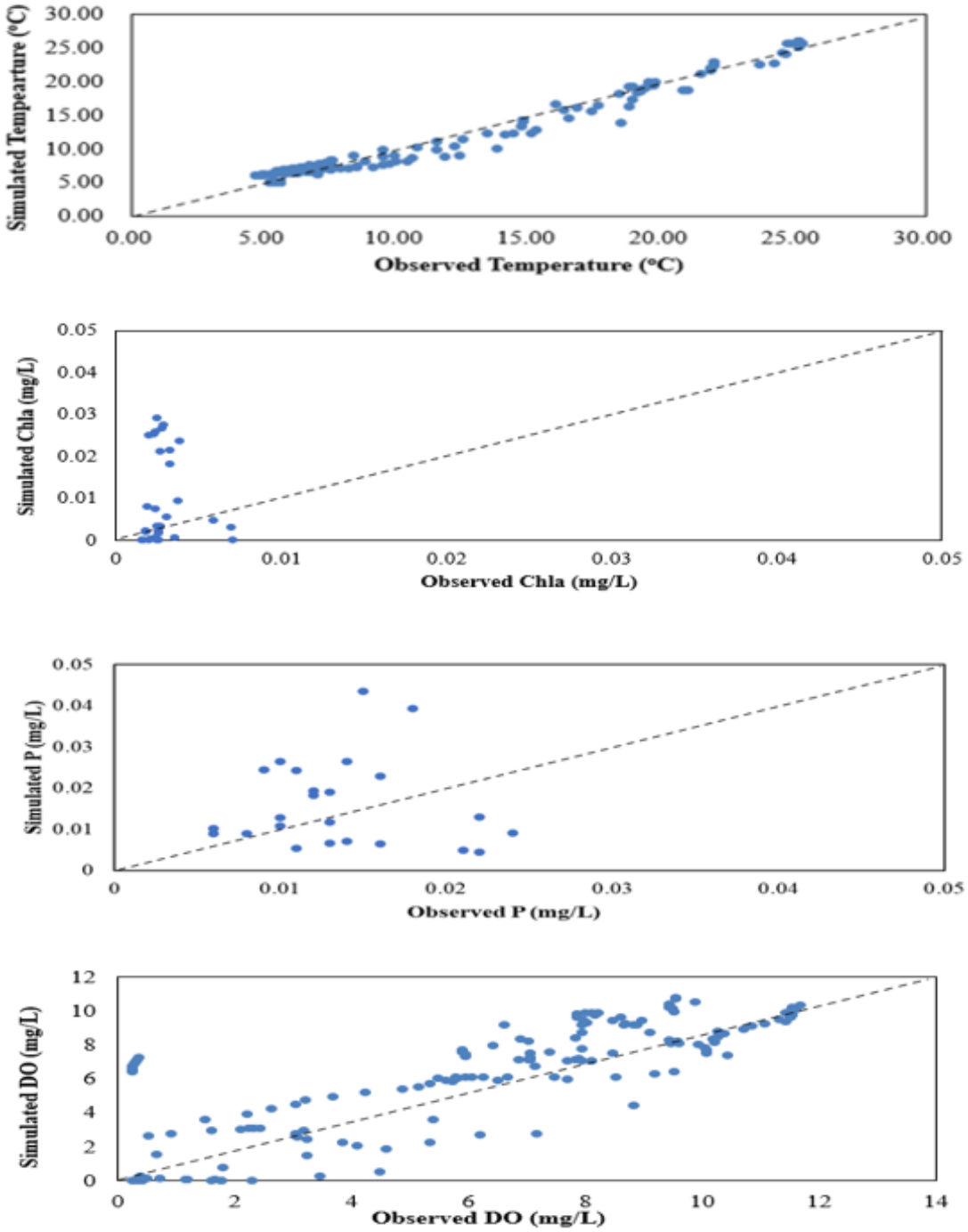

Figure 4.1 Comparison of the simulated and observed water quality values for Lake Elmo, 2007–2009

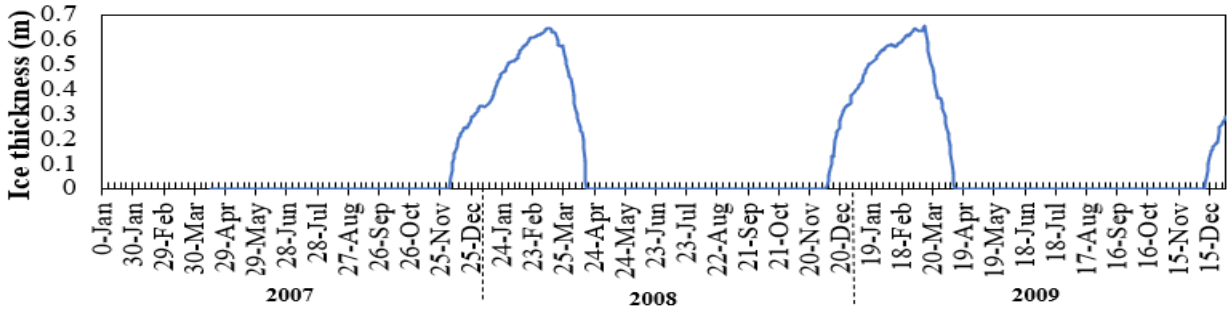

Figure 4.2 Simulated ice thickness on Lake Elmo in 2007–2009

Figure 4.4 shows simulated and observed Chl*a* and phosphorus at the surface of Elmo Lake. The simulation starts on 16th April 2007. Simulated Chlorophyll-a concentration (Fig. 4.4 a) is under 10 µg/L (0.01 mg/L) until the end of May 2008, then increases significantly causing algal bloom as a result of ice melting and surge of nutrients (Fig. 4.4 b). On 28th May 2008, simulated Chlorophyll-a concentration began to decrease but was still higher than the typical value for Elmo Lake. During the end of summer, Chl*a* comes to the usual range. Another factor contributing to the algal bloom is the warm water which stays close to the optimum temperature for algal growth (20°C, Fig. 4.3 b). In the fall, as the water cools down, the cooler water sinks into the deep and the lake mixes due to natural convection and wind mixing. This fall turnover unleashes/diffuses a large supply of phosphorus and nitrogen from the deeper layers into surface layers (Fig. 4.5) and causes a Chl*a* bloom at the surface. From Figure 4.4 (a), such fall blooms can be identified in mid-September to the early of December in 2008 and 2009. One thing that might be noticed is that the 2007 simulation does not comply with the algal bloom trend discussed above since it does not have high nutrients after ice melting (Fig. 4.4 b) specified at the initial conditions. The first year of simulation is considered as model warm-up period and the results are not considered to be accurate.

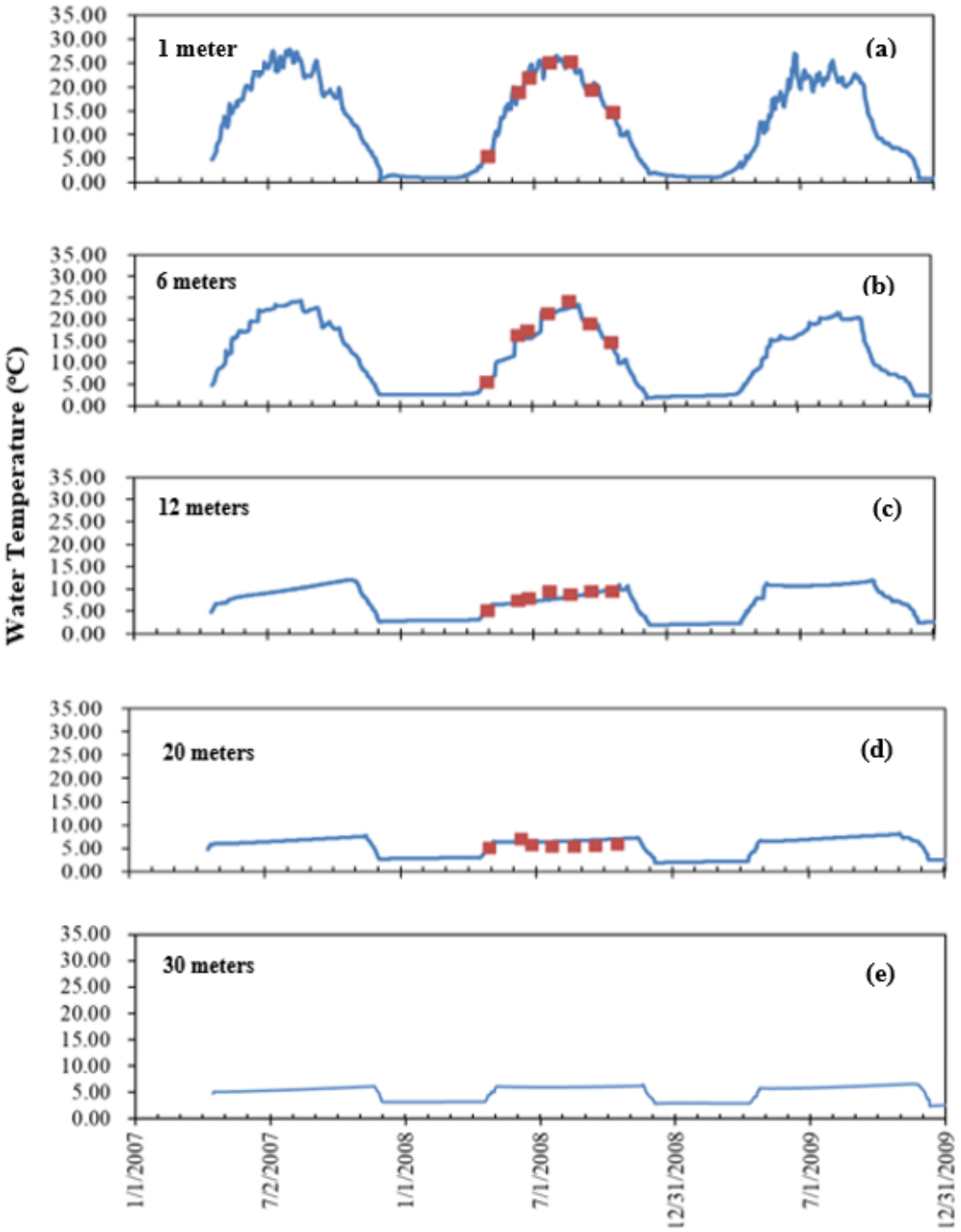

Figure 4.3 Simulated (solid line) and observed (dots) water temperatures at (a) surface (1.0 m), (b) 6 m, (c) 12 m, (d) 20 m, (e) 30 m below the surface for Lake Elmo, April 2007 to December 2009.

Figure 4.4 (a) indicates that the simulated Chl*a* concentrations near the water surface closely match the observed data except for June in 2008 and 2009. The simulated Chl*a* for the period of July to October 2008 and July to September 2009 follows the trend of the observed data. The model overpredicts Chl*a* on some days in May 2008 and 2009. The overprediction during May and June (Fig. 4.4 a) is probably due to the predicted surge of nutrients after ice melting in April (Figure 4.2). The model predicts this surge to occur rapidly resulting in a low concentration of phosphorus, which is used for photosynthesis and high concentration of chlorophyll-a.

The model underpredicts phosphorus concentration during May and June in 2008 and 2009, which could be due to not counting nutrient inputs from the runoff of snow melting. From late October to late November, before the ice starts to form at the surface of the lake (Figure 4.4 b), phosphorus at the surface and other surface layers (Fig. 4.5) starts to increase due to mixing and the fall overturns and remains more or less constant under the ice cover period. During the ice cover period, the phosphorus concentration becomes stable as the organic processes (photosynthesis) becomes slow due to the near-zero water temperature and/or low light. As the ice starts to melt, the surge of nutrients increases the phosphorus concentration for a brief period. Due to the conducive temperature, the phosphorus is used up by the algae for growth in May and June which results in a sudden decrease of phosphorus but an algal bloom, which significantly overpredicted Chla in May and June in 2008 and 2009.

Green algae and blue-green algae are simulated separately and then combined to represent the total chlorophyll-a. Time series of simulated chlorophyll-a and phosphorus at 1 m, 6 m, 12 m, 20 m, and 30 m below the surface are presented in Figure 4.5. The Chlorophyll-a concentration is higher at the topwater layers than that of the deeper layers due to photosynthesis with more

available light but fewer nutrients. The 6 m depth seems to have the highest Chl*a* peak during the summer, which could have adequate light from above and adequate nutrients from the lake bottom. In summer, 6 m depth is in metalimnion where the layers are more stable than the surface layer. The solar irradiance at 6 m depth could be close to optimum. Near the surface, too strong irradiance might create a problem for algal growth (light inhibition). In the deeper layers, the peak algal concentration in summer and fall flattens as the solar radiation cannot penetrate through the deepwater columns and there is no algal growth.

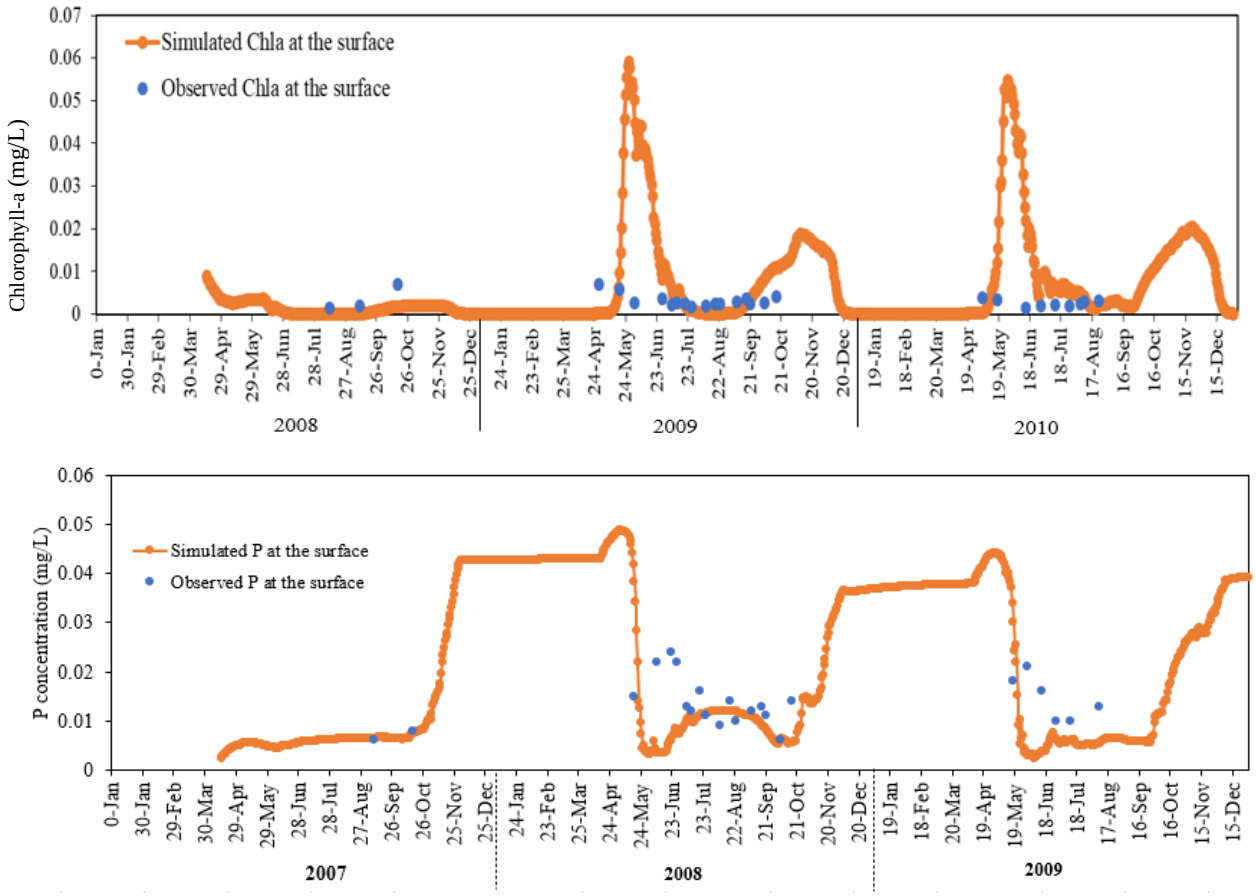

Figure 4.4 Comparison between simulated and observed chlorophyll-a and phosphorus at the surface of Lake Elmo, 2007–2009

Simulated phosphorus concentrations at 1 m show the lowest phosphorus concentration as a result of the phosphorus uptake of phytoplankton, which is the only sink term for Phosphorus. In the deeper layer, in addition to detrital decay and phytoplankton respiration, sediment release adds up to the available phosphorus. Since most of the deeper layers are anoxic during the summer (Figure 4.7) and phosphorus release happens in anoxic condition, phosphorus release from sediment contributes to a major portion of phosphorus in deep water layers. Phosphorus peaks were simulated in deep layers at the early fall as a result of sediment release just before the anoxic condition ends and then the fall mixing/overturn reduces phosphorus in deep layers and increases in surface layers.

The model is sensitive to several parameters. A sample sensitivity analysis was performed for chlorophyll-a simulation and the result is presented graphically. For Elmo Lake simulation (2007–009), the maximum growth rate of algae (Gmax) was set to 3 for both Green algae and Blue-green algae. To assess the effect of Gmax on final results, the simulated chlorophyll-a with Gmax =1.5 is compared with the simulated chlorophyll-a with Gmax of 3 in Figure 4.5. When Gmax decreases from 3 to 1.5, the summer peak Chla of 0.0578 mg/L reduces to 0.0138 mg/L in 2008. In 2009, the algal bloom occurs for a longer period at a stretch (end of May to December). When mass yield ration of phosphorus to chlorophyll-*a* is changed from 0.4 to 1.5, the chlorophyll-a concentration reduces for the whole period. The overall seasonal trend remains the same as shown in Figure 4.5. The summer peak in 2008 reduces to 0.0131 mg/L. In the fall, the chlorophyll-a concentration increases insignificantly which does not result in any bloom.

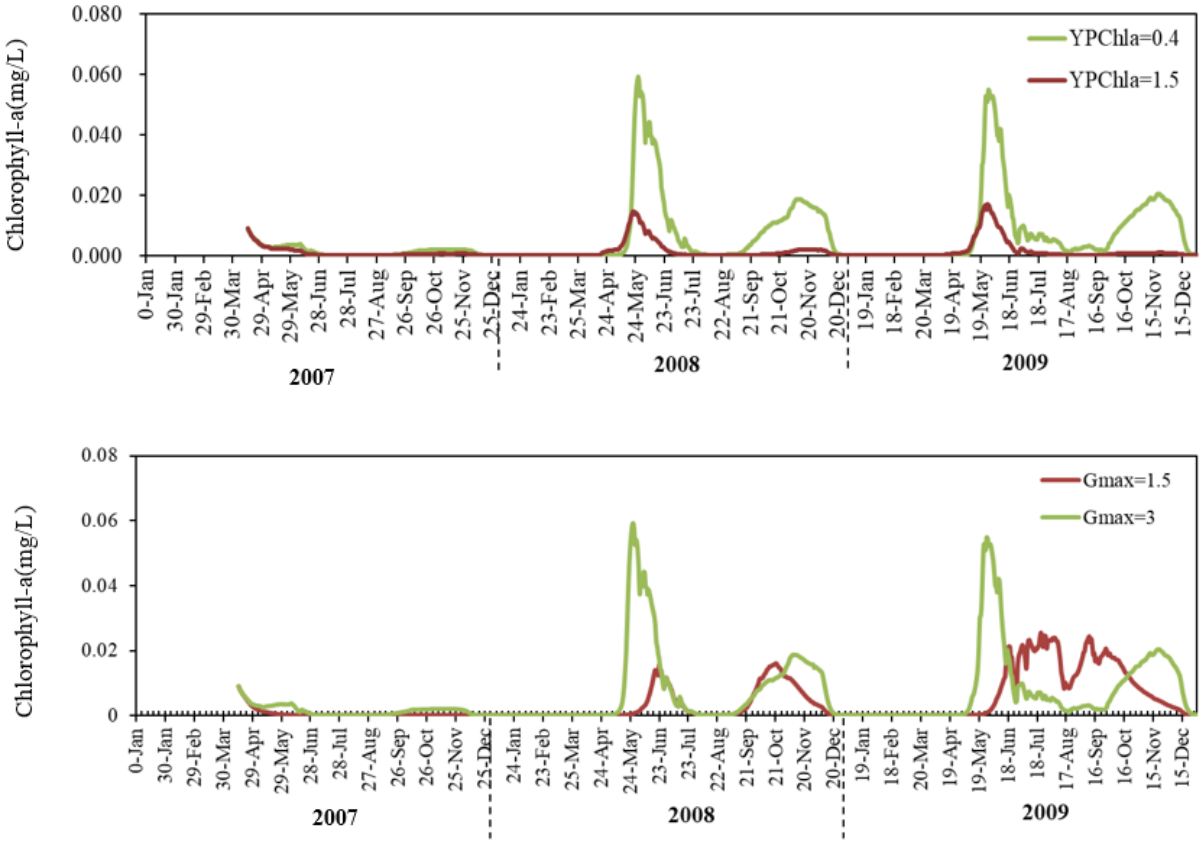

Figure 4.5 Sensitivity analysis of two calibration parameters for Chl*a* simulation

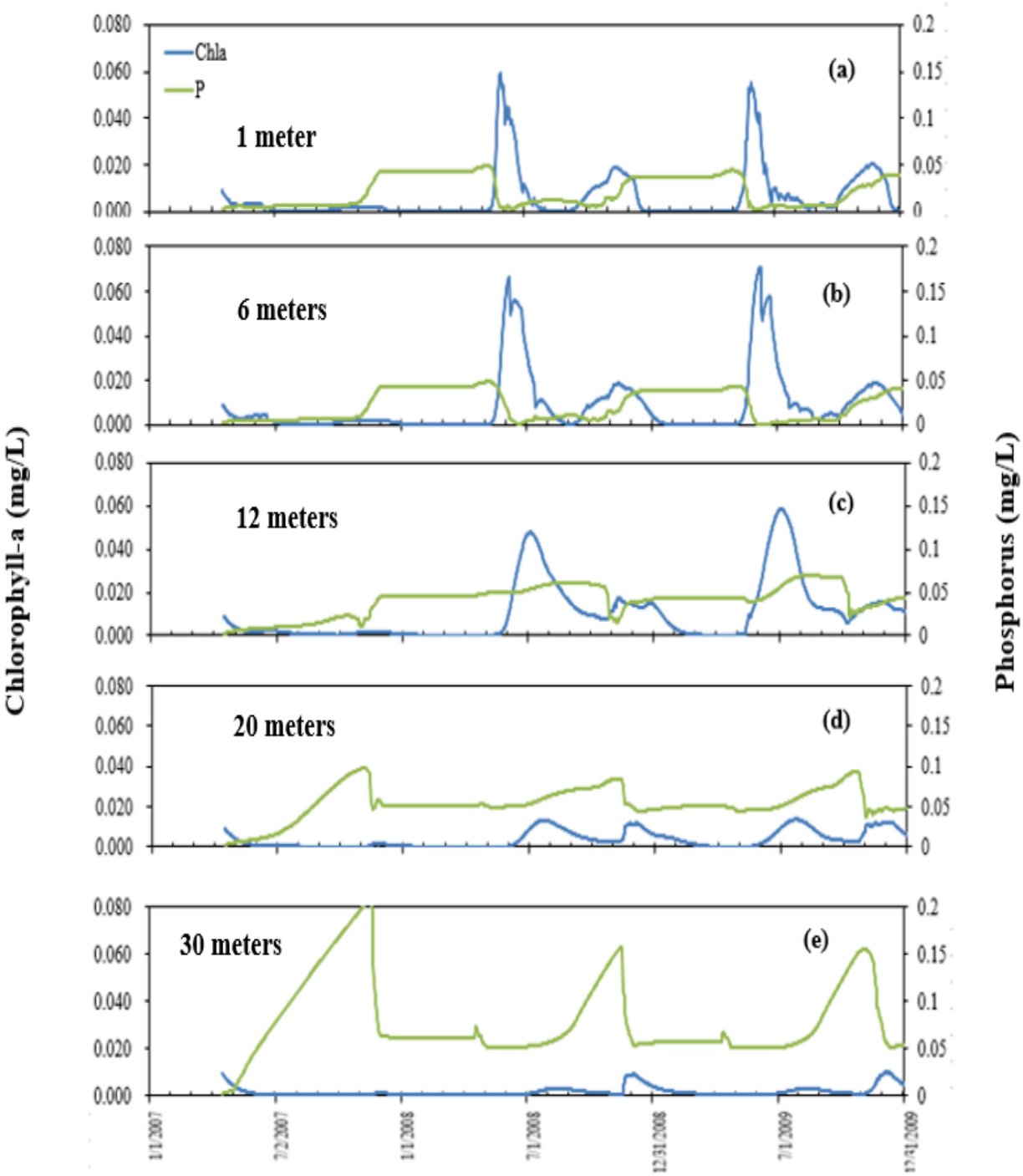

Figure 4.6 Simulated Chlorophyll-a and phosphorus (right y-axis) concentrations at (a) 1 m, (b) 6 m, (c) 12 m, (d) 20 m, and (e) 30 m below the surface for Lake Elmo, April 2007 to December 2009

DO and BOD concentrations at 1 m, 6 m, 12 m, 20 m, and 30 m below the surface are presented in Figures 4.7 and 4.8, respectively. Overall, the simulated DO in summer (no winter DO data) appears to have good agreement with the observed values except for one low value at 20 m below the surface (likely data issue). In the summer months, the lake is thermally stratified (Fig. 4.3). The thermocline prevents the DO produced by photosynthesis from reaching the cold hypolimnion water. The hypolimnion has the DO acquired during spring overturn which is gradually used for detrital decay.

A comparison between chlorophyll-a concentrations simulated by RegDO and NCDO models is presented in Figure 4.9. The RegDO model uses a general seasonal pattern of chlorophyll-a from the observed data to fill up the missing chlorophyll-a concentrations during the simulation period. This approach, though capable of producing satisfactory DO results, is not capable of detecting detailed water quality conditions in a lake. Moreover, sometimes this interpolating scheme results in some discrepancies in DO simulation. The NCDO model simulates Chl*a* concentration day by day accounting for all ecological changes happening inside the lake environment. From Figure 4.9, it can be observed that the Chl*a* concentration assumed from the RegDO model has a pretty consistent trend year by year. In reality, the water temperature, mixing, phytoplankton concentration at an earlier time step play a vital role in Chl*a* concentration. From the NCDO model simulation, it is visible that the chlorophyll-a concentration at the surface layer keeps increasing in summer due to increased photosynthesis. Ice melting, the surge of nutrients, and water temperature results in an algal bloom in lake water. In the fall, the lake mixes as the cooler water sinks into the deep. This fall turnover transfers phosphorus and nitrogen from the deeper layers to

surface layers and causes a bloom at the surface. From the NCDO plot, such fall blooms can be identified in mid-September to the end of December in 2008 and 2009 which cannot be predicted by the RegDO model. As the observed data were very scattered, the RegDO model predicts a declining trend of chlorophyll-a during summer months. One of the main drawbacks of the Chl*a* simulation in the RegDO model is its dependence on observed data. Out of 989 days of the simulation period, we had observed data for only 38 days. Though both of the models produce desirable DO results, the NCDO model works better in predicting the Chl*a* concentration.

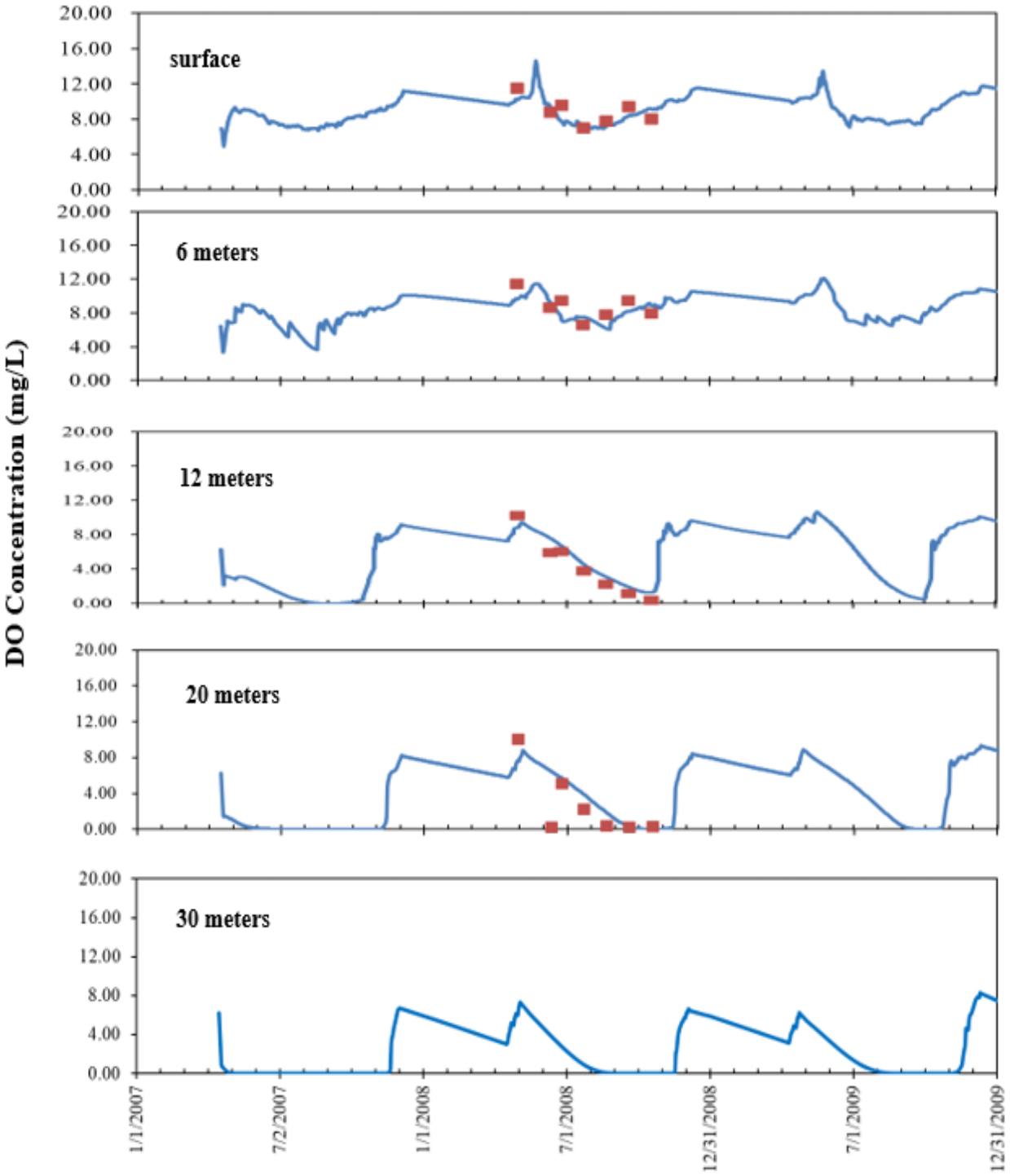

Figure 4.7 Simulated (solid line) and observed (dots) DO at (a) 1 m, (b) 6 m, (c) 12 m, (d) 20 m, (e) 30 m below the surface for Lake Elmo, April 2007 to December 2009.

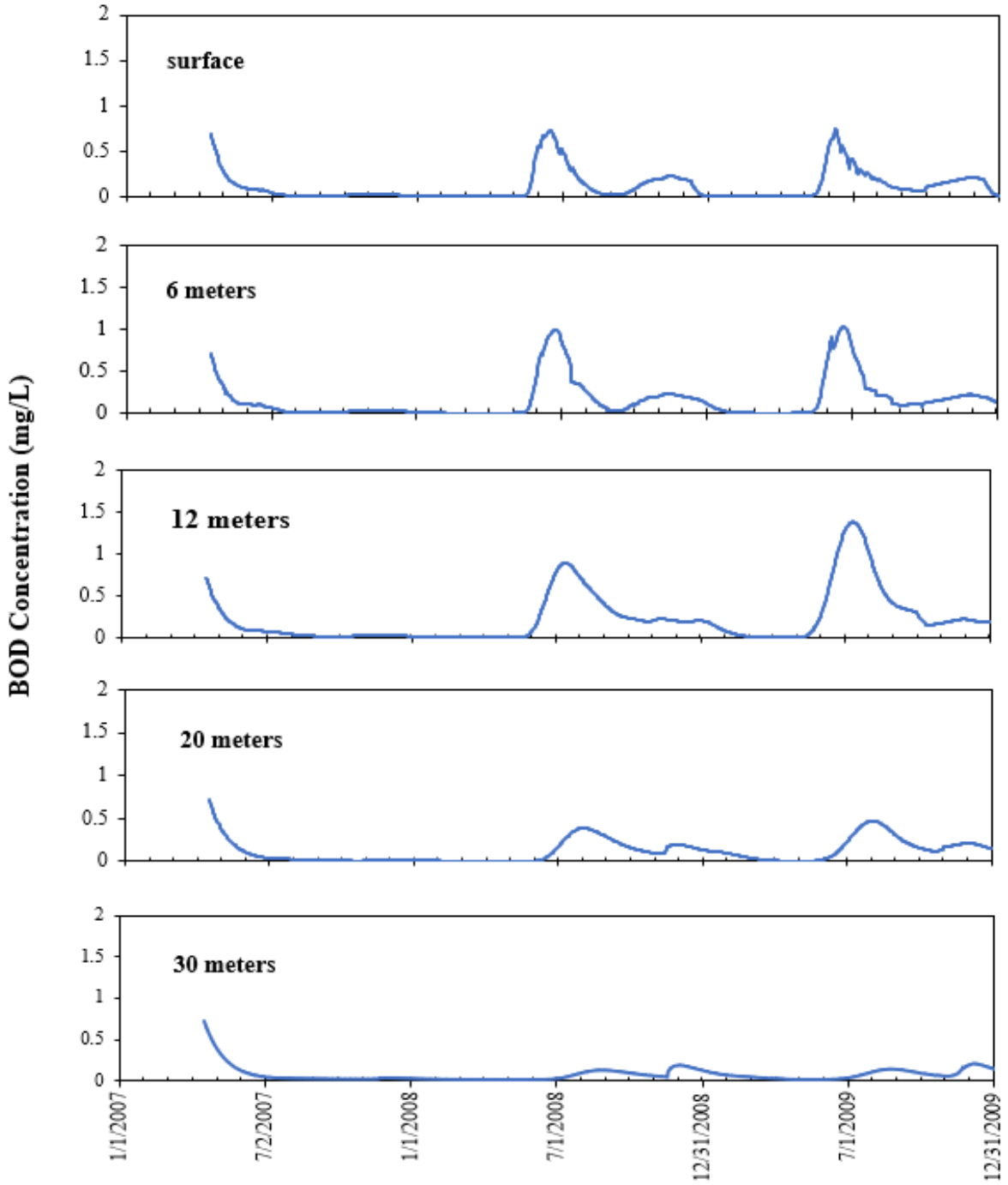

Figure 4.8 Simulated (solid line) and observed (dots) BOD at (a) surface, (b) 6 m, (c) 12 m, (d) 20 m, (e) 30 m below the surface for Lake Elmo, April 2007 to December 2009.

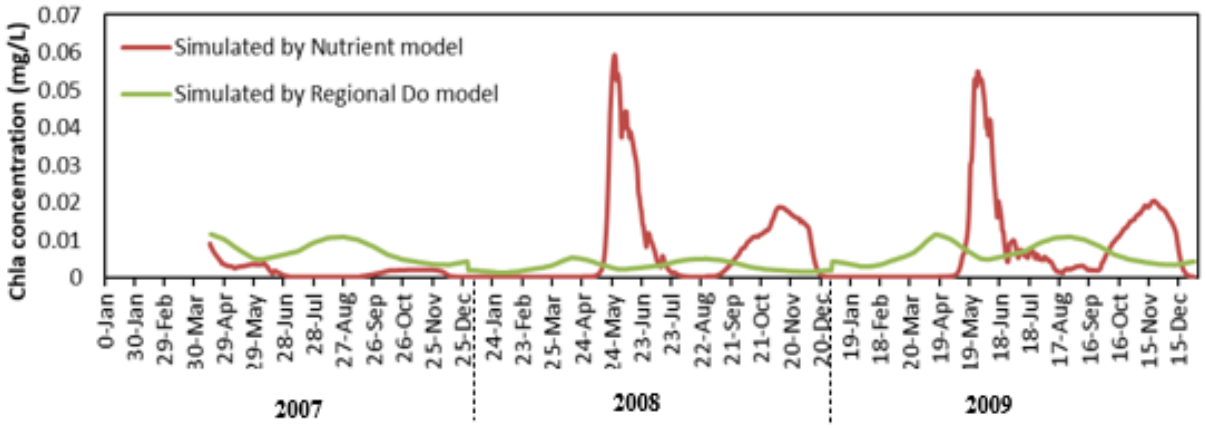

Figure 4.9 Comparison between simulated DO concentrations by two different simulation models: RegDO model and NCDO model

Phosphorus profile data of Lake Elmo were not available in 2007–2009. Lake Elmo was extensively monitored in 1988 and had measured phosphorus concentration data at five depths (0 m, 8 m, 16 m, 24 m, and 32 m) and dissolved oxygen data at 31 depths for open water season. The comparison between simulated and observed concentrations for phosphorus and DO at three days is presented in Figure 4.10. On April 11th, 1988, the lake is more or less well mixed and phosphorus concentration does not vary much throughout the depth but DO concentration gradually declines along depths due to the contribution of more sink terms (Equation 2.19) but for the profile plot, the slope is not steep. On 18th May 1988, the stratification increases and the simulated DO at the bottom is near to zero. On 19th October 1988, the Phosphorus near the surface layer is being used by the phytoplankton for growth. the lake became strongly stratified and the bottom layers of the lake become anoxic so that the phosphorus release from sediment contributed to the higher phosphorus concentration at the deeper depths – increase along depths from metalimnion and hypolimnion.

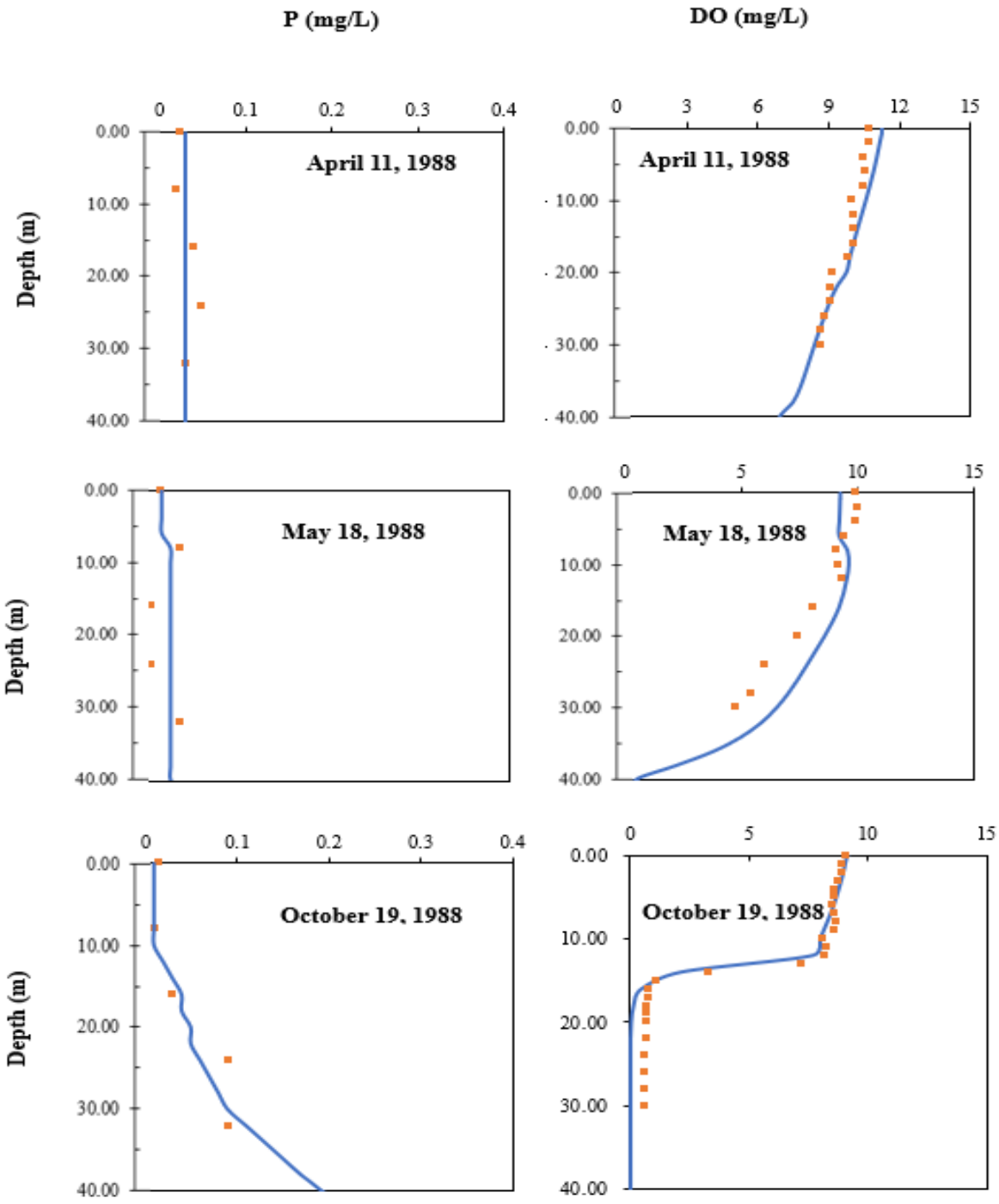

Figure 4.10 Simulated (line) and observed (dots) phosphorus and dissolved oxygen profiles for Lake Elmo, 1988

4.1.2 Long-term Simulation of Lake Elmo

West and Stefan (1988) tried multiple-year simulation using MINLAKE98 for lake Riley and Elmo. For Lake Riley, they could not simulate multiple years using the same set of calibration parameters. For Lake Elmo, the model could simulate successfully for 1985–1990. The regression coefficient for temperature and dissolved oxygen were 0.91 and 0.79, respectively. MINLAKE2020 model produced a much better result simulating the same lake for the same period. For a simulation of 1985–1990 using MINLAKE2020 NCDO model, the regression coefficient for temperature and DO are 0.9944 and 0.9715, respectively. Simulated phosphorus and chlorophyll-a concentrations at different depths were satisfactory as well. For a 30-year simulation (1979–2009) using MINLAKE2020 NCDO model, the regression coefficients for temperature and DO are 0.9888 and 0.9419, respectively. Moreover, the phosphorus and Chl*a* concentration at five simulation depths (1 m, 6 m, 12 m, 20 m, and 30 m) matches well with the available observed data. Observed Chl*a* and phosphorus data were available for 1980–1982, 1984, 1988, 1991, 1994, and 2005–2009. Figure 4.11 and Figure 4.12 present the comparison between simulated and observed Chl*a* and phosphorus at the surface. The simulated Chl*a* and phosphorus match reasonably well with the observed ones and the annual trend remains similar.

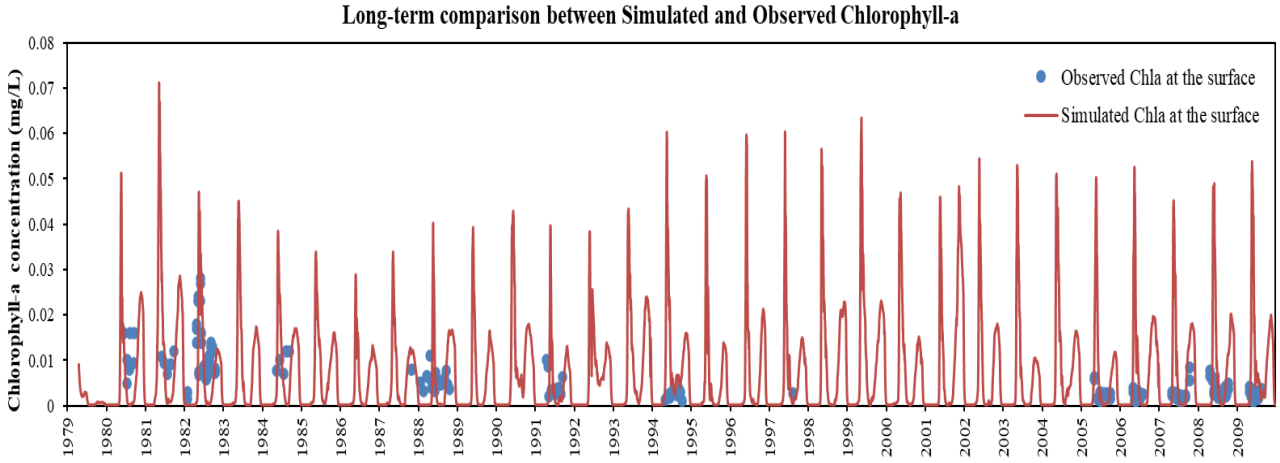

Figure 4.11 Simulated (line) and observed (dots) chlorophyll-a for long-term simulation of Lake Elmo from 1979 to 2009

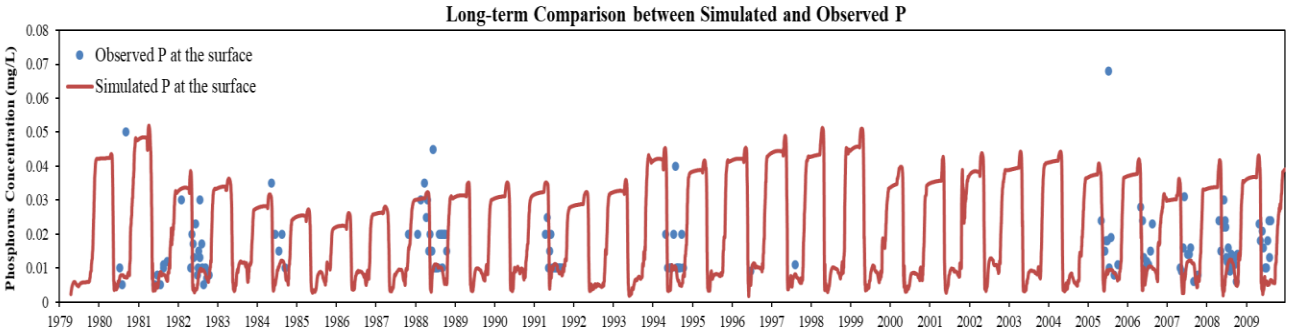

Figure 4.12 Simulated (line) and observed (dots) phosphorus for long-term simulation of Lake Elmo from 1979 to 2009

4.2 Lake Carrie simulation

MINLAKE2020 produced reproducible and satisfactory results for a 2-year and 30-year simulation for Lake Elmo. The model was also tested in a less stratified shallow lake, Carrie Lake in Minnesota, which has a maximum depth of 7.9 m. Unlike Lake Elmo, Carrie did not have MINLAKE2020 produced reproducible and satisfactory results for a 2-year and 30-year simulation

for Lake Elmo. The model was also tested in a less stratified shallow lake, Carrie Lake in Minnesota, which has a maximum depth of 7.9 m. Unlike Lake Elmo, Carrie did not have observed data for many years, we selected 2008–2010 as the simulation period that had an adequate number of days with field data for model calibration.

The lake has ice cover from late November to Mid-April as can be seen from Figure 4.13. The observed and simulated water temperature at 5 depths (1 m, 2.5 m, 4 m, 5.5 m, and 7 m) are presented in Figure 4.14. Near-zero temperatures are simulated to occur near the surface in late fall and winter. It can be concluded that the lake is not strongly stratified based on the differences between the maximum and average water temperatures at 1.0 m and 7.0 m, which are of 3.1 and 1.4 ^{o}C, respectively. The differences between simulated temperatures between 1 m and 7 m are less than 1.0 ^{o}C for 41.6% days during the open water seasons in 2008–2010. Simulated Chl*a* and phosphorus at 1 m, 2.5 m, 4 m, 5.5 m, and 7 m below the surface for 2008–2010 are presented in Figure 4.14. The lake is shallow and weakly stratified does not show a dramatic change of Chlorophyll-a over the depths (as observed for Lake Elmo). The seasonal pattern of the Chl*a* concentration remains the same throughout the depths. The Chl*a* concentration gradually decreases since the solar radiation is attenuated with depth. The lake has algal blooms in May 2009 and April 2010 after ice melting (Figure 4.15). That was because phosphorus is released from sediments when DO became anoxic under the ice cover periods for both 2009 and 2010 winter (Figure 4.16). There was small phosphorus release in the summer of 2008 and 2010 but it did not result in algal blooms (Figure 4.15). Gradually the algae die and add to the detritus biomass causing a decrease in algal biomass.

Figure 4.15 indicates that the lake experienced a much larger bloom in summer 2009 compared to summer 2010. Two reasons are contributing to this discrepancy: water temperature and nutrient availability. The simulated water temperatures in 2009 range from 20^{o}C to 25^{o}C for summer, which are respectively the optimum and maximum temperature set for this simulation. In 2010, the simulated water temperatures remain close to 25^{o}C and on some days, exceed 25^{o}C which hinders the algal growth. The phosphorus release in winter 2010 was simulated to be much lower than that of winter 2009 (Figure 4.16) due to a shorter ice cover period in 2010 (Figure 4.13).

Simulated BOD concentrations at five depths below the surface are presented in Figure 4.17. It can be observed that the BOD increases gradually from May 2009 to July 2009. The algal biomass from the algal bloom begins to die and adds to the BOD concentration. Therefore, simulated BOD from MINLAKE2020 directly corresponds to algal blooms. If there is a point source of BOD from somewhere (e.g. a wastewater treatment facility), it can be added from lake subroutine and the point source can be independent of algal blooms. It is also noticeable that the BOD at the surface layer is less than the BOD in the metalimnion. The algae after dying sink downwards and accumulate at more stable layers (metalimnion).

The zooplankton grazing at 1 m, 2.5 m, 4 m, 5.5 m, and 7 m below the surface is plotted together with chlorophyll-a concentration in Figure 4.18. The magnitude of Chla lost by grazing has very small magnitude. The grazing corresponds to chlorophyll-a but has a lag time. Grazing does not change much along the depth.

Simulated and observed DO concentrations match well at five depths (Figure 4.19). The DO concentration decreases with depth because of the low concentration of chlorophyll-a in the deeper layers plus sedimentary oxygen demands. The lake can be regarded as weakly stratified

based on the DO profiles in 2009 when summer bottom DO was above 4.0 mg/L in many days, while DO stratification in 2008 and 2010 was strong. Simulated DO at 5.5 and 7 m has some fluctuations in the summer of 2008 and 2009 due to a short period of strong mixing and results in anoxic conditions only in a few days. Stratification in 2010 summer was more stable with a steady anoxic condition about 1.5 months at the lake bottom. The anoxic conditions were also simulated at the end of winter ice cover periods in 2009 and 2010, which started from the lake bottom and reached 1 m below the ice. The ice cover period was shorter and ice thickness was smaller in the 2010 winter (Figure 4.13). These anoxic conditions during ice cover periods typically occur in shallow mesotrophic or eutrophic lakes (Fang et al., 2000) and result in high phosphorus concentration due to sediment release (Figure 4.15).

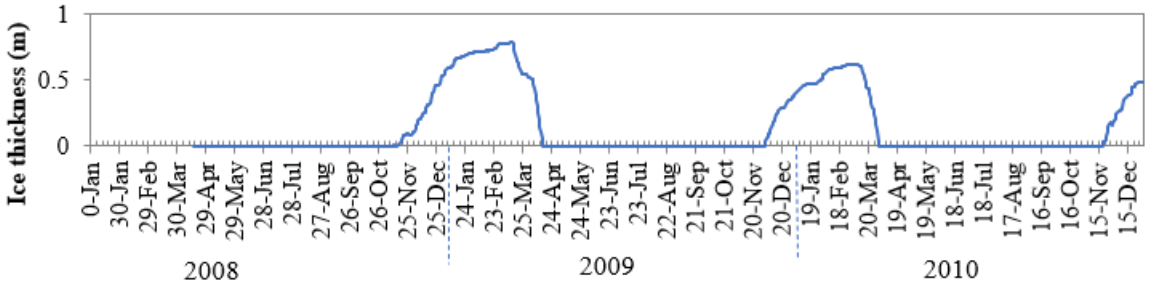

Figure 4.13 Simulated ice thickness on Lake Carrie in 2008–2010.

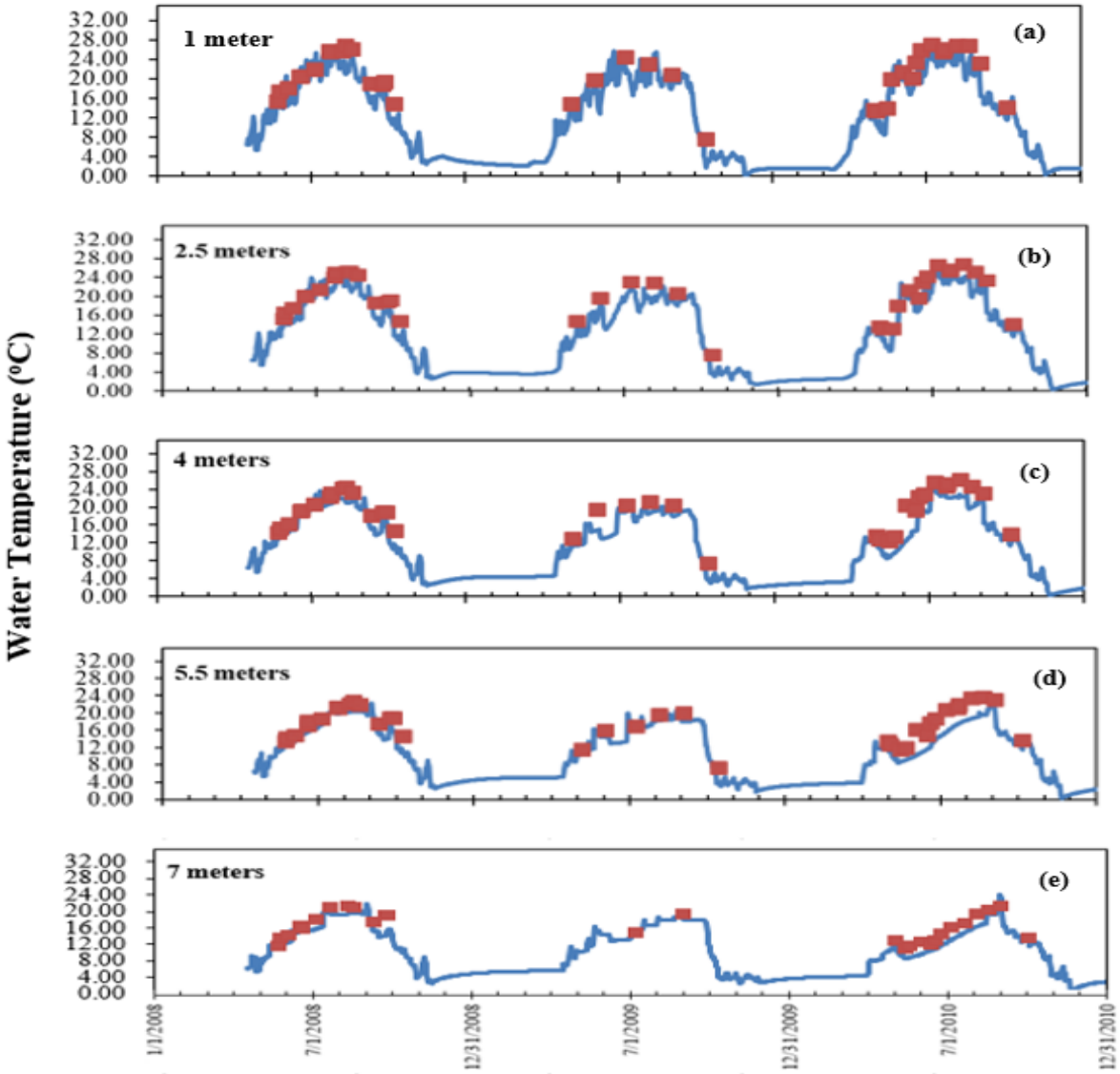

Figure 4.14 Simulated (solid line) and observed (dots) water temperature at (a) surface, (b) 2.5 m, (c) 4 m, (d) 5.5 m, (e) 7 m below the surface for Lake Carrie, April 2008 to December 2010

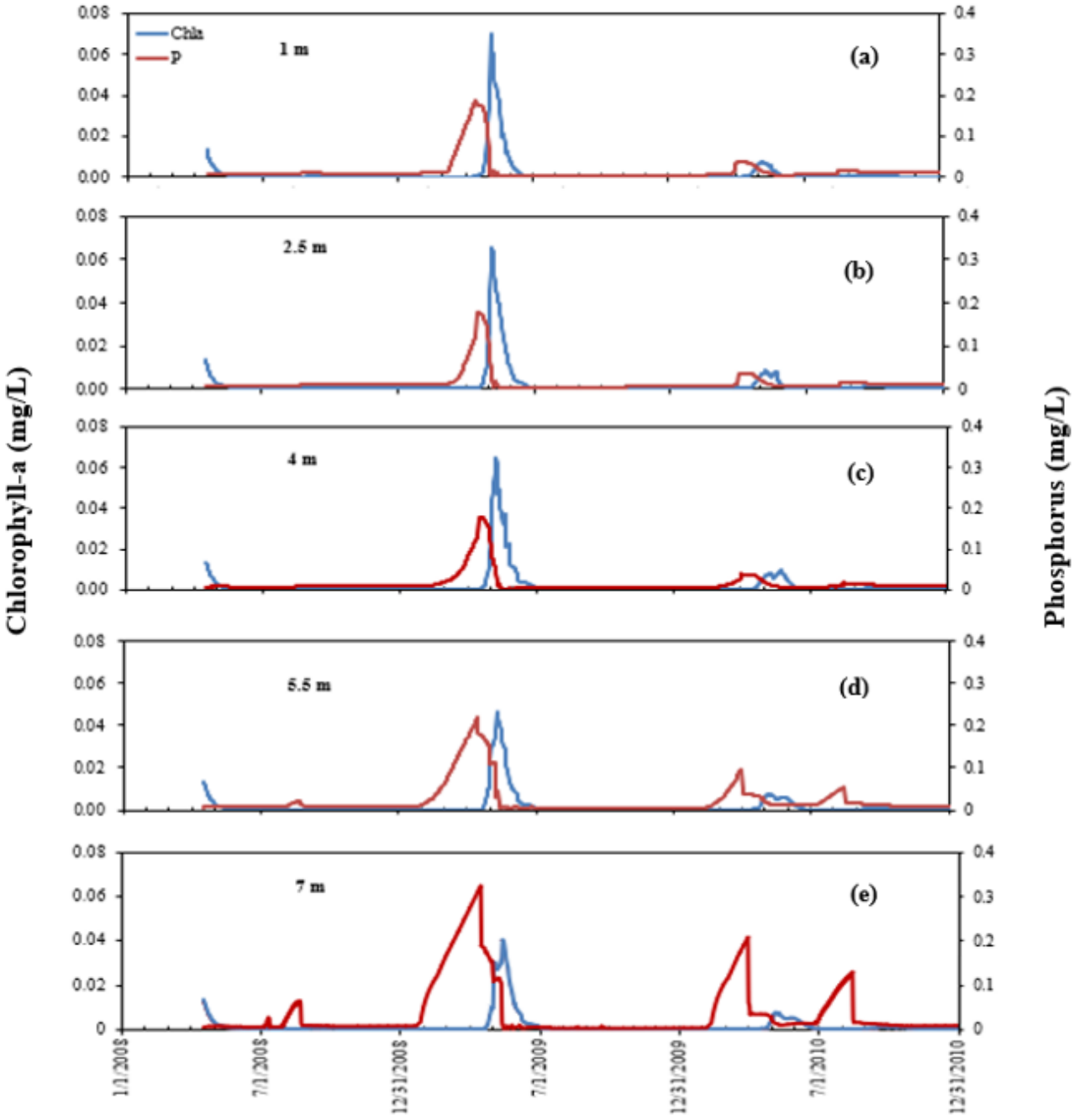

Figure 4.15 Simulated (solid line) and observed (dots) chlorophyll-a at (a) surface, (b) 2.5 m, (c) 4 m, (d) 5.5 m, (e) 7 m below the surface for Lake Carrie, April 2008 to December 2010.

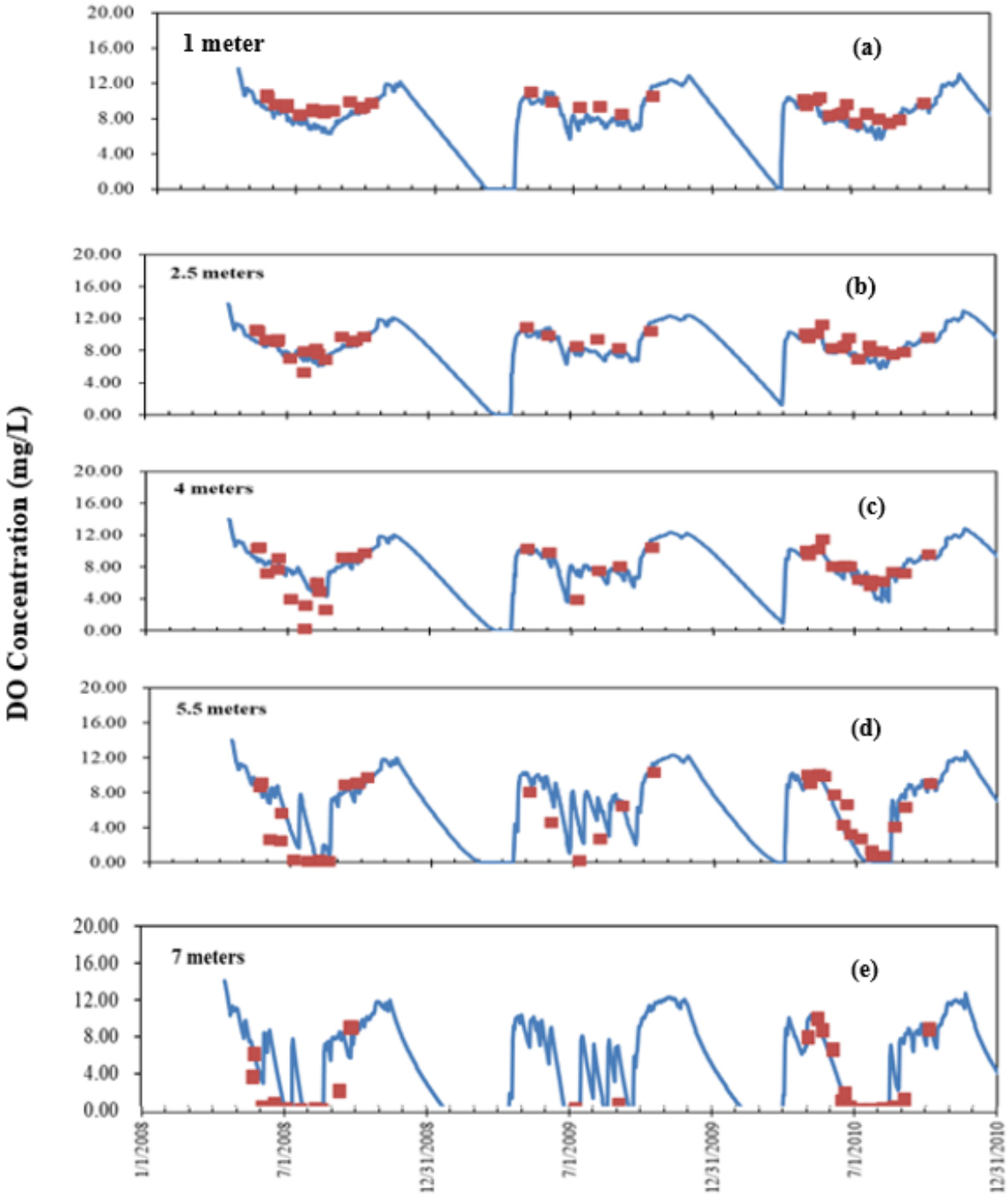

Figure 4.16 Simulated (solid line) and observed (dots) DO concentration at (a) surface, (b) 2.5 m, (c) 4 m, (d) 5.5 m, (e) 7 m below the surface for Lake Carrie, April 2008 to December 2010

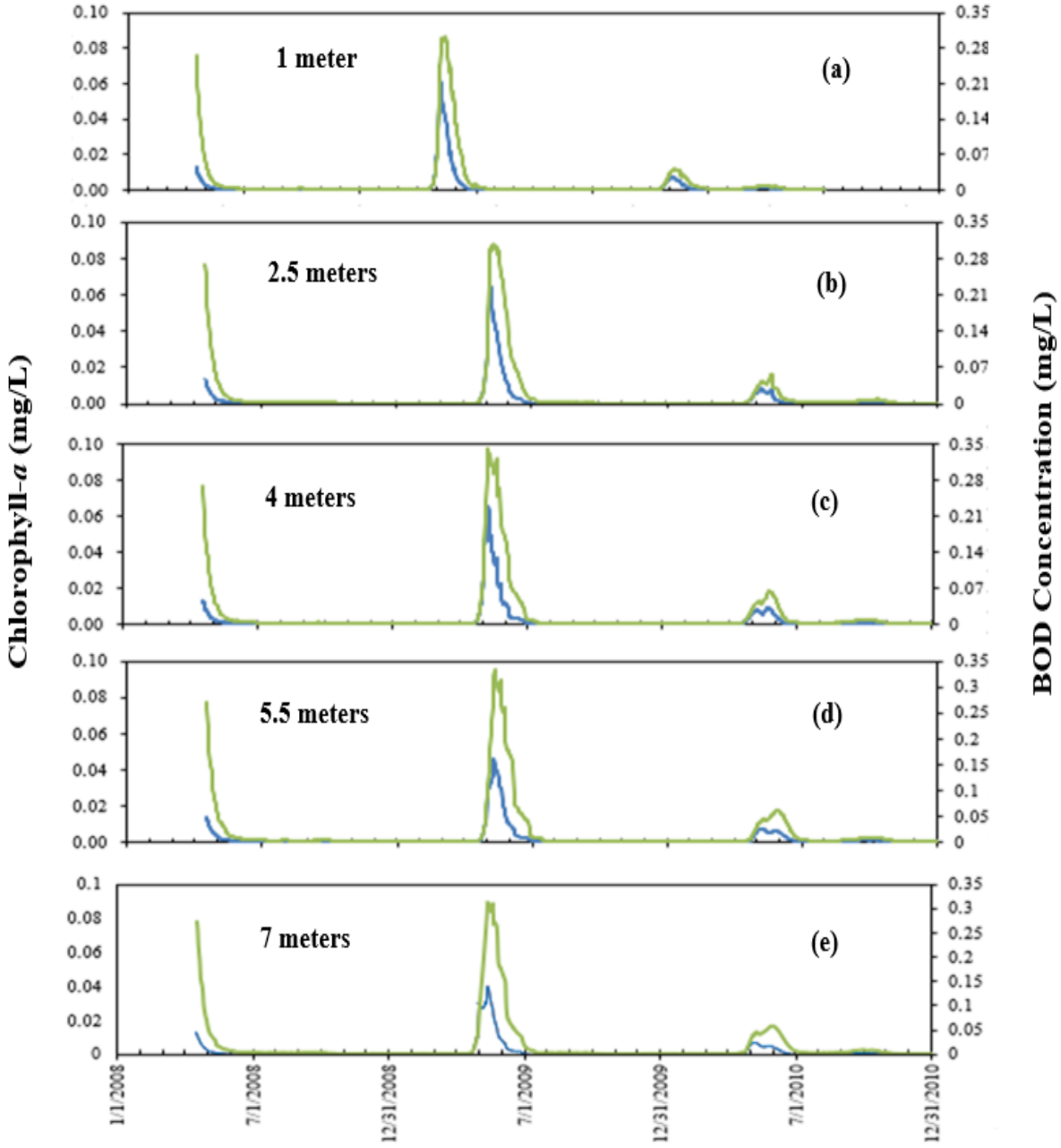

Figure 4.17 Simulated BOD and Chl*a* concentration at (a) surface, (b) 2.5 m, (c) 4 m, (d) 5.5 m, (e) 7 m below the surface for Lake Carrie, April 2008 to December 2010

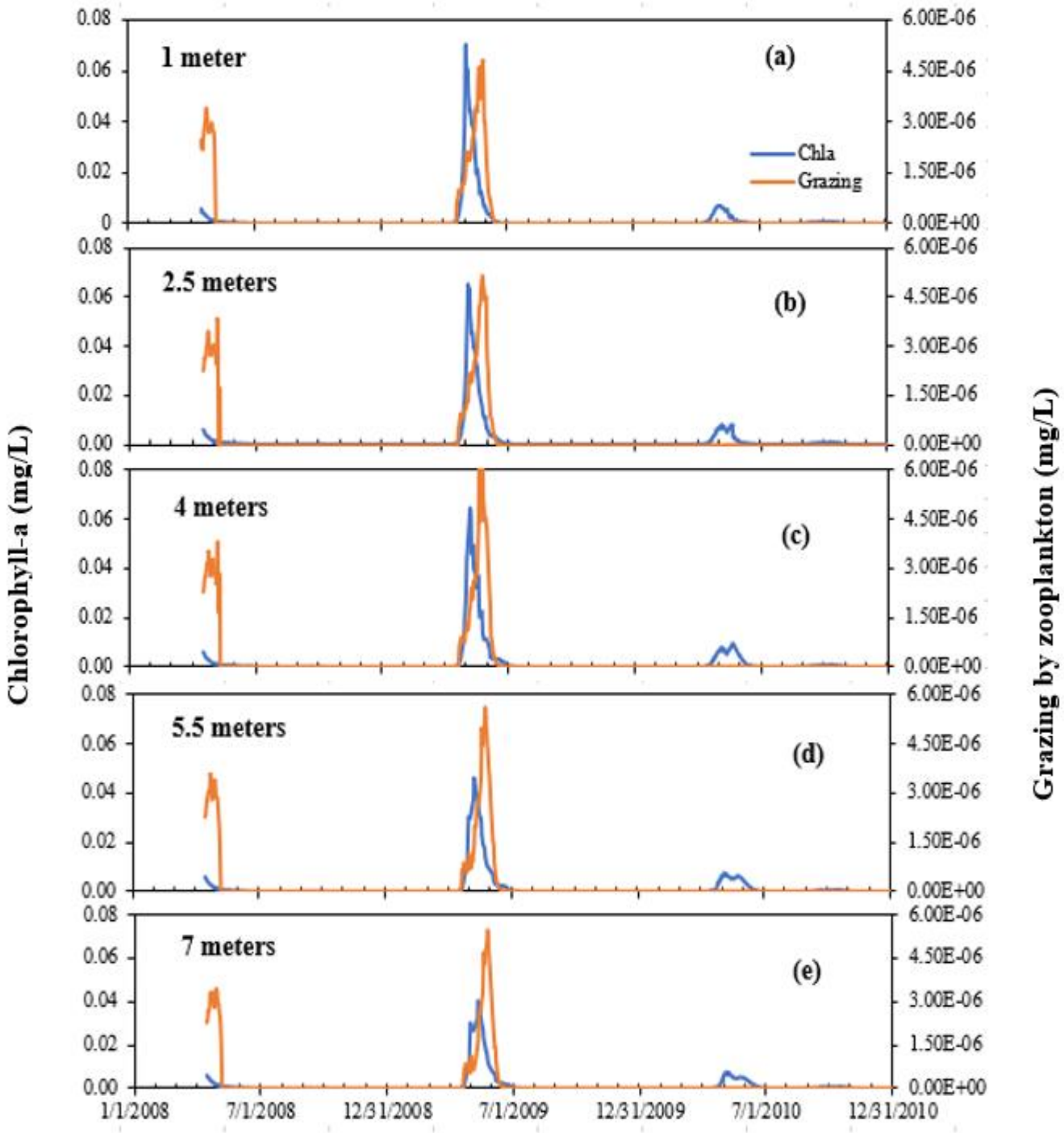

Figure 4.18 Simulated zooplankton grazing and Chl*a* concentration at (a) surface, (b) 2.5 m, (c) 4 m, (d) 5.5 m, (e) 7 m below the surface for Lake Carrie, April 2008 to December 2010

Lake Carrie had observed phosphorus data at the epilimnion and hypolimnion during the open water seasons for 2008–2010 that are compared with simulated phosphorus (Figure 4.19). The model simulated high phosphorus concentrations during the winter of 2009 but there are no winter phosphorus data for comparison. The simulated high phosphorus concentrations directly match well with the simulated anoxic DO conditions in 2009 and 2010 winters (Figure 4.16).

The simulated phosphorus does not vary much from April 16^{th,} 2008 to January 20^{th,} 2009. The lake has ice formation on the surface from November 2008 to April 2009 (Figure 4.13) but anoxic condition started in January 2009 from the lake bottom (Figure 4.16). The simulated DO at 1.0 m below the ice-water surface becomes anoxic at the beginning of February 2009. This results in increased release of phosphorus from the sediment and the phosphorus concentration begin to increase. In Mid-April, as the ice melts and the nutrients get unleashed into the water, an algal bloom occurs which utilizes phosphorus. The concentration of DO gradually increases at the surface and sediment phosphorus release decreases which result in a gradual decrease in phosphorus concentration during the summer of 2009. After this period, the processes governing the phosphorus concentration comes in equilibrium until April 2010.

The simulated phosphorus in April after ice melting is much higher than the observed data, but for other months matches reasonably well with the observed data. The phosphorus concentration at the bottom of the lake is much higher compared to the surface P concentration during the bloom. To better understand the relationship between DO and phosphorus, simulated DO and phosphorus are plotted together in Figure 4.20. During the winter, the bottom layer becomes anoxic and

sediment releases phosphorus to the water. During the spring after ice melts out, the lake water becomes warmer and algal bloom occurs.

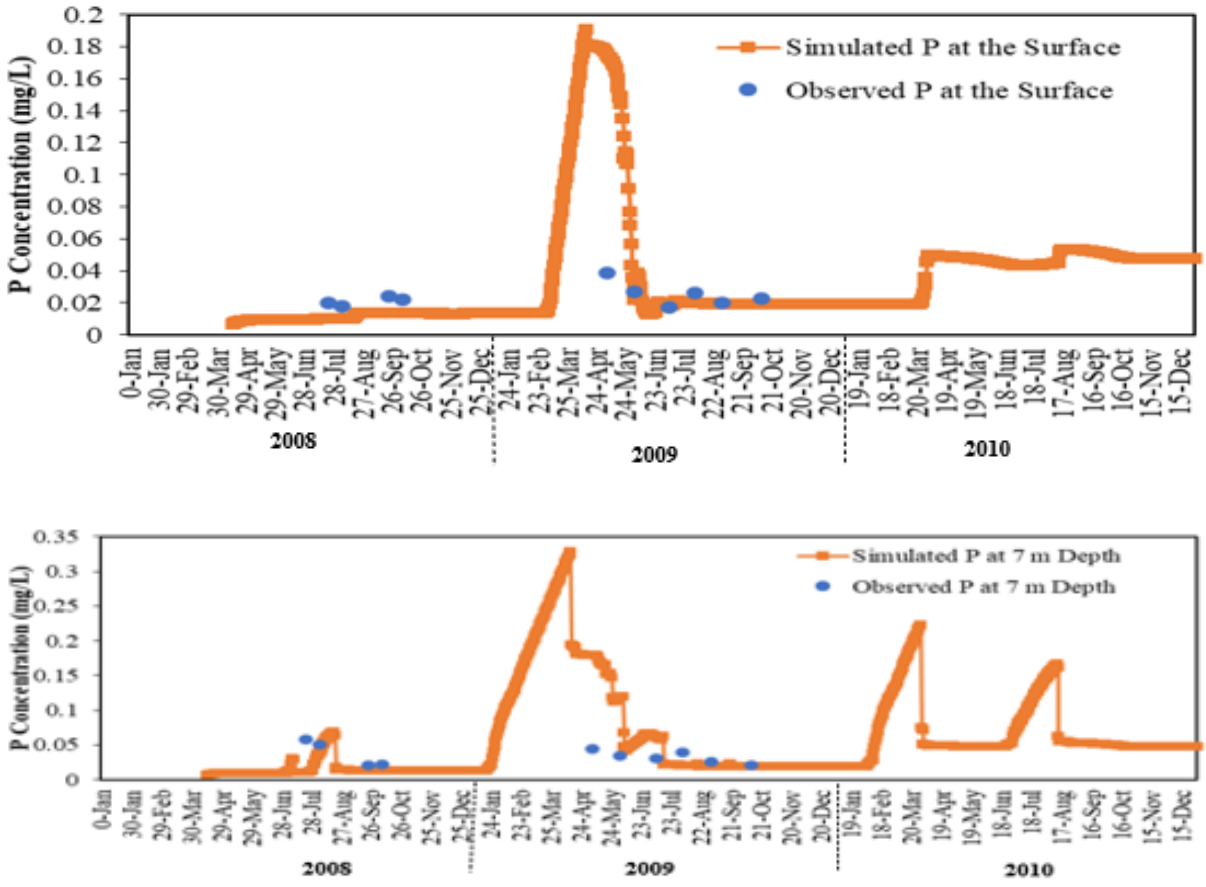

Figure 4.19 Simulated and observed phosphorus concentration at the bottom of Lake Carrie in 2008-2010

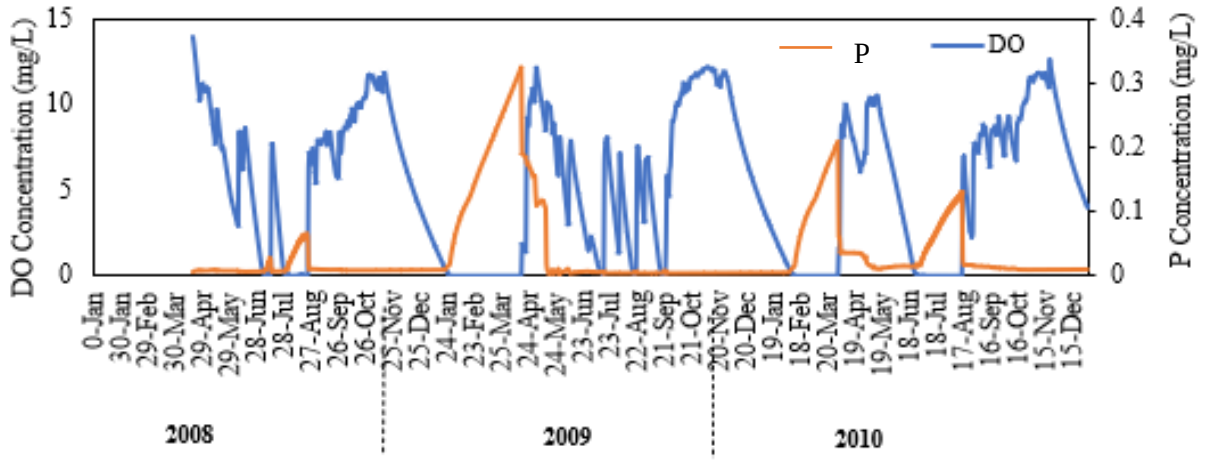

Figure 4.20 Simulated phosphorus and DO concentration at 7.0 m (near the lake bottom) of Lake Carrie in 2008-2010

Figure 4.21 presents phosphorus profiles of 3 days in 2008. It can be observed that on 4th July 2008, the lake is well mixed, and the small phosphorus concentration increases because of sediment release in the anoxic condition in the hypolimnion. On August 8th of 2008, the lake is stratified. The lake becomes well mixed again on September 13th, 2008.

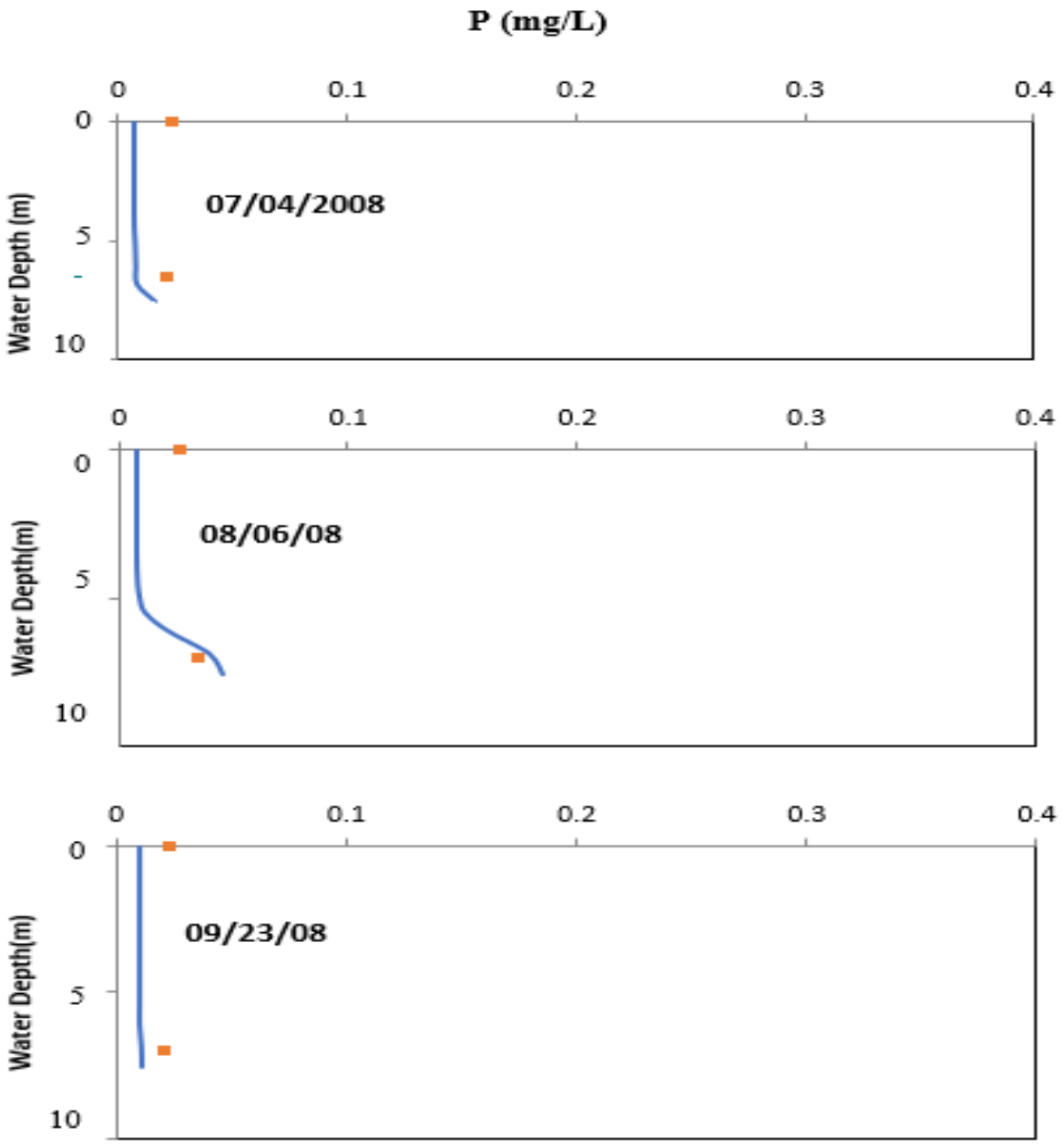

Figure 4.21 Simulated phosphorus with observed data for 3 selected days in 1988 in Lake Carrie

4.3 Pearl Lake Simulation

Deep lakes such as Lake Elmo does not exhibit a noticeable change in DO concentration based on the model used for simulation. However, Pearl lake, being very shallow, exhibits a noticeable change in DO concentration depending on the model (RegDO or NCDO model). Figure 4.22 shows the difference between the DO concentrations simulated by Model 3 (NCDO model) and Model 4 (RegDO model) and their comparison with the observed DO at the surface of Pearl Lake in 2010–2012. RegDO model overpredicts DO concentration throughout the simulation period except for March 2011. NCDO model results match well with the observed DO concentrations in 2010 and 2011. The model seems to underpredict DO in 2012 but the difference is in a reasonable range. Model 4's simulated DO concentrations soar up to 35 mg/L suddenly in early April 2011 under the ice cover when there was no snow, light permeated clear ice to have photosynthesis but surface reaeration was set to zero. The observed data in August–November 2011 matches well with the DO concentration simulated by the NCDO model whereas the RegDO model overpredicts DO to the highest magnitude difference of 10 mg/L for this period.

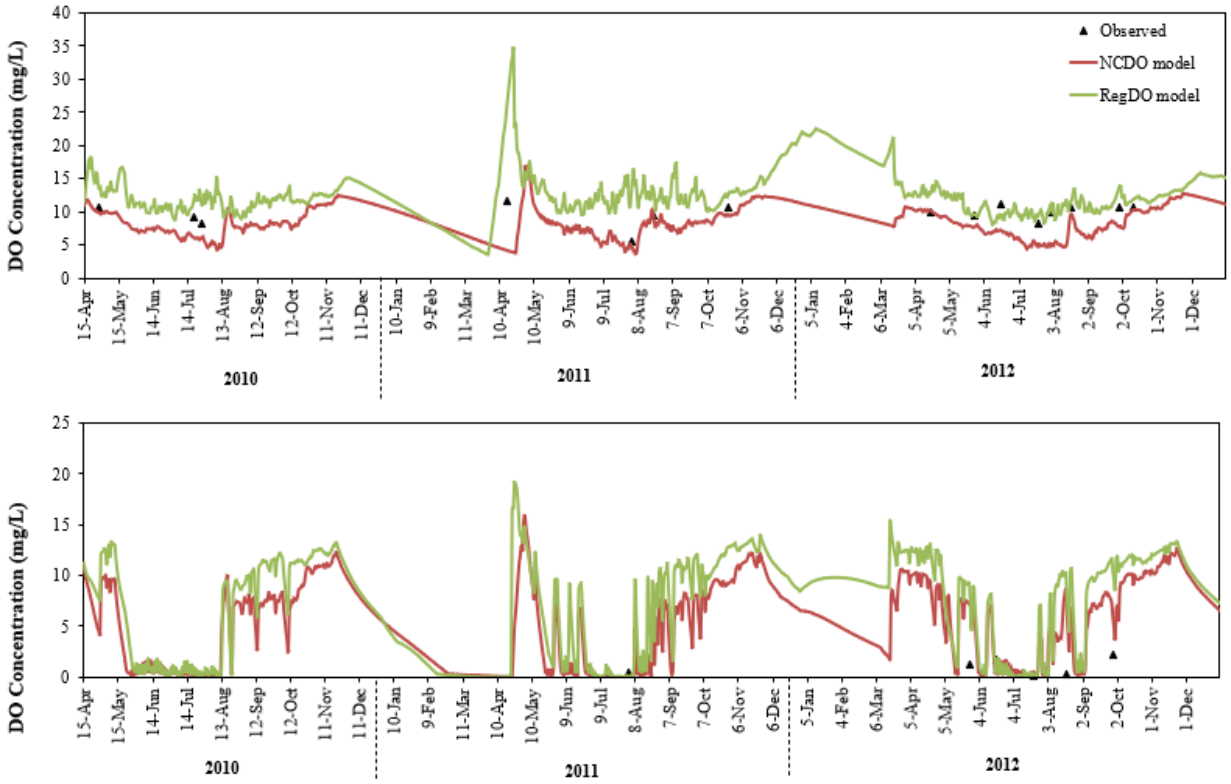

Figure 4.22 DO concentration at 1 m and 5 m depth of Pearl lake (2010 – 2012) using RegDO (Model 4) and NCDO (Model 3) model

A comparison between observed and simulated chlorophyll-a concentration in Pearl lake in 2010–2012 is presented in Figure 4.23. The observed pattern shows the trend of increasing chlorophyll-a in fall for all years and in summer for 2011. Fall turnover seems to be the influencing factor for an algal bloom. The simulated chlorophyll-a concentrations match well with the observed P concentrations except for some underprediction in summer 2012.

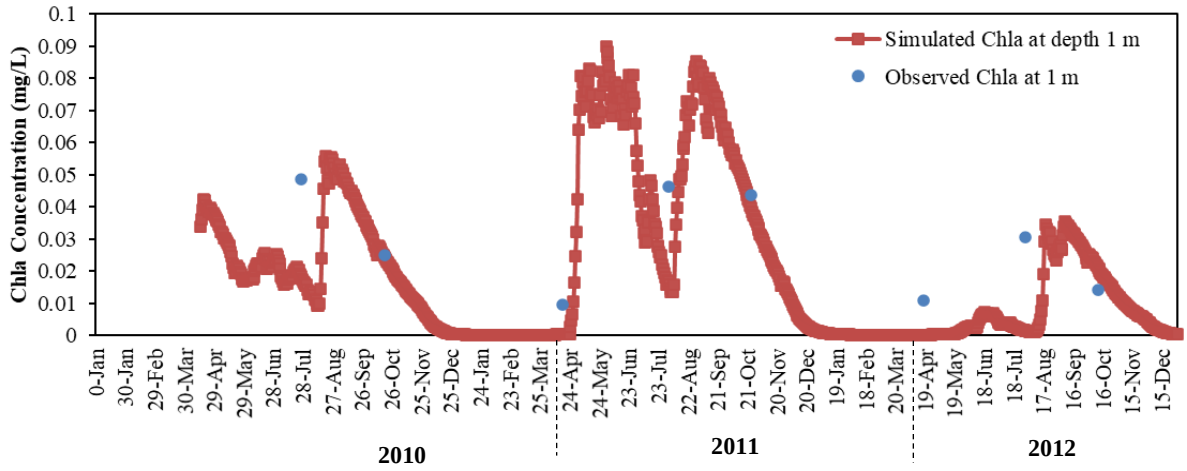

Figure 4.23 Comparison between simulated and observed Chlorophyll-a in Pearl lake in 2010-2012

4.4 Thrush Lake Simulation

For most of the lakes, only the surface chlorophyll-a data were available. Therefore, Thrush lake was chosen to be tested for Chl*a* simulation validation as it has Chl*a* data for both epilimnion and hypolimnion. The comparison between observed and simulated Chl*a* in Thrush lake is presented in Figure 4.24. The simulated Chl*a* at 1 m and 11 m were selected to be compared with the observed epilimnion and hypolimnion Chl*a* concentrations, respectively. Thrush lake is an oligotrophic lake. Hence, the Chl*a* concentrations in Thrush lake is much lower than that of the other simulated lakes. The simulated Chl*a* matches well with the observed Chl*a* concentrations at the epilimnion except for some overprediction from August 1986 to October 1986. However, in the hypolimnion, on 7/15/1986 and 8/12/1986, the observed Chl*a* is unusually high, even higher than the epilimnion. Overall, the model underpredicts chlorophyll-a for hypolimnion.

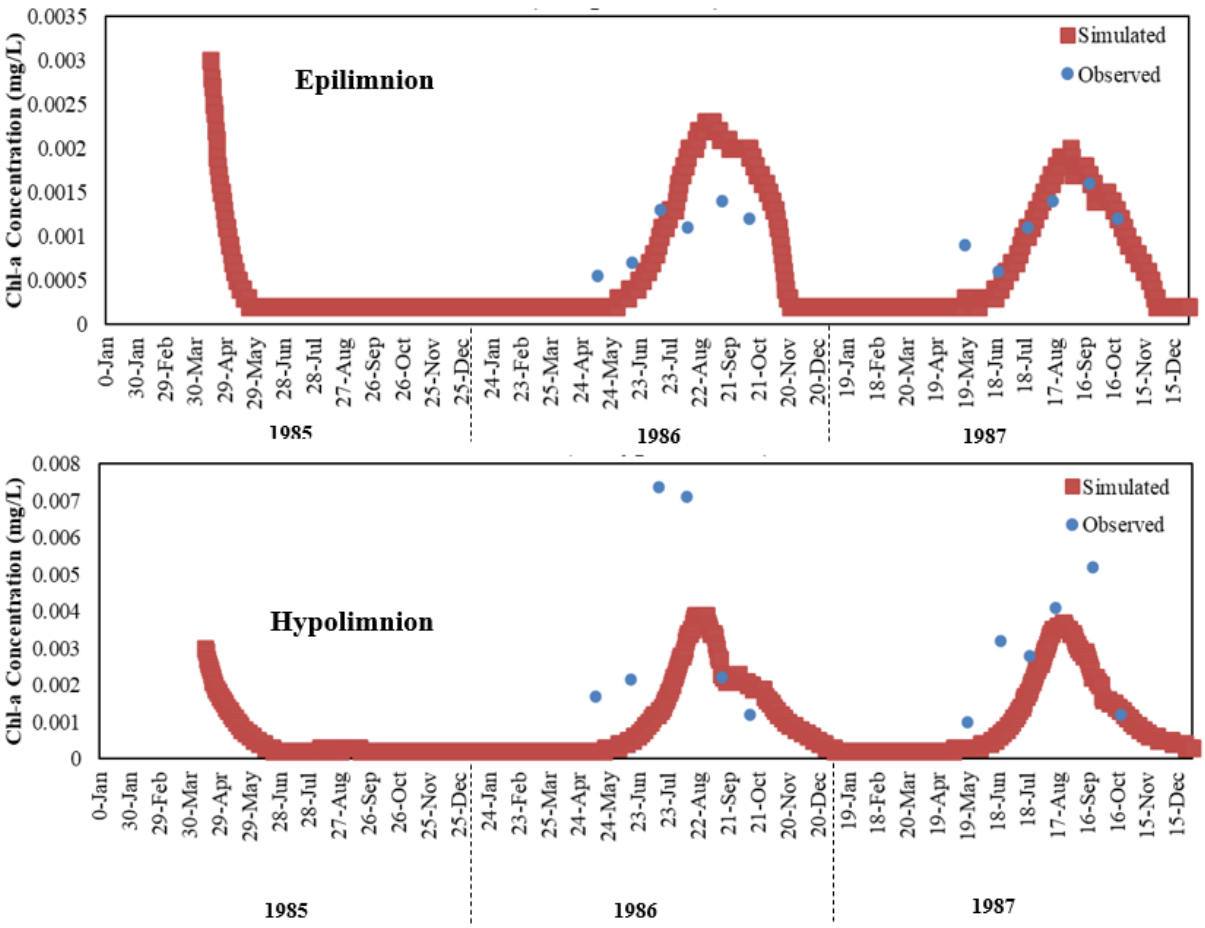

Figure 4.24 Comparison between simulated and observed Chl*a* in epilimnion and hypolimnion of Thrush lake in 1985-1987

4.5 Other Lakes Simulation - Riley and Carlos

Another medium depth lake, Lake Riley was also simulated for this study. Riley lake has data files for lake inflow and outflow from 1982 to 1983, which will be beneficial for the future study of MINLAKE2020. The simulation results of Lake Riley are presented in Appendix A.

Lake Carlos is a very deep lake in Minnesota. It is a mesotrophic and strongly stratified lake with a geometry ratio of 1.15. In Figure 4.25, a comparison between simulated and observed Chl*a* is presented for Lake Carlos in 2008–2012. Long-term simulation for a deep stratified lake is

challenging, especially without any data on the growth rate, zooplankton population, etc. From Figure 4.25, it can be observed that the lake follows a similar pattern for Chl*a* concentration in each year. The simulated and observed Chl*a* match closely in 2009 and 2012. In 2010 and 2011, the model underpredicts the chlorophyll-a concentration at the surface. The simulated phosphorus concentration follows the trend of the observed phosphorus data. The simulated phosphorus matches pretty well with the observed data as shown in Figure 4.26.

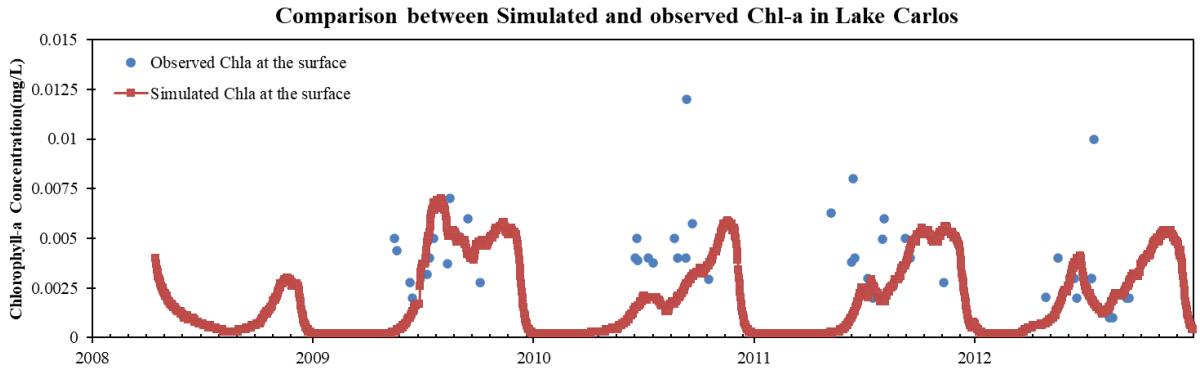

Figure 4.25 Simulated and observed Chl*a* concentration at the surface of Carlos lake

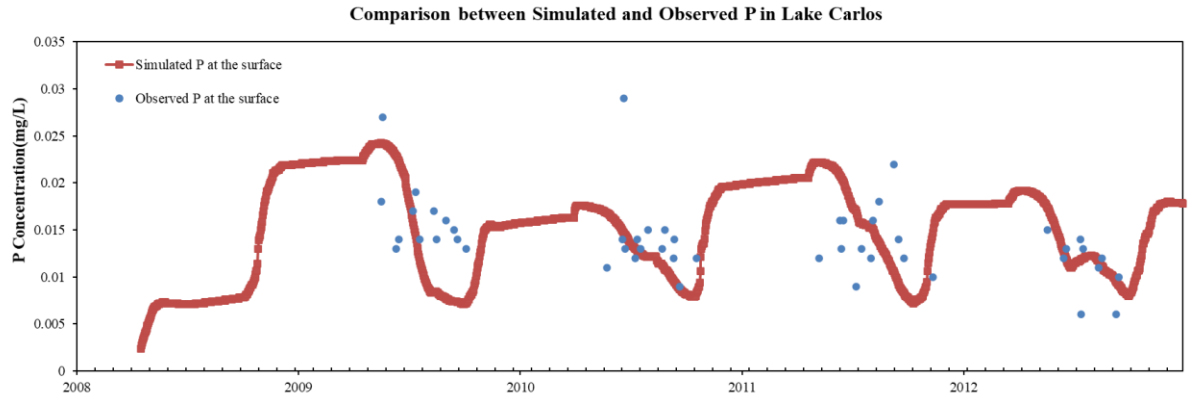

Figure 4.26 Simulated and observed P concentration at the surface of Carlos lake

4.6 Calibration Results

4.6.1 Calibration Parameter Values

To get better results from the model, some model parameters were calibrated for the six Minnesota lakes selected for the study. The calibrated values of the parameters are given in Table 4.1.

The study lakes had few days of observed data. The simulation period was selected based on the available observed data for temperature, DO, Chl*a*, and phosphorus. Most of the lakes were calibrated for a short period span (2–4 years). Lake Elmo was first calibrated for 2007–2009 but later the same calibration parameters were used for 30 years simulation (1979–2009). At first, the model was calibrated based on the water temperature model. Both time series and water temperature profiles were used for model calibration. Then the model was calibrated for the nutrient model. Algal growth rate, respiration rate, mortality rate, sediment phosphorus release, and yield coefficient of P to Chl*a* was calibrated simultaneously looking at the Chl*a* and P time series data. Most of the lakes had Chl*a* data for the surface layer only. The model was further calibrated for the detrital decay rate and SOD coefficient at 20^{o}C. If any of the parameters need further calibration, the parameter can be recalibrated based on the observed data. One challenge in calibrating the nutrient model is that one calibration parameter can affect several water quality variables. For example, the half-saturation coefficient of phosphorus affects Chl*a*, phosphorus, and DO simulation. The user might get satisfactory results for DO but not for Chl*a* and phosphorus. So, it is important to check on all the related water quality variables while calibrating the model. The model seems to be more sensitive for some parameters, and additional sensitivity analysis will be performed for Lake Elmo and other lakes.

Table 4.1 Calibrated values of parameters for MINLAKE2020 for six study lakes

Calibration Parameter	Unit	Calibrated value for lakes											
		Pearl		Carrie		Thrush		Riley		Riley		Carlos	
W_{str} (Summer, Fall)		0.6	0.6	1	0.5	0.5	0.2	0.7	0.2	1	0.6	1	1
K_{BOD}	/day	0.1		0.1		.05		.07		.05		0.1	
Sb20	$g/m^2/day$	1.5		0.75		0.2		2		1.7		0.5	
EMCOE(1)		1		2		3		0.5		1		1.5	
EMCOE(2)		1.5		1		3		3		1		2.2	
EMCOE(4)		1		3		0.5		1.5		1		1	
EMCOE(5)		1		1		1		1		1		1	
G_{max}(K)	/day	3	3	3	3	0.5	0.5	1.5	1.5	3	3	0.6	0.6
K_r(K)	/day	.03	.03	.09	.09	.04	.05	.04	.05	.09	.09	.03	.03
K_m(K)	/day	.015	.015	.03	.03	.03	.03	.03	.03	.05	.05	.03	.03
K_P(K)	m/day	.03	.03	.09	.09	.02	.03	.02	.03	.09	.09	.06	.06
V(K)	m/day	0.1	0.1	.25	.18	.2	.1	.2	.1	.25	.18	.25	.15
V(BOD)	m/day	0.1		0.15		0.15		0.13		0.15		0.15	
S_P	g/m^2-day	.01		.01		.01		.02		.01		.03	
T_{opt}(K)	^oC	20	20	20	20	25	25	27	27	20	20	20	20
T_{max}(K)	^oC	25	25	25	25	32	32	42	42	25	25	30	30
T_{min}(K)	^oC	0	0	3	10	0	0	0	0	3	10	0	0
ZP	$/m^3$	100		900		500		1300		500		10000	
ZPMIN	$/m^3$	10		50		10		100		10		200	
YPChl*a*	mg P/mg Chl*a*	0.4		1.1		1.1		1.1		0.4		0.9	

Note: K is the number of total algal classes

4.6.2 Effect of Calibration on Results

MINLAKE2020 has several parameters that need to be calibrated. Most of the parameters have a range of values suggested by other researchers from previous studies or based on model development theoretical background as described in section 2.2. Lake Riley and Lake Elmo were originally simulated using MINLAKE98 (West and Stefan, 1998). However, since MINLAKE2020 differs from MINLAKE98 and the simulation period was different, the calibration parameters used in MINLAKE98 could not be used for Lake Elmo 2007–2009 or 1979–2009 simulation. MINLAKE2020 could simulate water quality for both of these periods using the same set of calibrated parameters. This is a major advantage of MINLAKE2020 over MINLAKE98.

Lake Riley was simulated using the set of calibration parameters used in MINLAKE98 report since the same period was simulated. Most of the parameter values worked well. One of the most sensitive parameters for MINLAKE2020 is the settling velocity of algae. If the settling velocity is too large or too small, the model cannot operate. The settling velocity needed to be recalibrated for Lake Riley as the listed values caused the Chl*a* to become too large to simulate. In Table 4.2, the lists of calibration parameters and their suggested values are given for Lake Elmo.

For Chl*a* simulation, the most sensitive parameter was the settling velocity. If the settling velocity is too low or too high, the model will stop because of unreasonable Chl*a* concentration. Another important parameter that plays a vital role in MINLAKE2020 calibration is the zooplankton population and the minimum zooplankton population for predation. Zooplankton population is hard to predict without any observed data. A range of values was tested and the one giving the most reasonable result was chosen.

Optimum, minimum, and maximum temperatures are also important calibration parameters for algal growth. The combination of these three temperatures is very important for accurately simulating Chl*a*. For phosphorus and chlorophyll-*a* calibration, the benthic release rate (BRR), Mass yield ratio of phosphorus to chlorophyll-*a* (YPChla), and the half-saturation coefficient of phosphorus (HSCPA) are very sensitive parameters (Table 4.2). The combination of these three parameters correlates the Chl*a* and P concentration in MINLAKE2020. Though these parameters have very minimal effect on DO, they are very important for accurately simulating Chl*a* and P. For some lakes, if the considered BRR is very high, the Chl*a* will get out of range and the simulation will stop. Model parameters EMCOE(2), EMCOE(1), Sb20, and BODK20 are calibration parameters which were also used in MINLAKE2012. Among them, sediment oxygen demand at 20 ^{o}C (Sb20) is the most sensitive one for DO and P simulation.

Table 4.2 Calibration parameters used in MINLAKE2020 for Lake Elmo with a regression coefficient of the DO simulation

Sensitive Parameters	Description of Parameter	Uncalibrated value	Calibrated Value	Regression Coefficient (before calibration)	Regression Coefficient (after calibration)
BODK20	Detrital Decay rate	0.5	.05	0.8787	0.9247
SB20	SOD coefficient at 20^{o}C	0.5	1.7	0.5625	0.9247
ZP	Zooplankton population	2000	500	0.8695	0.9247
ZPMIN		100	10	0.8739	0.9247
PREDMIN		.1	.03	0.874	0.9247
FVCHLA(K+1)	Settling Velocity for algae and detritus	.05, .05, .05	0.25, 0.18, 0.15	0.8886	0.9247
TMAX(K)	Maximum temperature for algal growth	42, 42	25, 25	0.8877	0.9247
TMIN(K)	Minimum temperature for algal growth	0, 0	3, 10	Stopped at 4/1/09	0.9247
TOPT(K)	Optimum temperature for algal growth	27,27	20, 20	0.8877	0.9247
EMCOE(2)	Multiplier for calibrating SOD below euphotic zone	3	1	0.9146	0.9247
EMCOE(1)	Multiplier for calibrating diffusion in metalimnion	3	1	0.8877	0.9247
BRR	Benthic Phosphorus release rate	.001	.01	0.8856	0.9247
YPChl*a*	Mass yield ratio of P to Chla	1.1	0.4	0.8886	0.9247
HSCPA	Half saturation coefficient of Phosphorus	.02, .03	.09,.09	0.8854	0.9247
Gmax	Maximum growth rate of algae	1, 1	3, 3	0.886	0.9247
XKR2	Algal respiration rate	.03, .03	.09, .09	0.8385	0.9247
XKM	Algal mortality rate	.015, .015	.05, .05	0.9136	0.9247

4.7 Statistical Parameters

The statistical parameters were calculated for all of the simulated lakes for temperature and dissolved oxygen. Since the observed data for Chl*a* and phosphorus were scarce, the statistical analysis for them was not developed. The temperature model was not changed much (except for the change in sediment temperature model), so the statistical parameters for temperature simulated by MINLAKE2020 and MINLAKE2012 were not compared. We have compared the statistical parameters for DO simulated by MINLAKE2020 and MINLAKE2012. The regression coefficient R^2, the root mean square error (RMSE) in mg/L, and the Nash-Sutcliffe efficiency were calculated and are summarized in Table 4.3.

Table 4.3 Statistical Parameters for six lakes

Lake Name	Simulation Period	MINLAKE2020 (DO)			MINLAKE2012(DO)		
		RMSE (mg/L)	NSE	R^2	RMSE (mg/L)	NSE	R^2
Elmo	2007-2009	2.02	0.70	0.92	1.89	0.70	0.92
Carlos	2008-2010	2.39	0.61	0.90	6.06	-1.54	0.79
Riley	1982-1983	3.28	-0.14	0.85	3.08	0.38	0.85
Thrush	1985-1987	2.43	0.40	0.92	4.55	-1.09	0.88
Carrie	2008-2010	1.95	0.70	0.93	1.98	0.69	0.94
Pearl	2010-2012	3.42	-0.12	0.87	4.34	-0.80	0.87

The R^2 shows the goodness of fit between observed and simulated data. The closer it is to 1, the better the fit is. Nash-Sutcliffe Efficiency (NSE) is an important parameter to evaluate model performance. The predictions with an NSE value greater than 0.5 is considered to be good. The RMSE indicates the error associated with the predictions and their criteria depend on the magnitude of the original value.

From Table 4.3, we can see that the statistical parameters for DO do not vary much for lake Elmo. For Carlos, Thrush, and Pearl lake, the statistical parameters show better performance of

MINLAKE2020 DO simulation. In Riley Lake, though the R^2 remains the same for DO simulation, the RMSE and NSE indicates better results from MINLAKE2012 Regional DO model

4.8 Stratification

One of the main objectives of MINLAKE2020 model is to account for lake stratification so that it can accurately predict water quality parameters in all layers. The reservoir model in SWAT assumes the lakes to be well-mixed which does not apply to most of the lakes. Figure 4.25 shows that Lake Elmo was very strongly stratified in 2008. The simulated DO differences between 1 m and 40 m depth were much greater than 1 mg/L (stratification criteria) in all seasons. In Lake Carrie, the stratification changes abruptly with time during the spring and summer for a shallower, weakly stratified lake. Typically, the differences of 1 ^{o}C in temperature and 1 mg/L in DO are used for the stratification threshold limit.

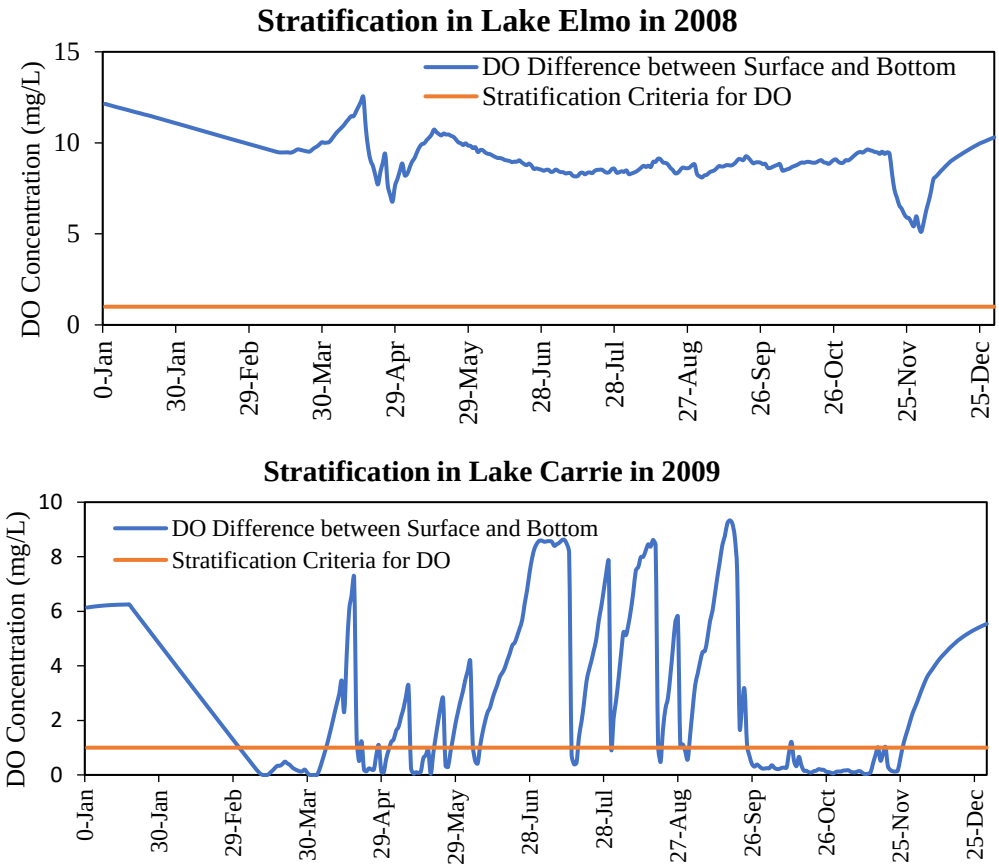

Figure 4.27 Simulated DO stratification in Lake Elmo and Lake Carrie

Chapter 5 Conclusions

5.1 Summary

Water quality is an important issue in the modern world. Several water quality models have been developed for different types of water bodies such as rivers, lakes, estuaries, and reservoirs. SWAT is a widely used model for water quality simulation of watersheds. SWAT assumes reservoirs (lakes) as well mixed waterbody which is not the real scenario in most of the cases. A simple one-dimensional daily lake model, MINLAKE was chosen to be integrated with SWAT modeling for simulating the lakes inside the watershed. Hence, a simple nutrient-chlorophyll-a-DO or NCDO model was developed and integrated with MINLAKE2012 to develop the final model, MINLAKE2020. MINLAKE model is comprised of many sub-models. MINLAKE2012 model simulates water temperature and DO in lakes with no significant inflows and outflows. It predicts the water temperature and DO in response to the ambient weather conditions such as solar radiation, air temperature, dew point temperature, wind speed, wind direction, sunshine percentage, and precipitation (snow and rain). A simplified Chla pattern (from the observed data) was used to predict daily Chla concentration in this model. In MINLAKE2020, separate sub-models were added for chlorophyll-a (representing phytoplankton) phosphorus and BOD. The DO model was modified accordingly to integrate the simulated nutrient and chlorophyll-a and zooplankton grazing.

MINLAKE is a reliable lake modeling tool used for different types of lakes over the years. Though the RegDO model provides satisfactory results for DO simulation, it cannot give the overall picture of the lake water quality due to simplified assumptions. For example, MINLAKE2012 cannot predict algal bloom in lakes which is a rising issue for many reservoirs. Therefore, in this study, the effort was made to provide the decision-makers and lake management

teams a more detailed yet simplified water quality model that can predict the water temperature and dissolved oxygen (DO) as well as the chlorophyll-a and nutrient concentration for each day. The one-dimensional deterministic water quality model MINLAKE2012 was reviewed carefully (section 2.1) and was modified to generate MINLAKE2020 (sections 2.2 and 2.3). The modification of the model incurred several model calibration parameters (section 3.2).

Six lakes were simulated using MINLAKE2020. The model was first tested in Lake Elmo simulation as this lake had calibration data from a previous study by West and Stefan (1988_. Lake Elmo produced reliable results for short term (2007–2009) and long-term (1979–2009) simulation (section 4.1). The lake was also simulated for another deep lake, Lake Carlos. The phytoplankton simulation of deep lakes showed a certain trend for every year. The model was tested for shallow lakes as well (section 4.2). The simulated values of chlorophyll-a and phosphorus were compared with that of the observed data. MINLAKE2020 produced satisfactory results for all lakes. In shallow lakes, the phytoplankton concentration changed abruptly because of mixing. In deep lakes, the difference in Chla simulation did not produce different DO values. On the contrary, in shallow lakes such as Pearl, the NCDO model simulation results are better aligned with the observed DO data than the RegDO simulation results.

5.2 Conclusions

The daily MINLAKE2020 model has been developed from MINLAKE2012 model and is capable of predicting the daily chlorophyll-a, phosphorus, BOD concentration in addition to water temperature and DO in stationary lake waters. The statistical results comparing simulated and measured water temperature and DO profile data show that the NCDO model works better than the RegDO model, especially in shallow lakes. MINLAKE2020 can successfully predict

chlorophyll-a, phosphorus, and DO for both timespans (short term and long term). The simulated results match reasonably well with the observed data for all lakes. This model can successfully predict algal bloom in lakes which can be beneficial for lake management teams. The stratification scenario of the lake can be perceived by the water temperature and DO results (section 4.5).

The deep lakes exhibit a certain trend for chlorophyll-a simulation year by year whereas the shallow lakes show abrupt change in chlorophyll-a concentration due to mixing. Moreover, the chlorophyll-a calculation method greatly affects the DO concentration in shallow lakes but the effect on deep lakes is minimal.

5.3 Future Studies

Though MINLAKE2020 is well capable of predicting the daily Chla, phosphorus, BOD, and DO, it can be improved further. One of the improvements that can be applied to the model is adding an inflow and outflow subroutine to the program. This will hopefully increase the model accuracy as well as the flexibility of the model to be integrated with other watershed-scale models. Most of the lakes receive inflows from upstream and phosphorus loading is the main cause of eutrophication in most of the cases. This integration of inflow will better mimic the real nutrient scenario of a lake and predict algal bloom. This modification will allow the model to be integrated with the SWAT model to increase the accuracy of the watershed model. The basic code for inflow and outflow parts was developed but has not comprehensively tested.

Model sensitivity analysis should be performed to get a better understanding of the effect of calibration parameters. This will further help to ease the process of calibration and increase model accuracy and applicability.

Most of the lakes have a small amount of data for chlorophyll-a and phosphorus which makes model calibration difficult. Moreover, most of the calibration parameters are chosen based on the user's experience. Short-term daily observed data at regular intervals in all seasons can be used to better validate the model. The data collection of the lakes will allow the user to better predict the calibration parameters as well.

MINLAKE2012 model was used to study the impact of future climate changes on water quality in lakes, first in the State of Minnesota (Stefan et al. 1995b) and then over the contiguous USA (Fang et al. 2004). How the MINLAKE2020 model affects the projection of water quality in lakes is an interesting topic for future studies. This future projection will allow the lake management professionals to predict algal bloom. It will be specifically more beneficial for the lakes which are used for drinking water supply.

References

Anderson, D.M., Cembella, A.D., Hallegraeff, G.M., 2012. Progress in understanding harmful algal blooms: paradigm shifts and new technologies for research, monitoring, and management. Annu. Rev. Mar. Sci. 4, 143–176. https://doi.org/10.1146/annurev-marine-120308-081121. Aquatic Sci. 65, 1779e1796

Bartram, J., Carmichael, W., Chorus, I., Jones, G., Skulberg, O., 1999. Introduction. In: Chorus, I., Bartram, J. (Eds.), Toxic Cyanobacteria in Water. World Health Organization, London, and New York.

Batick, B. M. (2011). "Modeling Temperature and Dissolved Oxygen in the Cheatham Reservoir with CE- QUAL-W2," Vanderbilt University.

Biology: 17-43.

Chapra, S. C. (2008). Surface water-quality modeling, Waveland press.

Chen, G., Fang, X., Li, J., and Gong, Y.,2018. "Influences of weather conditions and daily repeated upstream releases on temperature distributions in a river-reservoir system". ASCE Journal of Hydrologic Engineering, 23(1), 04017055-1-14, DOI:10.1061/(ASCE)HE.1943-5584.0001601

Coutant, C. C. (1985). "Striped bass, temperature, and dissolved oxygen: a speculative hypothesis for environmental risk." Transactions of the American Fisheries Society, 114(1), 31-61.

Craig, P. M. (2012). "User's Manual for EFDC_Explorer 7: A Pre/Post Processor for the Environmental Fluid Dynamics Code." Dynamic Solutions-International, LLC, Edmonds, Washington, USA.

De Senerpont Domis, L.N., Van de Waal, D.B., Helmsing, N.R., Van Donk, E., Mooij, W.M., 2014. Community stoichiometry in a changing world: combined effects of warming and eutrophication on phytoplankton dynamics. Ecology 95, 1485–1495. https://doi.org/10.1890/13-1251.1.

Devkota, J., and Fang X., 2015. "Numerical Simulation of Flow Dynamics in a Tidal River under Various Upstream Hydrologic Conditions." Hydrological Sciences Journal, DOI: 10.1080/02626667.2014.947989

Devkota, J., and Fang X., 2015. "Quantification of water and salt exchanges in a tidal estuary", Water, 7(5), 1769-1791; DOI: 10.3390/w7051769 (Online Open Access)

Dillon, P.J., Rigler, F.H., 1974a. The phosphorus-chlorophyll relationship in lakes: phosphorus-chlorophyll relationship. Limnol. Oceanogr. 19, 767–773. https://doi.org/10.4319/lo.1974.19.5.0767.

Ding, L., 2012, "Water Purification Demonstration Project: Limnology and Reservoir Detention Study of San Vicente Reservoir – Nutrient and Algae Modeling Results", City of San Diego.

Dodds WK, Bouska WW, Eitzmann JL, Pilger TJ, Pitts KL et al. (2009) Eutrophication of U.S. freshwaters: Analysis Analysis of potential economic damages. Environ Sci Technol 43: 12-19. doi:10.1021/es801217q.

Dodds, W.K., 2006. Eutrophication and trophic state in rivers and streams. Limnol. Oceanogr. 51, 671–680. https://doi.org/10.4319/lo.2006.51.1_part_2.0671.

Durrer, M., Zimmermann, U., Jüttner, F., 1999. Dissolved and particle-bound geosmin in a mesotrophic lake (Lake Zürich): spatial and seasonal distribution and Ecological Modelling, 43(3-4), 155-182.

Fang X., R. Shrestha, A.W. Gorger, J. Lin, and M. Jao, 2007. “Simulation of Impacts of Streamflow and Climate Conditions on Amistad Reservoir.” Invited paper for the Journal of Contemporary Water Research and Education. Published by the Universities Council On Water Resources (UCOWR), USA, 137 (September, 2007):14-20.

Fang, X. (1994). "Modeling of Dissolved Oxygen Stratification Dynamics in Minnesota Lakes under Different Climate Scenarios," Dissertation, University of Minnesota.

Fang, X., Alam, S. R., and Stefan, H. G. (1998). "Continental-scale projections of potential climate change effects on water temperature, dissolved oxygen and associated fish habitat of small lakes in the contiguous U.S., Vol. III - Effects of climate conditions on fish habitat." Project Report 421, St. Anthony Falls Laboratory, University of Minnesota, Minneapolis, MN.

Fang, X., Alam, S. R., Jacobson, P., Pereira, D., and Stefan, H. G. (2010a). "Simulations of water quality in cisco lakes in Minnesota." Project Report No. 544, St. Anthony Falls laboratory, University of Minnesota, Minneapolis, MN, Minneapolis.

Fang, X., and Stefan, H. G. (1994a). "Modeling of dissolved oxygen stratification dynamics in Minnesota lakes under different climate scenarios." Project Report 339, St Anthony Falls Hydraulic Laboratory, University of Minnesota, Minneapolis, MN 55414, 260pp.

Fang, X., and Stefan, H. G. (1994b). "Temperature and dissolved oxygen simulations for a lake with ice cover." St. Anthony Falls Hydraulic Laboratory, University of Minnesota, Project Report 356, Minneapolis, MN.

Fang, X., and Stefan, H. G. (1996a). "Dynamics of heat exchange between sediment and water in a lake." Water Resources Research, 32(6):1719-1727.

Fang, X., and Stefan, H. G. (1996b). "Long-term lake water temperature and ice cover simulations/measurements." Cold Regions Science and Technology, 24(3), 289-304.

Fang, X., and Stefan, H. G. (1998). "Temperature variability in the lake sediments." Water Resources Research, 34(4), 717-729.

Graham, J.L., Loftin, K.A., Meyer, M.T., Ziegler, A.C., 2010. Cyanotoxin mixtures and taste-and-odor compounds in cyanobacterial blooms from the Midwestern

Gu, R., and Stefan, H. G. (1990). "Year-round temperature simulation of cold climate lakes." Cold Regions Science and Technology, 18(2), 147-160.

Hannoun, I.A., List, E., Kavanagh, K.B., Chiang, W.L., 2006, "Use of Elcom and Caedym for Water Quality Simulation in Boulder Basin", Proceedings of the Water Environment Federation 2006(9):3943-3970

Hasler AD (1969) Cultural eutrophication is reversible. Journal of Biosciences 19: 425-431.

Hayes, J., (2020) "Lake Erie fishing dependent on competing Ohio toxic algal abatement plans", post-gazette.com

Hondzo, M., and Stefan, H. G. (1993a). "Lake water temperature simulation model." Journal of Hydraulic Engineering, 119(11), 1251-1273.

Hondzo, M., and Stefan, H. G. (1993b). "Regional water temperature characteristics of lakes subjected to climate change." Climatic Change, 24, 187-211.

Hudnell HK (2010) The state of U.S. freshwater harmful algal blooms assessments, policy and legislation. Toxicon 55: 1024-1034. doi:10.1016/j.toxicon.2009.07.021. PubMed: 19646465.

Hudnell HK, Dortch Q (2008) A synopsis of research needs identified at the Interagency, International. Symposium on Cyanobacterial Harmful Algal Blooms (ISOC-HAB). Advances in Experimental Medicine and

Hutchinson, G. E. (1957). A treatise on limnology, Wiley, New York.

Idso, S. B., and Jackson, R. D. (1969). "Thermal radiation from the atmosphere." Journal of Geophysical Research, 74(23), 5397-5403.

Imboden, D.M., 1974. Phosphorus model of lake eutrophication: P model of lake eutrophication. Limnol. Oceanogr. 19, 297–304. https://doi.org/10.4319/lo.1974.19.2.0297.

Janssen, A.B.G., Teurlincx, S., Beusen, A.H.W., Huijbergts, M.A.J., Rost, J., Schipper, A.M., Seelen, L.M.S., Mooji, W.M., Janse, J.H., 2019, "PCLake+: A process-based ecological model to assess the trophic state of stratified and non-stratified freshwater lakes worldwide", https://doi.org/10.1016/j.ecolmodel.2019.01.006

Ji, Z.-G. (2008). Hydrodynamics and water quality: modeling rivers, lakes, and estuaries, John Wiley & Sons.

Koenings, J. P., and Edmundson, J. A. (1991). "Secchi disk and photometer estimates of light regimes in Alaskan lakes: Effects of yellow color and turbidity." Limnology and Oceanography, 36(1), 91-105.

lakes in Manitoba. J. Fish. Res. Board Can. 33 (1), 25e35.

Le Moal, M., Gascuel-Odoux, C., Ménesguen, A., Souchon, Y., Étrillard, C., Levain, A.,Moatar, F., Pannard, A., Souchu, P., Lefebvre, A., Pinay, G., 2018. Eutrophication: a new wine in an old bottle? Sci. Total Environ. https://doi.org/10.1016/j.scitotenv.2018.09.139.

Le Moal, M., Gascuel-Odoux, C., Ménesguen, A., Souchon, Y., Étrillard, C., Levain, A., Moatar, F., Pannard, A., Souchu, P., Lefebvre, A., Pinay, G., 2018. Eutrophication: a new wine in an old bottle? Sci. Total Environ. https://doi.org/10.1016/j.scitotenv.2018.09.139.

Lee, R.G., Biggs, T.W., and Fang, X.,2018. "Thermal and hydrodynamic changes under a warmer climate in a variably stratified hypereutrophic reservoir", Water, 10(9); DOI: 10.3390/w10091284, (Online Open Access).

Leon, L.F., Smith R.E.H., Romero, J.R., Hecky, R.E., 2006. “Lake Erie Simulations with ELCOM-CAEDYM”, International Congress on Environmental Modeling and Software.

Liu Y, Villalba G, Ayres RU, Schroder H (2008) Global phosphorus flows and environmental impacts from a consumption perspective, Journal of Industrial Ecology 12: 229-247. doi:10.1111/j.1530-9290.2008.00025.x.

Lock, G. S. H. (1990). The growth and decay of ice, Cambridge University Press. Lundquist, J. B. (1975). "A primer on limnology."

Mani, A., and Rangarajan, S. (1982). Solar radiation over India, Allied Publishers.

Markfort, C. D., Perez, A. L. S., Thill, J. W., Jaster, D. A., Porté-Agel, F., and Stefan, H. G. (2010). "Wind sheltering of a lake by a tree canopy or bluff topography." Water Resour. Res., 46(3), W03530, doi:10.1029/2009wr007759.

Marshall, C. T., and Peters, R. H. (1989). "General patterns in the seasonal development of chlorophyll a for temperate lakes." Limnology Oceanography, 34(5), 856-867.

Martin, J. L. (2013). Hydro-environmental analysis: freshwater environments, CRC Press.

Megard, R. O., S., C. J. W., Smith, P. D., and Knoll, A. S. (1979). "Attenuation of light and daily integral rates of photosynthesis attained by planktonic algae." Limnology and Oceanography, 24(6), 1038-1050.

Megard, R. O., Tonkyn, D. W., and Senft, W. H. (1984). "Kinetics of oxygenic photosynthesis in planktonic algae." Journal of Plankton Research, 6(2), 325-337.

Moomaw WR, Birch MB (2005) Cascading costs: an economic nitrogen cycle. Science in China Series C, Life Sciences. Chinese Academy of Sciences 48 Spec No. 2: 678-696

Moss, B., 2012. Cogs in the endless machine: lakes, climate change and nutrient cycles: a review. Sci. Total Environ. 434, 130–142. https://doi.org/10.1016/j.scitotenv.2011.07.069 (Climate Change and Macronutrient Cycling along the Atmospheric, Terrestrial, Freshwater and Estuarine Continuum - A Special Issue dedicated

Nash, J. E., and Sutcliffe, J. V. (1970). "River flow forecasting through conceptual models part I - a discussion of principles." Journal of Hydrology, 10(3), 282-290.

Pivovarov, A. A. (1972). Thermal condition in freezing lakes and rivers, Wiley, New York.

Pomati, F., Matthews, B., Seehausen, O., Ibelings, B.W., 2017. Eutrophication and climate warming alter spatial (depth) co-occurrence patterns of lake phytoplankton assemblages. Hydrobiologia 787, 375–385. https://doi.org/10.1007/s10750-016-2981-6.

Pretty JN, Mason CF, Nedwell DB, Hine RE, Leaf S et al. (2003) Environmental costs of freshwater eutrophication in England and Wales. Environ Sci Technol 37: 201-208. doi:10.1021/es032467q.

Reckhow KH, Arhonditsis GB, Kenney MA, Hauser L, Tribo J et al. (2005) A predictive approach to nutrient criteria. Environ Sci Technol39: 2913-2919. doi:10.1021/es048584i. PubMed: 15926533

Reynolds, C.S., Irish, A.E., Elliott, J.A., 2001a. The ecological basis for simulating phytoplankton responses to environmental change (PROTECH). Ecol. Model. 140, 271–291.

Reynolds, C.S., Irish, A.E., Elliott, J.A., 2001b. The ecological basis for simulating phytoplankton responses to environmental change (PROTECH). Ecol. Model. 140, 271–291. https://doi.org/10.1016/S0304-3800(01)00330-1

Riley, G. A. (1947). "Factors controlling phytoplankton populations on Georges Bank." J. Marine Research, 6, 54-73.

Riley, M. J., and Stefan, H. G. (1987). "Dynamic lake water quality simulation model" MINLAKE"." Riley, M. J., and Stefan, H. G. (1988). "MINLAKE: A dynamic lake water quality simulation model."

Rubin, H. (2001). Environmental fluid mechanics, CRC Press.

Schindler DW, Vallentyne JR (2008) The algal bowl: Overfertilization of the world's freshwaters and estuaries. Edmonton: University of Alberta Press. 348 pp.

Smith VH, Tilman GD, Nekola JC (1999) Eutrophication: impacts of excess nutrient inputs on freshwater, marine, and terrestrial ecosystems. Environ Pollut 100: 179-196.

Smith, V.H., Joye, S.B., Howarth, R.W., 2006. Eutrophication of freshwater and marine ecosystems. Limnol. Oceanogr. 51, 351–355.

Stefan, H. G., and Fang, X. (1994). "Model simulations of dissolved oxygen characteristics of Minnesota lakes: past and future." Environmental Management, 18(1), 73-92.

Stefan, H. G., Cardoni, J. J., and Fu, A. Y. (1982). "RESQUALL II: a dynamic water quality simulation program for a stratified shallow lake or reservoir: application to Lake Chicot, Arkansas." University of Minnesota, Minneapolis, MN 55414, 154.

Stefan, H. G., Fang, X., David, W., Eaton, J. G., and McCormick, J. H. (1995a). "Simulation of dissolved oxygen profiles in a transparent, dimictic lake." Limnology and Oceanography, 40(1), 105-118.

Stefan, H. G., Hondzo, M., and Fang, X. (1993). "Lake water quality modeling for projected future climate scenarios." Journal of Environmental Quality, 22(3), 417-431.

Stefan, H. G., Hondzo, M., Eaton, J. G., and McCormick, J. H. (1995b). "Predicted effects of global climate change on fishes in Minnesota lakes." Fisheries and Aquatic Sciences (Special Publication), 121, 57- 72.

Stefan, H., and Ford, D. E. (1975). "Temperature dynamics in dimictic lakes." Journal of the Hydraulics Division, ASCE, 101(HY1, January, 1975), 97-114.

Stepanenko, V.M., A. Martynov, K.D. Jöhnk, Z.M. Subin, M. Perroud, X. Fang, F. Birch, D. Mironov, and S. Goyette, 2013. “A One-dimensional Model Intercomparison Study of Thermal Regime of a Shallow Turbid, Midlatitude Lake”. Geoscientific Model Development, Discussion Paper, 5:3993-4035 and Final Paper, 6:1337-1352 with supplemental information.

Tabachek, J.L., Yurkowski, M., 1976. Isolation and identification of blue-green algae producing muddy odor metabolites, geosmin, and 2-methylisoborneol in saline

Takolander, A., Cabeza, M., Leskinen, E., 2017. Climate change can cause complex responses in Baltic Sea macroalgae: a systematic review. J. Sea Res. 123, 16–29. https://doi.org/10.1016/j.seares.2017.03.007.

Terry, J.A., Sadeghian, A., Lindenschmidt, K.-E., 2017. Modelling dissolved oxygen/sediment the effect of grazers. Water Res. 33 (17), 3628e3636.

Thiery, W., Stepanenko, V.M., Fang X., Jöhnk K.D., Li Z., Martynov A., Perroud M., Subin, Z.M., F. Darchambeau, Mironov D., Lipzig, N.P.M.V., 2014. "LakeMIP Kivu: Evaluating the representation of a large, deep tropical lake by a set of one-dimensional lake models." Tellus A 2014, 66, 21390, http://dx.doi.org/10.3402/tellusa.v66.21390.

Thomann, R. V., and Mueller, J. A. (1987). Principles of surface water quality modeling and control, Harper Collins Publishers Inc, New York, xii, 644 p.

Torregrossa, M., (2019)."Lake Erie harmful algae bloom expanding rapidly as seen from imagery", https://www.mlive.com/weather/2019/08/lake-erie-harmful-algae-bloom-expanding-rapidly-as-seen-on-imagery.html

Townsend AR, Howarth RW, Bazzaz FA, Booth MS, Cleveland CC et al. (2003) Human health effects of a changing global nitrogen cycle. Frontiers in Ecology and the Environment 1: 240-246.

Truax, D. D., Shindala, A., and Sartain, H. (1995). "Comparison of two sediment oxygen demand measurement techniques." Journal of Environmental Engineering, 121(9), 619-624.

Turner RE, Rabalais NN (2003) Linking landscape and water quality in the Mississippi river basin for 200 years. Journal of Biosciences 53: 563-572.

USACE. (1995). "CE-QUAL-R1: A Numerical One-Dimensional Model of Reservoir Water Quality; User's manual." US Army Corps of Engineers (ACE), Waterways Experiment Station.

USEPA (1994) National water quality inventory: 1994 report to Congress. Washington, D.C. Available: Available online at: http://water.epa.gov/lawsregs/guidance/cwa/305b /94report_index.cfm.

USEPA (1996) National water quality inventory: 1996 report to Congress. Washington, D.C. Available: Available online at: http://water.epa.gov/lawsregs/guidance/cwa/305b /96report_index.cfm.

USEPA (1998) National strategy for the development of regional nutrient criteria. Available: http://water.epa.gov/scitech/swguidance/waterquality/standards/criteria/aqlife/pollutants/nutrient/nutsi.cfm.

USEPA (1998) National water quality inventory: 1998 report to Congress. Washington, D.C. Available: Available online at: http://water.epa.gov/lawsregs/guidance/cwa/305b/98report_index.cfm.

USEPA (2000) National water quality inventory 2000 report. Washington, D.C. Available: Available online at: http://water.epa.gov/lawsregs/guidance/cwa/305b/2000report_index.cfm.

USEPA (2002) National water quality inventory: Report to Congress 2002 reporting cycle. Washington, D.C. Available: Available online at: http://water.epa.gov/lawsregs/guidance/cwa/305b/2002report_index.cfm.

USEPA (2009) EPA needs to accelerate adoption of numeric nutrient water quality standards. Available: http://www.epa.gov/oig/reports/2009/20090826-09-P-0223.pdf.

Utley, B. C., Vellidis, G., Lowrance, R., and Smith, M. C. (2008). "Factors affecting sediment oxygen demand dynamics in blackwater streams of Georgia's coastal plain." JAWRA Journal of the American Water Resources Association, 44(3), 742-753.

Vollenweider, R.A., Kerekes, J., 1982. Eutrophication of Waters. Monitoring, Assessment and Control. OECD Cooperative Programme on Monitoring of Inland Waters. OECD, Paris.

Wake, A., and Rumer Jr., R. R. (1979). "Modeling ice regime of Lake Erie." Journal of the Hydraulics Division ASCE, 105(7), 827-844.

Walley, R. (2011). "University Lakes." Louisiana Department of Wildlife and Fisheries.

Wanninkhof, R., Ledwell, J., and Crusius, J. (1990). "Gas transfer velocities on lakes measured with sulfur hexafluoride." Air-water mass transfer, ASCE, 441-458.

Water Resources Research, 32(6), 1719-1727.

Watson, S.B., Ridal, J., Boyer, G.L., 2008. Taste and odour and cyanobacterial toxins: impairment, prediction, and management in the Great Lakes. Can. J. Fish.

Wetzel, R. G. (1975). Limnology, Saunders, Philadelphia, xii, 743 p.

Wetzel, R.G., 2001. Limnology: Lake and River Ecosystems. Academic Press.

Wolfe AH, Patz JA (2002) Reactive nitrogen and human health: Acute and long-term implications. Ambio 31: 120-125. Available online at: doi:10.1579/0044-7447-31.2.120;2. PubMed: 12078000

Xie Q., Liu X., Fang X., Chen Y., Li, C., and MacIntyre S., 2017. "Understanding temperature variations and thermal structure of a subtropical deep river-run reservoir

before and after impoundment." Water, 9(8), 603; DOI: 10.3390/w9080603, (Online Open Access).

Xu, Z., and Xu, Y. J. (2015). "Determination of trophic state changes with diel dissolved oxygen: A case study in a shallow lake." Water Environment Research, 87(11), 1970-1979.

Xu, Z., and Xu, Y. J. (2016). "A deterministic model for predicting hourly dissolved oxygen change: Development and application to a shallow eutrophic lake." Water (Switzerland), 8(2), doi:10.3390/w8020041.

Yao, X., Zhang, Y., Zhang, L., Zhou, Y., 2018. A bibliometric review of nitrogen research in eutrophic lakes and reservoirs. J. Environ. Sci. 66, 274–285. https://doi.org/10.1016/j.jes.2016.10.022.

Zison, S. W., Mills, W. B., Diemer, D., and Chen., C. W. (1978). "Rates, constants and kinetic formulations in surface water quality modeling." Tetra Tech, Inc., for USEPA, ORD, Athens, Georgia, 317.

Appendix A

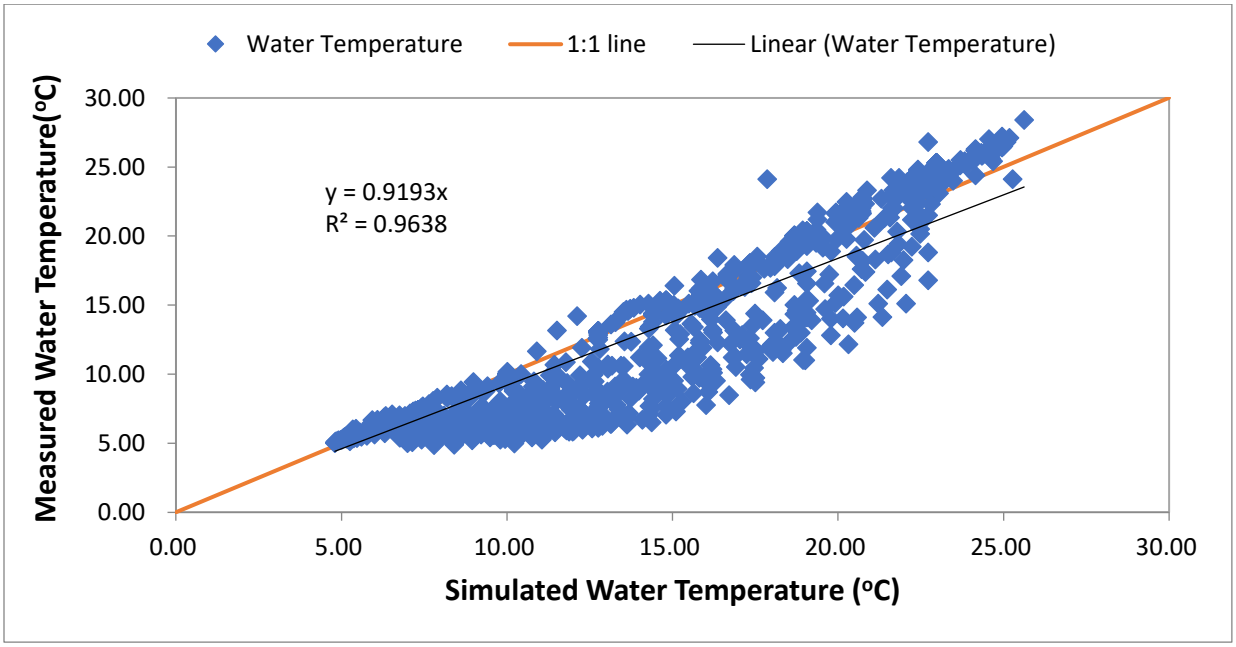

Figure A.1 Statistical comparison between simulated and observed water temperature in Riley Lake in 1985-1987

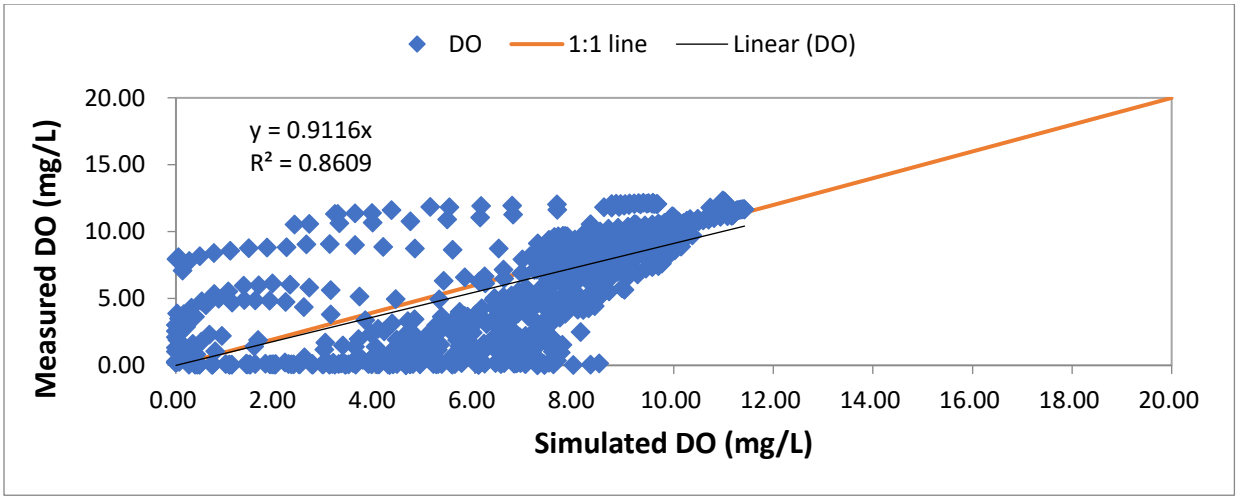

Figure A.2 Statistical comparison between simulated and observed DO in Riley Lake in 1985-1987

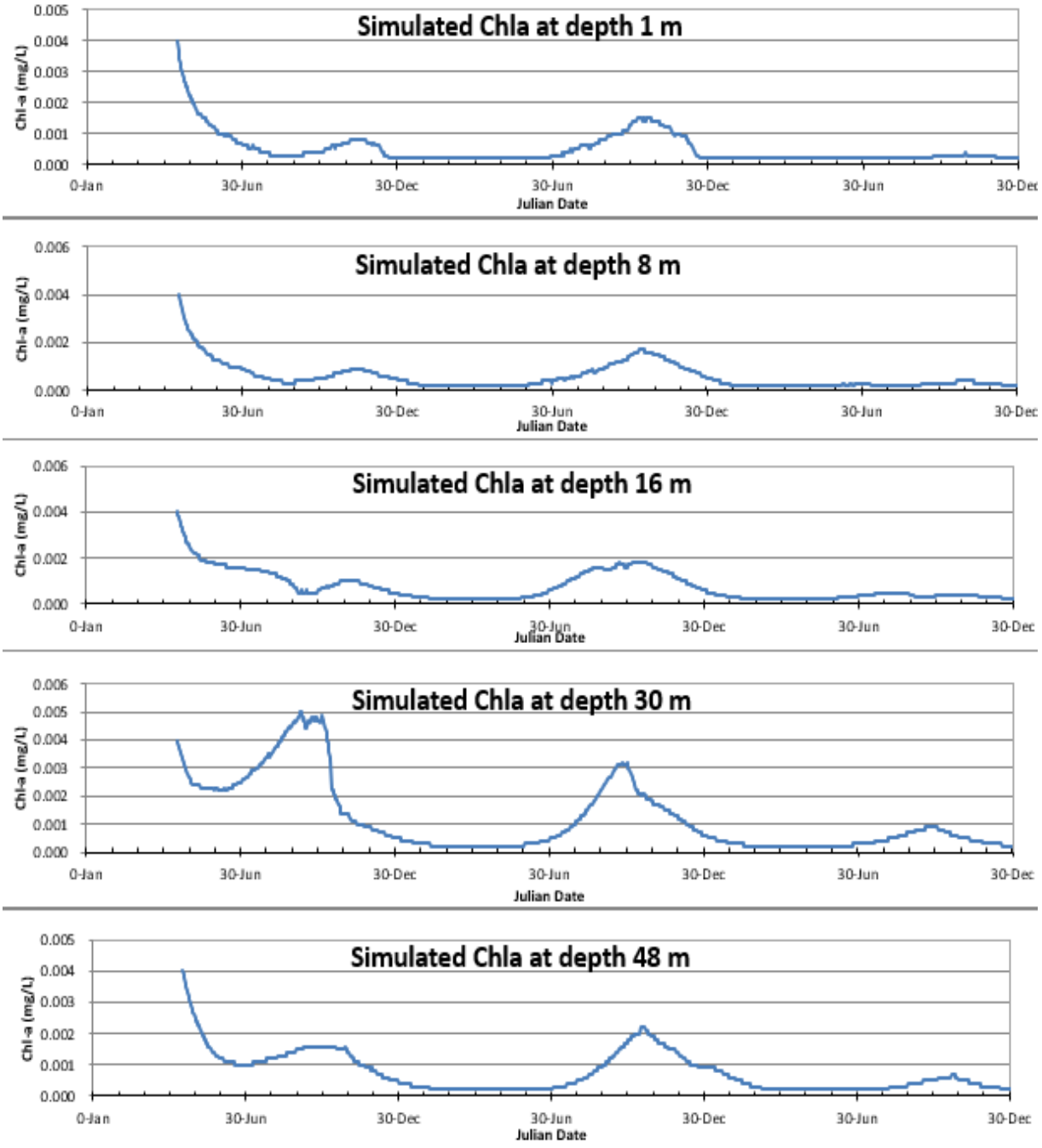

Figure A.3 Simulated chlorophyll-*a* at 1 m, 8 m, 16 m, 30 m and 48 m depth from the surface in Lake Riley in 1985-1987

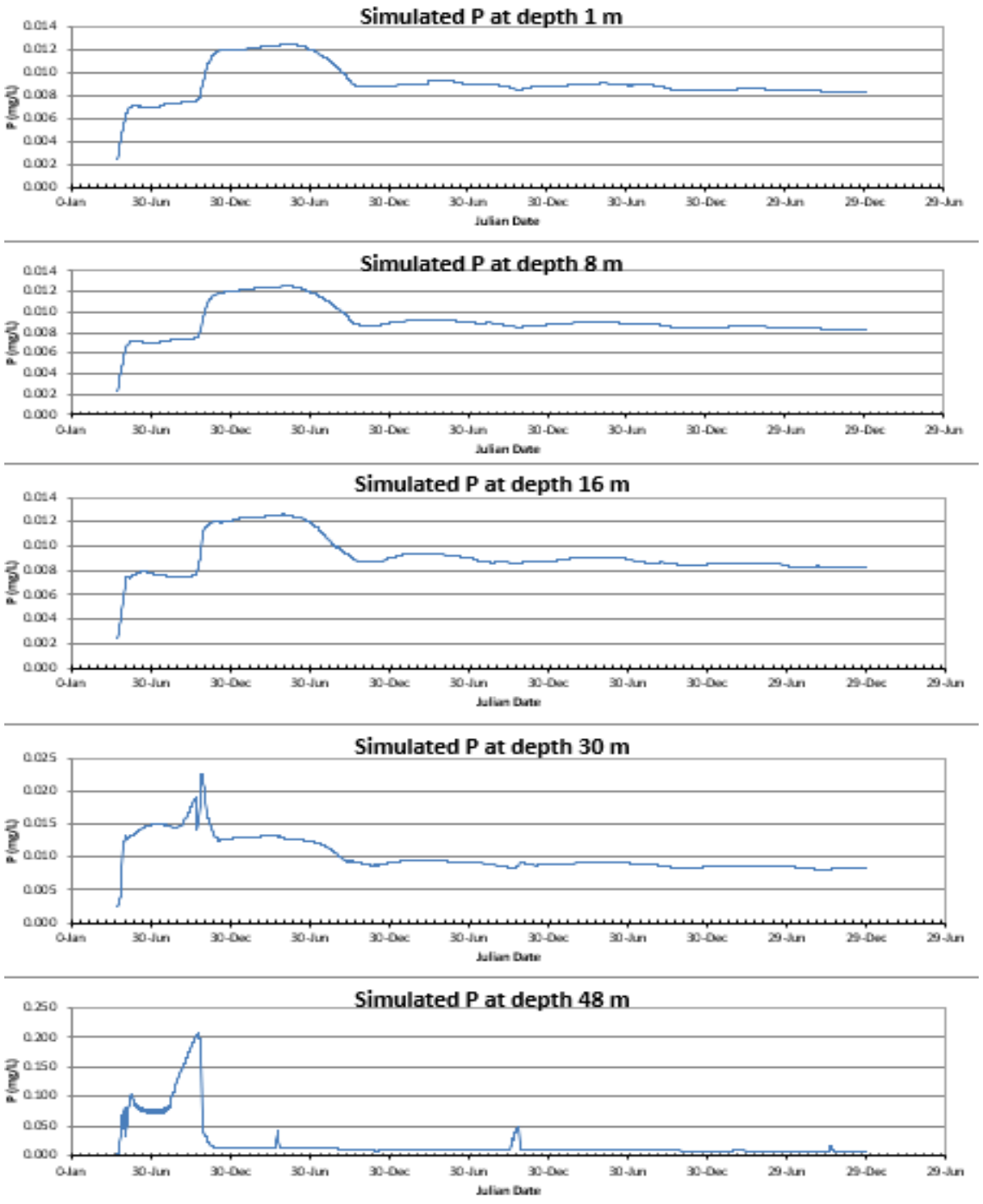

Figure A.4 Simulated phosphorus at 1 m, 8 m, 16 m, 30 m and 48 m depth from the surface in Lake Riley in 1985-1987